2008

The Role of GDF-3 in Patterning the Early Embryo

Ariel Levine

THE ROLE OF GDF-3 IN PATTERNING THE EARLY EMBRYO

A Thesis Presented to the Faculty of

The Rockefeller University

in Partial Fulfillment of the Requirements for

the degree of Doctor of Philosophy

by

Ariel Levine

June 2008

THE ROLE OF GDF-3 IN PATTERNING THE EARLY EMBRYO

Ariel Levine, Ph.D.

The Rockefeller University 2008

The central aim of modern embryology is the resolution of the signaling pathways and transcriptional networks that direct embryonic development. After a century of rich experimental embryology, more recent molecular analyses of embryogenesis have revealed that communication between cells drives some of the most important events of development, including cell fate determination, growth, and morphogenesis. Among signaling factors, the TGF-β superfamily regulates all of these phenomena, and is the focus of this work. Despite significant progress in understanding the role of individual TGF-β ligands, their ultimate integration as a pathway is not fully understood and several ligands remain unexplored.

In this work, I present the first comprehensive, comparative analysis of a mammalian-specific, structurally atypical TGF-β ligand, GDF-3. This work was first motivated by the finding that GDF-3 is strongly associated with the pluripotent state, and is one of the earliest ligands expressed in the mammalian embryo. However, nothing was previously

known about its function in stem cells, or in normal embryonic development.

Using frog embryos, mouse embryos, and mouse and human embryonic stem cells, I found that GDF-3 is a BMP-inhibitory ligand, adding to its unusual properties and extending the variety of regulatory strategies governing the TGF-β pathway. This inhibitory function endows GDF-3 with multiple activities, including the ability to directly induce neural tissue in frog embryos, thus highlighting the evolutionary conservation of mechanisms for neural formation. In mammalian embryonic stem cells, we found that GDF-3 opposes BMPs to regulate the balance of stemness and differentiation. These findings reveal the importance of negative, inhibitory information in the determination of the earliest embryonic cell fates.

Further, I found that GDF-3 is required for normal patterning of the mouse embryo; its reduction causes a dramatic and unprecedented phenotype. In genetrap GDF-3 mutants, disorganized, distal migration of the notochord results in dorso-ventral rearrangment of the entire embryo. This finding provides a genetic basis for dissecting the tightly coupled processes of morphogenesis and cell fate determination in the mammalian embryo.

This work establishes a clearer picture of the pleitropic TGF-β superfamily and contributes to an understanding of the conserved molecular basis of embryonic development.

DEDICATION:

This work is dedicated to my son, Max, whose inquisitiveness reminds me to always ask "Why"

ACKNOWLEDGEMENTS:

I am so grateful for the mentoring and friendship of Dr. Ali Brivanlou. He is an outstanding teacher, who has provided me with a balance of independence and guidance, encouragement and criticism, enthusiasm and perspective. His thought-provoking ideas on embryogenesis will continue to inform my work in the future. I am fortunate to have studied with him and I will always carry his vision and my appreciation.

The contribution of Dr. Brivanlou is complemented by the students and post-docs in his lab. They have created an exciting, intellectual environment, and have given me their patient advice, support, and criticism. I particularly acknowledge the help of Dr. Ignatio Munoz-Sanjuan and Dr. Francesca Spagnoli.

This work would have been impossible without the loving support of my husband, Barry Klein. Throughout my thesis, he has been a source of strength, a patient sounding board, a steady advisor, and an inspiration. He is a true partner, and this has been a very special time together in our lives.

My interest in science began with my parents. From my father, I have a passion for inquiry and thoughtful investigation, and he has contributed his advice and editing to each manuscript and talk I have prepared. His advice on presenting scientific ideas is invaluable, and stems from his love of knowledge and the sharing of it. From my mother, I have an intensity and a focus that has been very helpful during this work, and she has frequently been a sympathetic listener during my trips to and from the lab at all hours of the night.

I sincerely appreciate the advice and contributions of my thesis advisory committee, Dr. Elaine Fuchs, Dr. Lee Niswander, and Dr. Richard Harland. Their insightful questions have stimulated much of this work and their support in my professional development has been incredibly helpful. My thesis is a better work because of each of them, and I am so thankful for their time, attention, and mentoring.

This work was done as part of my progress in the MD-PhD program. This amazing program is coordinated by Dr. Olaf Andersen and by Ruth

Gotian, who have provided me with important help and advice throughout my training.

TABLE OF CONTENTS:

LIST OF FIGURES

LIST OF TABLES:

CHAPTER 1: BACKGROUND

In metazoans, the union of sperm and egg, two highly differentiated cell types, gives rise to the zygote – the totipotent cell. The zygote has the potential to form every cell type of the embryo and the adult organism through a series of sequential cell fate decisions that successively limit its range of potency. For example, the cells of the very early mammalian embryo divide, maintaining their totipotency until they reach sixteen to thirty-two cells, at which point outer cells will give rise to extra-embryonic tissues, such as the placenta, and inner cells are fated to give rise to the embryo proper (Pedersen et al., 1986; Ziomek and Johnson, 1982). This, the choice between the outer trophoblast and the 'inner cell mass', represents the first recognized restriction in cell fate potential.

The development of the embryo then follows from the establishment of the major axes: head versus tail (anterior-posterior axis), front versus back (dorsal-ventral axis), and the left-right axis. These coordinates are not merely geometric but are associated with the development of specific patterns of cell fate. Within this context, the germ layers form - ectoderm, mesoderm, and endoderm – and progressively differentiate into the various tissues of the final organism. These cell fate decisions occur as the result of communication between cells.

The extrinsic information that cells receive must be transferred into intrinsic cellular responses at the protein and transcriptional levels, a process

known as signal transduction (Brivanlou and Darnell, 2002). Several inter-connected signal transduction pathways have been identified and these play critical roles in both development and disease. These pathways involve an extra-cellular protein signal that binds to a receptor on the surface of the target cell. Upon binding this protein 'ligand', the receptors initiate a cascade of rapid, amplified reactions that send intracellular transducers to mediate the cellular response. Most commonly, these responses impinge on other signal transduction pathways and, ultimately, on target gene transcription levels in the nucleus. This 'locks down' the flexible extrinsic signal into a stable, cell autonomous response.

1.1 - TGF-β Signal Transduction in Embryogenesis

In development and adulthood, one of the most important signal transduction pathways is the Transforming Growth Factor-β (TGF-β) pathway. This pathway has a primary role in the formation of each of the germ layers of the early embryo: ectoderm, mesoderm, endoderm, and of germ cells (Conlon et al., 1994; Hemmati-Brivanlou et al., 1994; Hemmati-Brivanlou and Melton, 1992; Hemmati-Brivanlou and Melton, 1994; Hemmati-Brivanlou et al., 1992; Lawson et al., 1999; Smith, 1987; Sokol et al., 1990; Thomsen et al., 1990). Concurrently, TGF-β signaling helps to establish all three axes of polarity in the organism (the anterior-posterior axis, the dorsal-ventral axis, and the left-right axis) (Ariizumi et al., 1991; Harland, 2004; Levin et al., 1995; Perea-Gomez et

al., 2002; Robertson et al., 2003; Varlet et al., 1997; Vonica and Brivanlou, 2007; Wilson et al., 1997; Yost, 2001). Later in development, this pathway has diverse effects on cell fate, cell shape, and organ formation in many of the various tissues of the organism. TGF-β signaling has pleiotropic effects on many cell types and, not surprisingly, there are many different TGF-β ligands, several signal transducers, and a very large variety of TGF-β target genes. In the mammalian genome, there are approximately 40 TGF-β ligands (Lander et al., 2001). The basic features of a TGF-β ligand are a secretion signal, and a prepro domain that is cleaved to form the mature form that has a cysteine knot protein structure. The TGF-β ligands are divided roughly by homology into two major branches, the BMP/GDF (Bone Morphogenetic Protein/Growth and Differentiation Factor) branch and the TGF-β/Activin/Nodal branch. A classification of TGF-β ligands, based on the cysteine knot structural backbone, is shown in Figure 1.

Figure 1: The TGF-β superfamily ligands, classified by cysteine arrangment of the mature domain. The prepro region of the ligands (green) is cleaved from the mature region (red). The mature region contains cysteines (numbered from –1 through 7) that characterize the different subfamilies of TGF-β ligands. Type 1 ligands, the Activins and classic TGF-β ligands, contain the seven canonical cysteines (1-7) in addition to two additional cysteines. Type 2 ligands contain the seven canonical cysteines (1-7) and represents the BMP/GDF subfamily of ligands. Type 3 contains cysteines 1-6 and only represents one ligand, Xnr3. Type 4 ligands are missing the 4th canonical cysteine, the one involved for intermolecular interactions. From Levine and Brivanlou, 2006a.

Figure 1

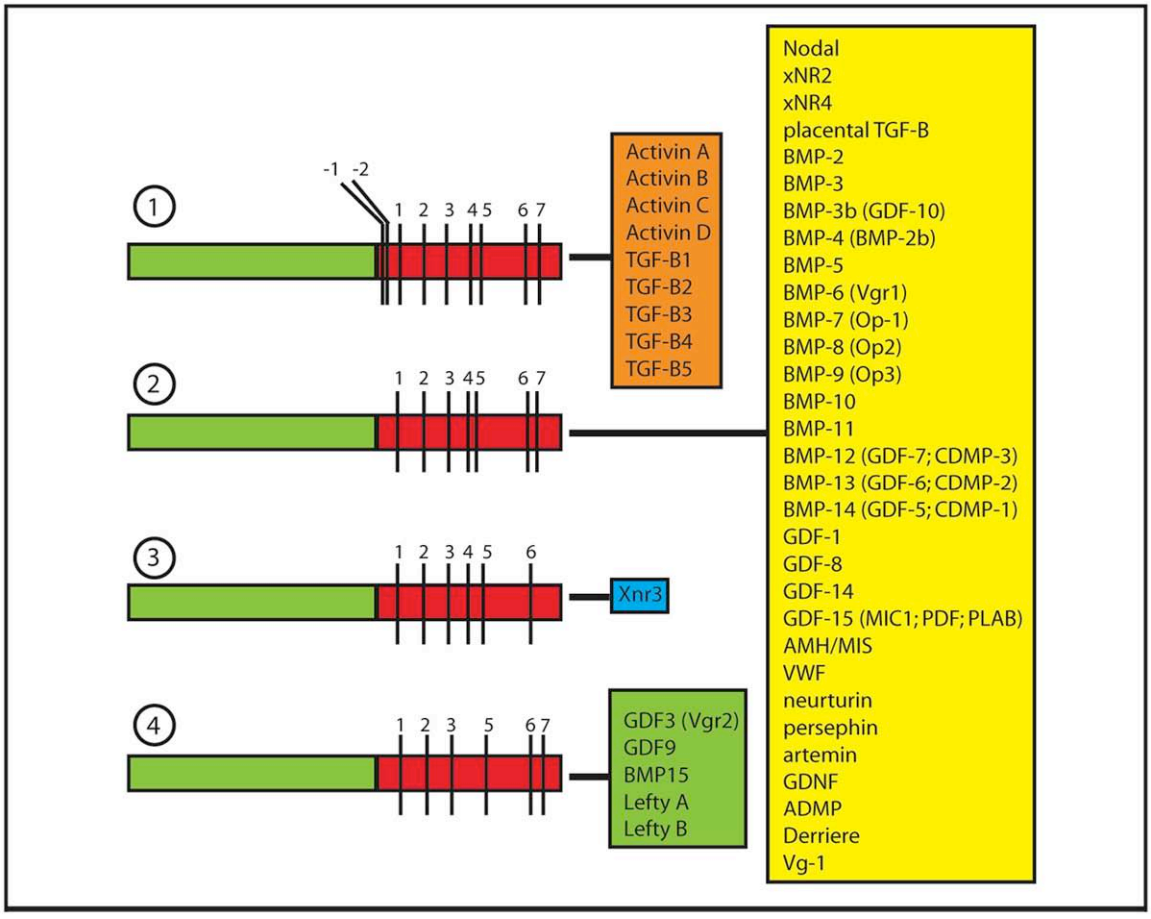
-1 -2
1 2 3 4 5 6 7
1
1 2 3 4 5 6 7
2
1 2 3 4 5 6
3
1 2 3 5 6 7
4
Activin A
Activin B
Activin C
Activin D
TGF-B1
TGF-B2
TGF-B3
TGF-B4
TGF-B5
Xnr3
GDF3 (Vgr2)
GDF9
BMP15
Lefty A
Lefty B
Nodal
xNR2
xNR4
placental TGF-B
BMP-2
BMP-3
BMP-3b (GDF-10)
BMP-4 (BMP-2b)
BMP-5
BMP-6 (Vgr1)
BMP-7 (Op-1)
BMP-8 (Op2)
BMP-9 (Op3)
BMP-10
BMP-11
BMP-12 (GDF-7; CDMP-3)
BMP-13 (GDF-6; CDMP-2)
BMP-14 (GDF-5; CDMP-1)
GDF-1
GDF-8
GDF-14
GDF-15 (MIC1; PDF; PLAB)
AMH/MIS
VWF
neurturin
persephin
artemin
GDNF
ADMP
Derriere
Vg-1

TGF-β ligands are secreted as dimers and bind to a two-part receptor on the surface of the target cell that is made by the association of a two Type 1 and two Type 2 TGF-β receptors (Shi and Massague, 2003). The classic TGF-β ligands, together with Activin, Nodal, and related ligands (including GDF1), are grouped together. The activating ligands of this group bind the Type 1 receptors Alk4, Alk5, and Alk7 and activate the pathway through C-terminal phosphorylation of the signal transducers Smad2 and Smad3. These Smads then bind to a common transcriptional co-regulator, enter the nucleus, and activate transcription of target genes, together with other transcriptional co-regulators, such as Smad4 (Figure 2). The other major branch of the TGF-β family includes BMP and most GDF ligands. The activating ligands of this group bind the Type 1 receptors Alk2, Alk3, and Alk6 and activate Smad1, Smad5, and Smad8 that regulate transcription together with a common co-regulator and another co-regulator such as OAZ (Figure 2) (Shi and Massague, 2003). However, some GDF ligands, for instance GDF-1, signal through the Smad2/3 branch of the pathway (Wall et al., 2000).

Figure 2

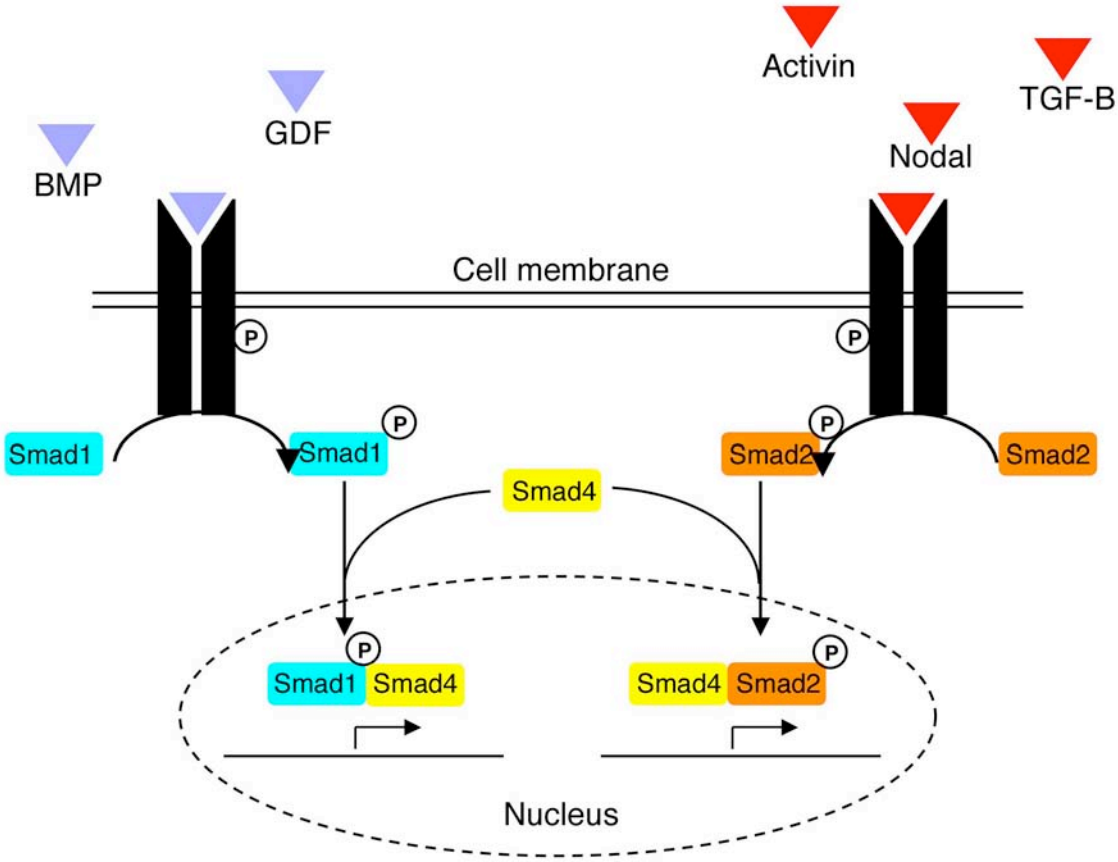

Figure 2: A simplified version of the TGF-β superfamily signaling pathways. The TGF-β ligands are divided into two families, the TGF-β/Activin/Nodal ligands on the right, and the BMP/GDF ligands on the left. The classic ligands bind to a heterodimeric receptor and activate Smads in the cell to regulate transcription. Smad1, Smad2, and Smad4 are shown as representative of the Smad1,5,8 subgroup, the Smad2,3 subgroup, and the Smad4a, 4b subgroups, respectively.

While the above abstract summary of a signal transduction pathway describes a linear path from extra-cellular signal to nuclear response, it is becoming clear that the TGF-β pathway is much more complex. One of the most important complex characteristics is the ability of TGF-β ligands to act as morphogens (Ariizumi et al., 1991; Green and Smith, 1990; Vincent et al., 2003; Wilson et al., 1997). This means that at different thresholds of signal transducer activation, TGF-β signaling can elicit different effects on the target cell, within a given window of time.

Another major feature of TGF-β signaling is that there are several mechanisms of Smad-independent signal transduction, for instance, through Tak/TAB (TGF-β Activated Kinase 1/Tak1 Binding Protein 1) signaling onto the MAPK pathway (Munoz-Sanjuan et al., 2002; Shibuya et al., 1996; Yamaguchi et al., 1995). Interestingly, some divergent TGF-β family members may not signal through Smads at all. For instance, GDNF and similar ligands signal through the Ret receptor to activate tyrosine kinases (Durbec et al., 1996; Jing et al., 1996; Trupp et al., 1996). Further complexities of TGF-β pathway signaling include the following: each ligand, receptor, signal transducer, and effector are regulated spatially and temporally within the embryo; similar ligands can have different strengths of activity (Aono et al., 1995); some ligands require co-receptors while others do not (Gritsman et al., 1999); related signal transducers may bind co-regulators with different affinities (Hata et al., 1998); and the

ongoing signaling status of other signal transduction pathways co-regulate all levels of the TGF-β pathway.

1.2 TGF-β signaling in early embryos: lessons from the frog

Many of the fundamental findings on the embryonic roles of this pathway were first characterized in the frog embryo, where TGF-β signaling has been shown to play a role in the development of every germ layer and most tissues analyzed. TGF-β ligands were first found to be regulators of cell fate in early embryos when Activin was identified as a mesoderm inducer in Xenopus cells and embryos (Smith, 1987; Thomsen et al., 1990). It was subsequently found to act as a morphogen, inducing distinct cell fates at different doses (Ariizumi et al., 1991; Green et al., 1992; Green and Smith, 1990). Low doses induce postero-lateral mesoderm, intermediate doses induce dorsal mesoderm, and high doses induce endoderm. *In vivo*, the Nodal-related ligands, Xnrs, probably account for the Activin-like mesoderm activity as a Nodal inhibitor abrogates mesoderm induction and the Xnrs are expressed in dorsal endoderm – precisely the predicted location to account for the cell fate gradient readout (Agius et al., 2000; Takahashi et al., 2000).

BMP signaling acts similarly in the ectoderm, inducing epidermis at high doses, placodes/cement gland at intermediate doses, and in the absence of BMP signaling, neural tissue is formed (Wilson and Hemmati-Brivanlou, 1995; Wilson et al., 1997). This latter phenomenon provides the mechanistic basis for the ‘neural default’ model (Hemmati-Brivanlou et al., 1994; Hemmati-Brivanlou

and Melton, 1992; Hemmati-Brivanlou and Melton, 1994; Hemmati-Brivanlou et al., 1992; Munoz-Sanjuan and Brivanlou, 2002). This model was based on two linked initial observations, both of which were conducted in the animal cap region of the frog embryo (Figure 3). This region is the prospective anterior end of the embryo and is fated to give rise to ectoderm. When explanted and cultured alone, the animal cap forms epidermis. However, if the cells of the animal cap are dispersed, thereby inhibiting cell-cell communication, these cells become neural tissue – this is the first important observation that led to the neural default model (Grunz and Tacke, 1989). The second observation was that over-expression of a truncated TGF-β type II receptor (that functions as a dominant negative receptor by forming inactive receptor heterodimers) in the animal cap gives rise to neural tissue (Hemmati-Brivanlou and Melton, 1992; Hemmati-Brivanlou and Melton, 1994). Together, these two findings suggested that a TGF-β related signal was normally signaling to cells of the animal cap to inhibit differentiation to neural tissue. It was found that this factor is BMP signaling, as exogenous BMPs can convert dispersed animal cap cells back into epidermis (Wilson and Hemmati-Brivanlou, 1995).

Figure 3

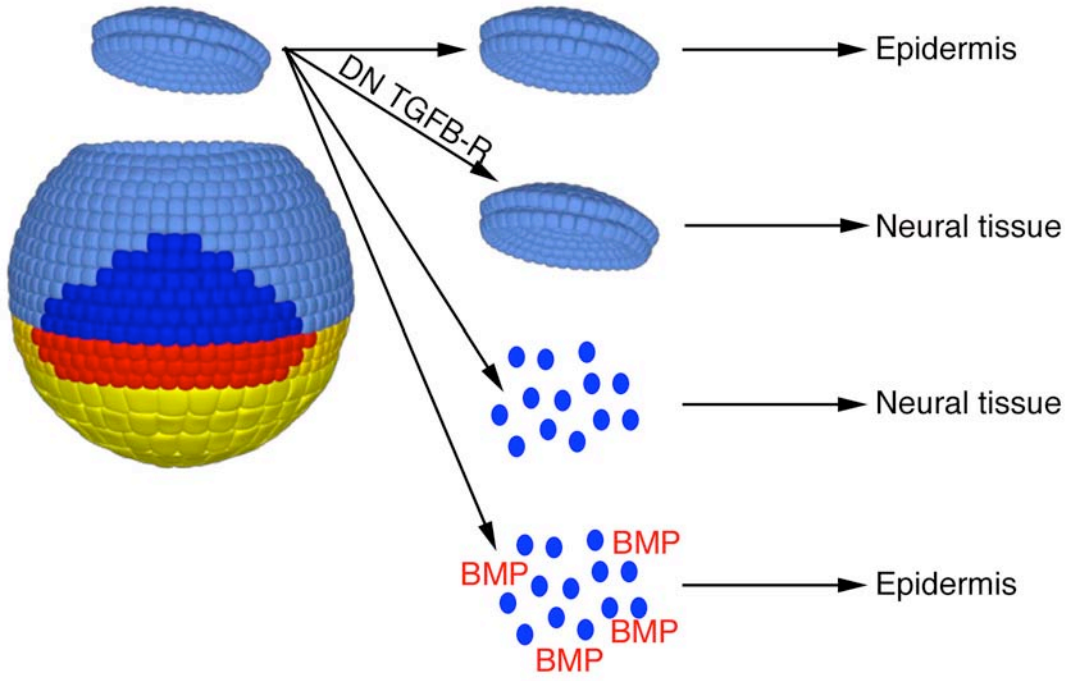

Figure 3: The experimental basis of the 'neural default' model. The animal cap of a blastula stage frog will give rise to ectoderm (blue) at gastrula stages. If the animal cap is isolated and cultured alone, it will give rise to epidermis. If the frog embryo was previously injected with a dominant-negative type II TGF-β receptor (DN ActRIIB), this tissue becomes neural. Conversion of the animal cap from epidermal to neural fates can also be accomplished by dispersion of the cells to prevent cell-cell signaling, a phenomenon that can be reversed by culture of the cells with BMP proteins. The future dorsal mesoderm is shown in red, endoderm in yellow.

BMP inhibition is the molecular basis by which neural induction and patterning can be 'organized' by a region of dorsal mesoderm. Historically, the first experimental embryology on neural induction was done by Spemann and his group (Spemann and Mangold, 1924). In his seminal work with Hilde Mangold, published in 1924, they found that the dorsal blastopore lip of the gastrulating *Triturus* (newt) embryo "exerts an organizing effect on its environment in such a way that, following its transplantation to an indifferent region of another embryo, it there causes the formation of a secondary embryo" (Spemann and Mangold, 1924). This 'secondary embryo' was fused to the host embryo at the ventral mid-line; it had two complete heads, two hearts, two of each of the main dorsal structures (the notochord, neural tube, and somites) and one gut tube.

Surprisingly, early lineage tracing demonstrated that while the entire axial mesoderm (notochord) of the secondary embryo is derived from the progeny of the graft, the nervous system (except the floorplate) was derived from the host (Mangold, 1933). This clearly indicates a non-autonomous, extrinsic influence of the graft on its neighboring host cells. The term 'neural induction' therefore comes from an observation made in the last century that a small region of dorsal mesoderm can initiate formation of the entire nervous system. Secreted inhibitors of BMPs, such as Noggin and Chordin, were subsequently localized to correspond spatio-temporally with the functional organizer, as defined by Spemann and Mangold to be the source of neural inducing signals. This tissue

then gives rise to the notochord, accounting for the graft-based origin of this tissue in the secondary embryo.

In addition to regulating cell fate in the ectoderm, BMP signaling helps to establish the dorso-ventral arrangement of cell fates within the mesoderm. Over-expression of BMP4 in the mesoderm causes extreme ventralization (Dale et al., 1992; Jones et al., 1992a), while over-expression of BMP inhibitors is sufficient to induce dorsal mesoderm (Smith and Harland, 1992). In between these extremes, increasing doses of classic BMPs progressively pattern notochord, muscle, kidney, and, at the highest doses, blood (Dosch et al., 1997; Hemmati-Brivanlou and Thomsen, 1995).

Figure 4: Spemann's organizer and neural induction by BMP inhibition in frog embryos. (A) A gastrula stage frog (stage 10+) is shown, detailing the location of critical signaling factors that induce neural tissue *in vivo*. In the frog embryo, BMP signaling is active in the ventral (yellow) part of the embryo. This is limited by BMP inhibitors in the dorsal organizer (maroon) and allows neural formation in the dorsal animal region (blue). Explantation and transfer of the organizer to a host embryo (B), results in formation of a 'secondary embryo' (C), in which the double neural plate is pseudocolored in blue. A cross section of the primary and secondary embryo (D), shows the two notochords (maroon), and two neural tubes (blue). The single endoderm is shown in yellow. The secondary structures are on the right in (D). (C,D) are from Figure 7 and Figure 23, respectively, of Spemann and Mangold, 1924.

Figure 4

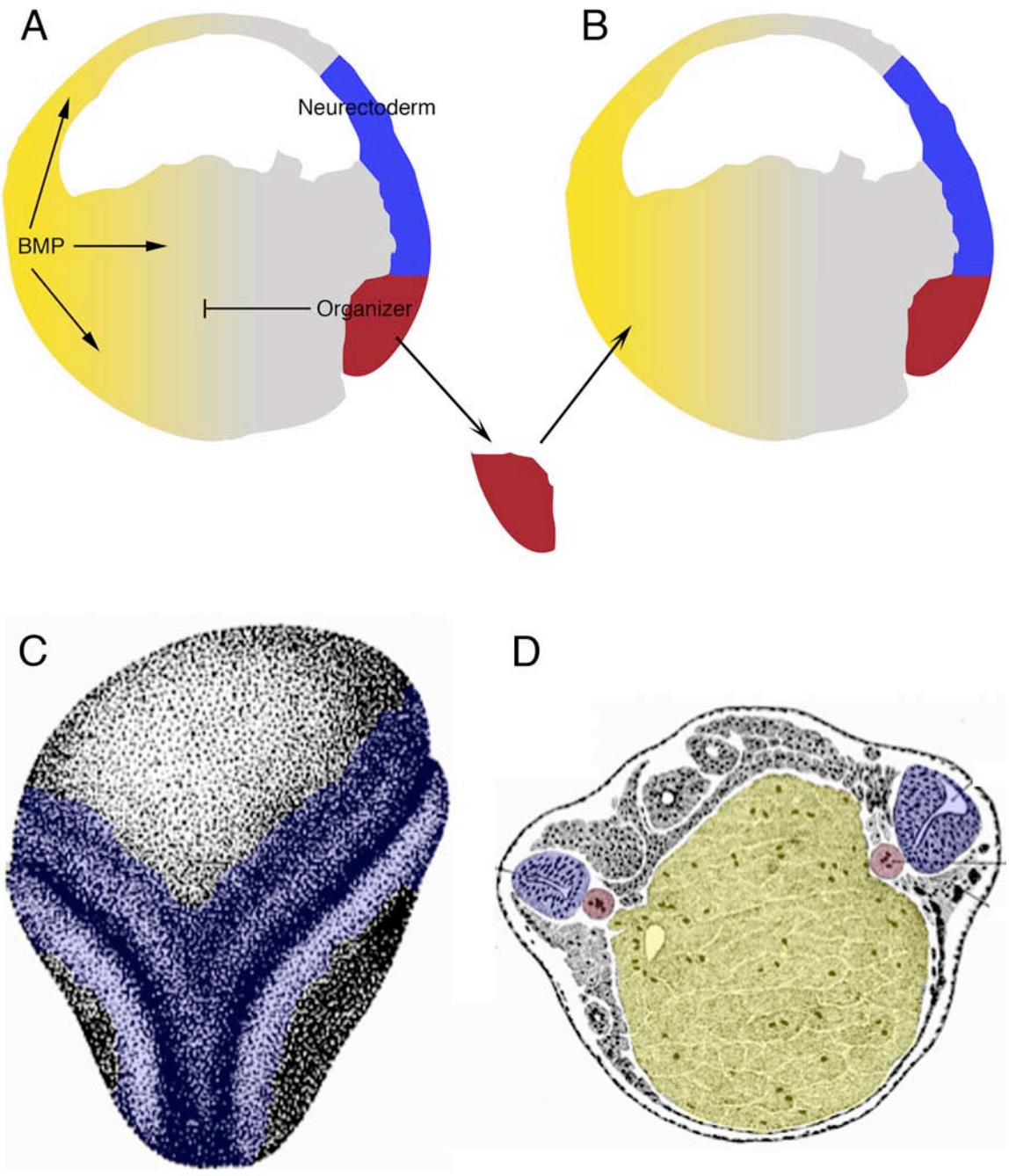

1.3 - TGF-β signaling in early embryos: conserved roles in the mouse

Many of the findings regarding TGF-β signaling in the frog embryo were confirmed and extended using genetic loss-of-function analysis in mouse embryos, particularly the classic examples of Activin/Nodal signals in mesoderm formation and inhibition of BMP signaling in neural induction. For instance, the mouse mutant of Nodal fails to form mesoderm and dies at peri-gastrulation stages (Conlon et al., 1994). Reduction of Nodal signaling through partial loss of its signal transducers, its transcriptional targets, or through a hypomorphic Nodal allele reveal that the highest levels of Nodal signaling in the embryo proper are required to induce anterior definitive endoderm and anterior axial mesoderm (Lowe et al., 2001; Vincent et al., 2003; Yamamoto et al., 2001). This was predicted from the morphogen gradient experiments in frog embryos, showing that the highest doses of Activin induce dorsal endoderm and notochord (Ariizumi et al., 1991; Green et al., 1992; Green and Smith, 1990).

In mouse development, the molecular and tissue basis of neural inducing signals have not been determined, though new evidence suggests an important conserved role for BMP inhibition, together with Nodal inhibition, in establishing the neural tissue. Importantly, recent work found that loss of the BMP receptor Alk3 (Di-Gregorio et al., 2007) or of Nodal (Camus et al., 2006) each result in a dramatic and precocious conversion of almost the entire epiblast into anterior neural tissue that expresses Otx2 and Sox1 as well as markers of anterior forebrain such as Six3, Dlx5, and Hesx1. Thus, it seems that, normally, Nodal

and BMP signaling are required during pre-gastrulation stages to prevent a default acquisition of neural fate and to maintain a pluripotent epiblast that also can form epidermis, mesoderm, and endoderm.

While the molecular mechanism of BMP inhibition is conserved in the mouse as the primary mode of neural induction, the identity of the tissues that mediate these signals are not clearly understood (Levine and Brivanlou, 2007). Briefly, neural tissue is first specified in the distal epiblast by mid streak stages, by signals emanating from the organizer (Figure 5). More posterior neural tissue is induced by the node, which has full organizer-like properties and the ability to induce an ectopic secondary axis upon transplantation. Subsequently, the node gives rise to the notochord, which serves as an organizing center for axial structures and plays a role in patterning the neural tube, foregut, and paraxial mesoderm. Therefore, as in the frog, the organizer and its derivatives direct the ongoing formation of the neural tube and dorsal axis.

Figure 5

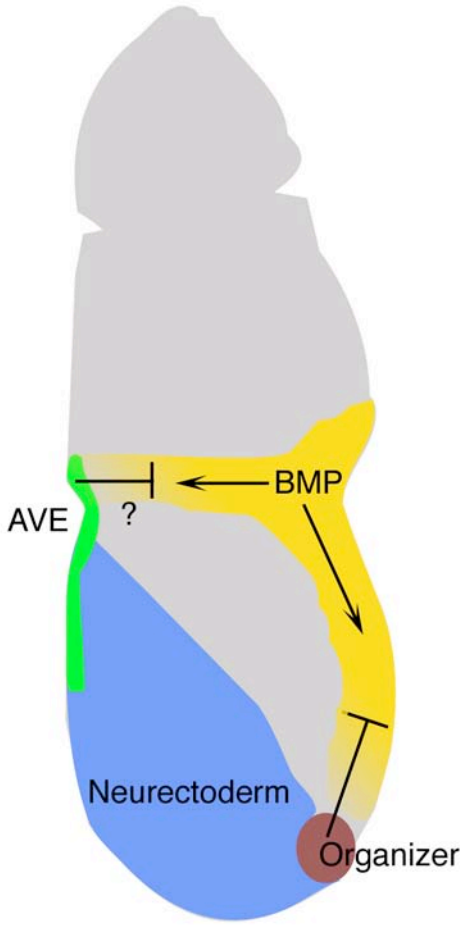

Figure 5: Neural induction in mouse embryos. At approximately e7.0 (mid-streak stage), the gastrula organizer (maroon), possibly in cooperation with the anterior visceral endoderm (AVE, green) allow neural induction to occur in the anterior epiblast (blue). This involves limiting BMP signaling (yellow) to the posterior/proximal embryo and may also involve regulation of other pathways such as Nodal and FGF.

1.4 TGF-β signaling in embryonic stem cells

To study new layers and functions of this complex pathway in early embryonic cell fate determination, I analyzed the TGF-β pathway in embryonic stem cells – an in vitro system in which differentiation recapitulates many of the early steps of normal embryogenesis. Embryonic stem cells are derived from the inner cell mass of the blastocyst and can self-renew in the undifferentiated state and can differentiate into all of the cell types of the embryo proper (reviewed in (Brivanlou et al., 2003). This latter characteristic allows a rapid analysis of factors involved in cell fate determination. More importantly, embryonic stem cells provide an opportunity to extend analysis of differentiation to a human embryological system.

Together with my colleagues, I found that Activin/Nodal signaling is active in early mouse embryos and in both mouse and human embryonic stem cells, as revealed by phosphorylation and nuclear localization of Smad2/3 (James et al., 2005). This activation is significant for the pluripotent state as exogenous Activin or Nodal promote pluripotency in human embryonic stem cells (Beattie et al., 2005; James et al., 2005; Vallier et al., 2004). Further, Activin/Nodal signaling is required for the maintenance of stemness in human embryonic stem cells (James et al., 2005; Vallier et al., 2005). While inhibition of Alk4/5/7 signaling in mouse embryonic stem cells does not affect pluripotency (Dunn et al., 2004; James et al., 2005; Vallier et al., 2005), blocking Nodal signaling in blastocyst outgrowths severely reduces levels of the inner cell mass and stem cell marker,

Oct4 (James et al., 2005). These findings show that Activin/Nodal signaling is important for pluripotency in human embryonic stem cells, mouse embryos, and mouse epiblast stem cells, although it is unclear why mouse embryonic stem cells do not require activation of this pathway.

In contrast to Activin/Nodal signaling, the role of BMP signaling in embryonic stem cells is somewhat controversial. In human embryonic stem cells, BMPs promote rapid differentiation to extra-embryonic cell fates even when these cells are cultured in feeder conditioned media that normally maintains their pluripotent state (Xu et al., 2002), despite the facts that stem cells express both the BMP inhibitor GDF-3 and the inhibitor Lefty (Sato et al., 2003) and that feeder cells secrete a BMP inhibitor as well (Xu et al., 2005). Further, human embryonic stem cells can be maintained without conditioned media by an exogenous combination of FGF activation and BMP inhibition (Xu et al., 2005). These findings suggest that the normal inhibition of BMP signaling in stem cells and early embryos is required to suppress differentiation to extra-embryonic fates.

In mouse embryonic stem cells, BMP signaling through Smad1/5/8 is normally minimally activated. However, moderate levels of exogenous activation of the BMP pathway may cooperate with other stemness pathways to support the undifferentiated state (Levine and Brivanlou, 2006b). However, as BMPs are morphogens (Wilson et al., 1997), it is possible that low levels of BMP signaling support pluripotency while higher levels push the cells to differentiate. This role

of BMPs is supported by *in vivo* evidence showing that reduced BMP signaling (in the BMPR1A knockout) results in loss of epiblast markers Oct4 and FGF5 at pre-gastrula stages (Di-Gregorio et al., 2007).

1.5 - GDF-3 is a TGF-β family member associated with stemness

After contributing to a broad analysis of the roles of TGF-β/Activin/Nodal signaling in embryonic stem cells, I chose to focus on specific ligands. A rich literature has shown that there can be subtle and dramatic functional differences between ligands, even those that are closely related**.** While many TGF-β superfamily members have well characterized functions in development and disease, several remain unexplored.

I studied a comparison of genes expressed in cells maintained in the undifferentiated state with genes expressed in their differentiated progeny (Sato et al., 2003), and focused my analysis on genes related to TGF-β signaling. Interestingly, three TGF-β ligands were enriched in the undifferentiated, 'stemness' population and displayed a sharp decline in expression when cells were pushed towards differentiation: Nodal, its antagonist ligand Lefty, and the relatively unstudied TGF-β ligand GDF-3 (Sato et al., 2003; Zeng et al., 2004). In fact, GDF-3 has become one of the most reliable markers of stemness (Adewumi et al., 2007), although almost nothing is known about its mechanism of action and its normal roles in stem cells and embryogenesis.

In this work, I address the role of GDF-3 in regulating diverse processes in early vertebrate development. To this end, I first characterized the biochemical mechanism of GDF-3, revealing that, surprisingly, it is a BMP inhibitor. I next sought to understand the functions of GDF-3 in each of its primary endogenous contexts of early development and began by analyzing its expression pattern in early embryogenesis, where it was found in the inner cell mass of the blastocyst (and its corollary, embryonic stem cells), and in the node and notochord. I found that GDF-3 is an endogenous BMP inhibitor in embryonic stem cells, and that it acts in a species-specific manner to regulate the undifferentiated state and the capacity for differentiation in human and mouse embryonic stem cells, respectively. To analyze the role of GDF-3 in the node and notochord, I studied a genetrap mutation of the GDF-3 locus, and found that in 42% of embryos, GDF-3 is required for correct dorsal-ventral arrangement of the body plan. Mutant embryos display a notochord at the ventral extreme of the embryo and a neural tube that opens into the body cavity of the embryo, with heart and endoderm at the extreme dorsal side of the embryo – the opposite of their position in normal embryos. This unusual phenotype is the result of perturbed migration of the notochord, a structure that organizes the axial tissues. This highlights the conserved role of BMP inhibitors and the node in embryonic patterning and reveals a requirement for normal BMP/GDF regulation in the chemotaxis of this structure, independent of its classic regulation of cell fates. In summary, this work provides the first comprehensive analysis of GDF-3, and

thereby illuminates novel aspects of TGF-β superfamily regulation, mechanisms of stemness, and basic strategies of early embryonic patterning.

CHAPTER 2: MECHANISM OF GDF-3 FUNCTION

2.1 GDF-3 is an atypical TGF-β ligand

GDF-3 is a TGF-β superfamily member sub-classified into the BMP/GDF (Bone Morphogenetic Protein/Growth and Differentiation Factor) branch of this family, based on homology (Jones et al., 1992b). Of note, GDF-3 is an atypical ligand, that has only six of the classical seven cysteines present in other TGF-β superfamily members (Jones et al., 1992b). It is missing the fourth cysteine – the one involved in inter-molecular interactions amongst TGF-β family members and with their secreted inhibitors (Figure 6) (Groppe et al., 2002).

Figure 6

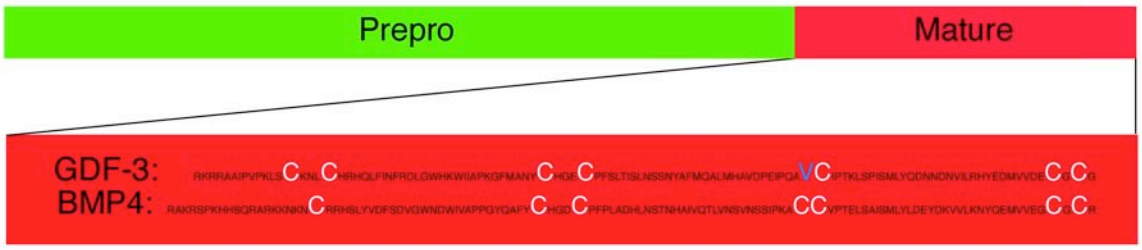

Figure 6: Primary structure of GDF-3 protein. GDF-3, like all other TGF-β ligands, contains a prepro domain and a mature domain. This mature domain (sequence shown) is atypical, containing only six of the canonical seven cysteines found in the cysteine knot structure of nearly all other TGF-β ligands (plus an additional, non-canonical cysteine). All cysteines are shown in white and the 'missing' fourth cysteine of GDF-3 is shown in blue. The sequence of BMP4 is shown for comparison.

I performed electronic library searches for homologues of GDF-3 in non-mammalian species such as Danio rerio and Xenopus laevis. However, the putative homologues given by Ensemble all possess the seven canonical cysteines characteristic of most TGF-β family members instead of the six present in GDF-3, suggesting that they are not true homologues.

More importantly, these putative 'homologues', such as xVg1, are not syntenic with GDF-3, but instead correspond to GDF-1. For instance, human GDF-3 is on chromosome 12p and is flanked by ApoBec1 and Stella, genes that are not found in the chick or in Xenopus tropicalis. Xenopus tropicalis Vg1 (CAJ82217, peptide Tegg005K01.1) is next to the genes COPE, Ddx49, then Homer3, the precise arrangement of genes neighboring human GDF-1 on chromosone 19.

I also designed several sets of degenerate primers based on mouse GDF-3 sequence and screened pools of frog cDNAs but did not find any Xenopus homologs (data not shown). Therefore, I tentatively conclude that GDF-3 is a recent evolutionary addition, present only in mammals.

The above analysis of the GDF-3 genomic region highlights another unusual characteristic of GDF-3. In humans, GDF-3 is located at 12p13, a region that strongly enriched for genes associated with pluripotency, including Nanog and Stella, which are immediately 5' of GDF-3. 12p13 is over-expressed in 80% of male germ cell tumors (Rodriguez et al., 2003), and down-regulation of the genes at this locus is associated with in vivo differentiation of these tumors

(Korkola et al., 2006). In these tumors, GDF-3 is specifically over-expressed (Korkola et al., 2006; Skotheim et al., 2006).

I began my analysis of GDF-3 by studying its activity and biochemical mechanism, so that I could interpret the function of GDF-3 in the results of gain and loss-of-function experiments that were performed in parallel. I chose to characterize GDF-3 activity in an unbiased way in the frog embryo because the effects of TGF-β pathway signaling in Xenopus are well established through phenotype and marker gene expression analysis. I reasoned that if GDF-3 is an agonist or antagonist of this pathway, or even of another pathway, its function might be partially determined through its effect on normal frog embryogenesis. Working with a mouse gene in a frog context provided the additional advantage that there is no 'background' GDF-3.

2.2 - GDF-3 elicits secondary axis induction in the frog embryo

I microinjected capped GDF-3 mRNA into the frog embryo. Unexpectedly, I found that injection of mGDF-3 mRNA in the ventral marginal zone of the four cell embryo, induces secondary axis formation (Figure 7A). In six batches of embryos (n = 151), I found this phenotype in 61% of embryos. Secondary axis induction of this type can occur by two mechanisms: induction of the Smad2/3 pathway by Nodal/Activin signaling (Thomsen et al., 1990), or inhibition of ongoing BMP signals (Smith and Harland, 1992; Suzuki et al., 1994). In contrast,

classic BMP/GDF ligands cause ventralization of the embryo, rather than a second dorsal axis (Dale et al., 1992; Jones et al., 1992a).

2.3 - GDF-3 inhibits BMP-induced cell fates and BMP-induced transcription

To determine which of these mechanisms is used by GDF-3, I performed a cell fate assay in the animal cap region of the frog embryo. As summarized in Figure 3, this tissue forms epidermis when isolated and cultured, due to ongoing BMP signaling. However, inhibition of this pathway activation can convert the animal cap into neural tissue. In contrast, Activin/Nodal signaling induces mesoderm in the animal cap, consistent with the role of these factors in the whole embryo.

Two cell embryos were microinjected in the animal pole with mRNA encoding mGDF-3 and allowed to develop to blastula stages. Animal caps were isolated and cultured to either late gastrula (stage 11.5) or late neurula (stage 21). The explants were then harvested and analyzed by RT-PCR for the detection of cell type specific markers. My analysis of expression of early and late markers shows that in contrast to other BMP family members, GDF-3 acts as a direct neural inducer. GDF-3 decreased expression of an immediate early response gene to BMP signaling, Msx-1, and increased expression of both early (Sox2) and late (Otx2 and NCAM) neural markers (Figure 7B,C). This conversion was direct because it was not concomitant with mesoderm induction, as demonstrated by the lack of induction of the pan-mesodermal marker

Brachyury (BU), the ventral marker Wnt8, and the marker of axial mesoderm collagen type II. These data demonstrated that over-expression of GDF-3 can block BMP-induced cell fates.

Figure 7: Activity of GDF-3 over-expression in frog embryos. (A) 1.5-3 ng GDF-3 RNA was injected into two out four cells of frog embryos in the future region of the ventral marginal zone and embryos were cultured until stage 32 (left panel) or stage 41 (right panel). Control uninjected sibling embryos are shown beneath an injected embryo in each panel. Scale bar is 1 mm. (B,C) RT-PCR of animal caps uninjected or injected with 1 ng of GDF-3 RNA collected at stage 12.5 (left panel) or stage 21 (right panel) to analyze early and late neural markers. Msx1 is an epidermal marker; Sox2 is an early neural marker; Otx2 and NCAM are late neural markers; BU, Wnt8, and Collagen type II (Coll II) are mesodermal markers. ODC is shown as a loading control. Whole embryos with and without reverse transcription ('E' and 'no RT', respectively) are shown as positive and negative controls for each RT-PCR marker. (D) Luciferase assay, in arbitrary units, from a BMP-respnsive element driving a luciferase reporter. Two cell frog embryos were injected with reporter alone (first column), BMP4 alone (100 pg RNA, second column), BMP4 (100 pg) and GDF-3 (500 pg) RNA (third column) or GDF-3 RNA (500 pg) alone. Whole embryos were harvested at stage 11 and assayed for luciferase activity.

Figure 7

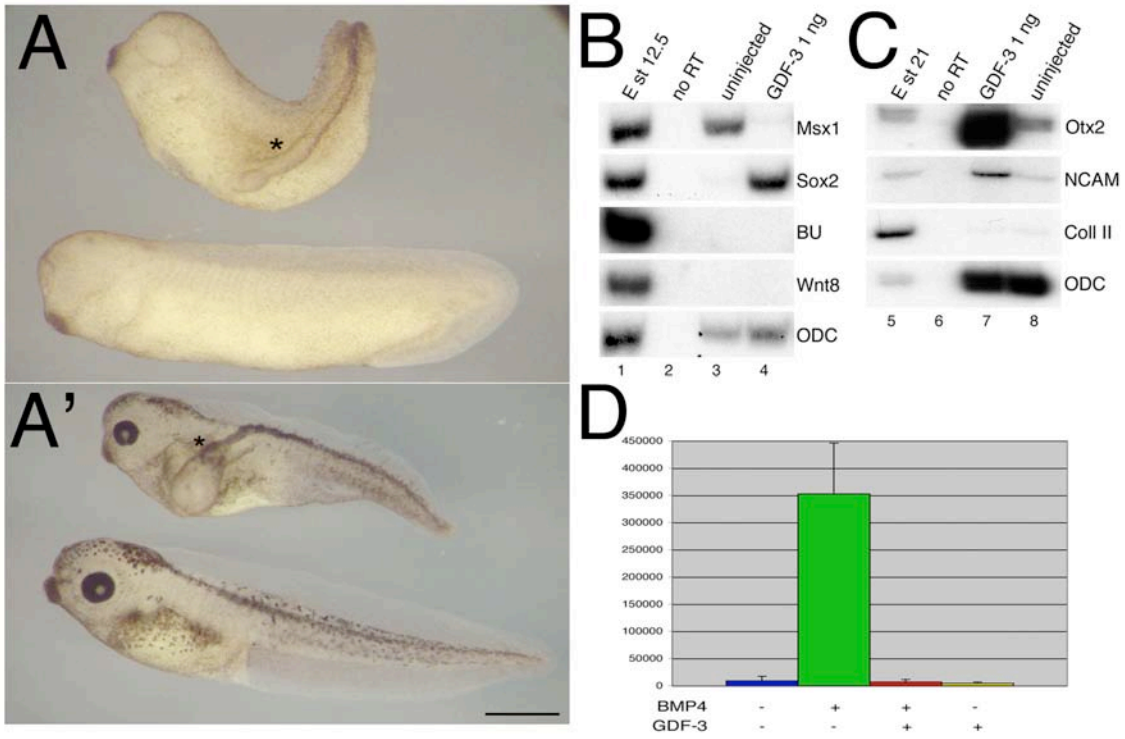
A
A'
B
E st 12.5
no RT
uninjected
GDF-3 1 ng
Msx1
Sox2
BU
Wnt8
ODC
1 2 3 4
C
E st 21
no RT
GDF-3 1 ng
uninjected
Otx2
NCAM
Coll II
ODC
5 6 7 8
D
450000
400000
350000
300000
250000
200000
150000
100000
50000
0
BMP4 - + + -
GDF-3 - - + +

To confirm that GDF-3 can inhibit BMP signaling, I analyzed the effect of GDF-3 over-expression on the ability of BMP to activate a reporter gene via Smad1/5/8. I injected two cell frog embryos with a BMP-responsive element driving a luciferase reporter (BRE-Lux), together with RNAs for BMP4 and GDF-3. Although BMP4 alone gave strong activation of the reporter gene, this signaling was almost completely inhibited by the presence of GDF-3 (Figure 7D).

2.4 - GDF-3 mature protein inhibits BMP-induced cell fates

The activities observed for several TGF-β ligands upon over-expression of mRNA may not reflect true functions of the protein. Therefore, I used two approaches to study the activities of the mature protein. In the first strategy, I produced GDF-3 protein by microinjection of 50 ng GDF-3 mRNA into Xenopus oocytes, followed by collection of GDF-3-containing medium after 48 hours. I examined the oocyte lysate and the conditioned media for GDF-3 protein to check for processing and secretion of GDF-3. In the oocyte lysate, I found both the prepro and mature forms of GDF-3 but only the mature form is secreted into the conditioned media (Figure 8A).

I tested the activity of GDF-3 conditioned media on two mesodermal explants derived from the marginal zone of the frog embryo. BMPs are normally expressed throughout the early embryo but the local secretion of BMP inhibitors in the dorsal marginal zone (DMZ) establishes the dorsal axis in normal Xenopus embryos; therefore, creating a second region of BMP inhibition in the

ventral marginal zone (VMZ) results in a secondary axis. The conditioned medium was then presented to both DMZ and VMZ and the behavior of the explants was compared to controls. Figure 8B shows that VMZ explants normally form a sphere in culture, whereas DMZ explants elongate due to the formation of tissues such as muscle and notochord that undergo convergent extension. GDF-3 protein dorsalizes VMZ tissue, creating elongation and the appearance of anterior structures such as the cement gland. Analysis of molecular markers by RT-PCR in these explants agrees with the conclusion that GDF-3 has strong dorsalizing activity in the mesoderm, as GDF-3 protein decreased the expression of the ventral mesodermal marker globin and induced the expression of dorsal paraxial markers such as m-actin in the VMZ explants (data not shown).

Figure 8: GDF-3 mature protein is a BMP inhibitor. (A) Western blot of GDF-3 protein produced by injection of GDF-3 RNA into frog oocytes and collection of oocyte lysate and conditioned medium (CM) after 48 hours. Lanes 1 and 3 show water injected oocyte lysate and CM; lanes 2 and 4 show GDF-3 injected lysate and CM. The upper band shows GDF-3 prepro form and the lower band shows GDF-3 mature protein, the only form seen in the oocyte conditioned medium. (B) Effect of diluted oocyte conditioned medium containing Activin or GDF-3 protein on frog embryo mesodermal explants – the ventral and dorsal marginal zones (VMZ and DMZ). Activin CM is shown as a positive control for causing VMZ elongation. The ratio of dilution is shown beneath each label. (C) Effect of recombinant human GDF-3 protein (rhGDF-3) on cell fate in intact and dispersed animal caps. RT-PCR on untreated (-) or rhGDF-3 or recombinant mouse Nodal (rmNodal) treated intact animal caps are shown in lanes 3-7 at the indicated doses. In lanes 8-12, disassociated animal caps were untreated or treated with recombinant human BMP4 protein (rhBMP4) and challenged with increasing doses of rhGDF-3. Sox2 is a neural marker, Msx1 is an epidermal marker, BU is a mesodermal marker, ODC is shown as a loading control. Whole stage 11.5 embryo, with and without reverse transcription ('E st 11.5' and 'no RT', respectively), are shown as positive and negative controls for each marker.

Figure 8

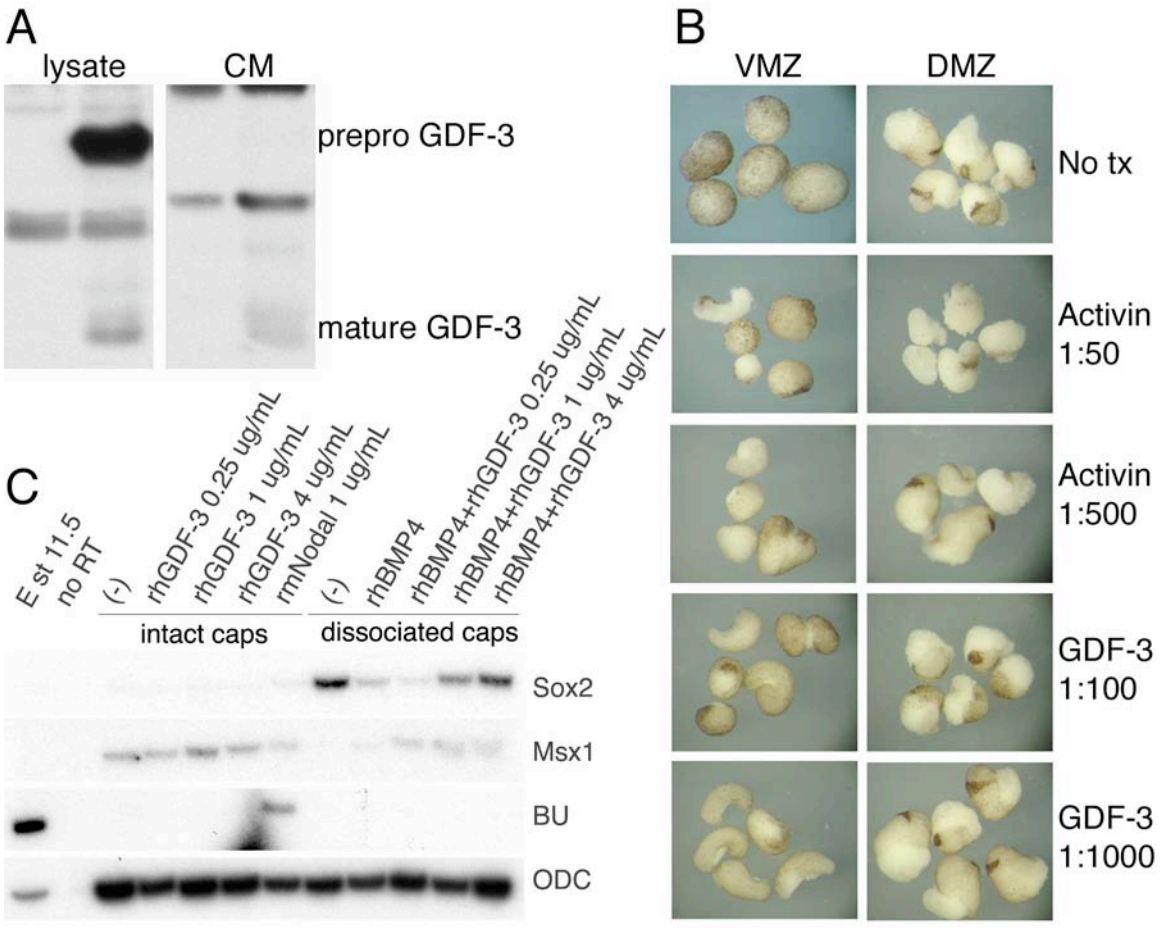
A
lysate
CM
prepro GDF-3
mature GDF-3
B
VMZ
DMZ
No tx
Activin 1:50
Activin 1:500
GDF-3 1:100
GDF-3 1:1000
C
E st 11.5 no RT
(-)
rhGDF-3 0.25 ug/mL
rhGDF-3 1 ug/mL
rhGDF-3 4 ug/mL
rmNodal 1 ug/mL
(-)
rhBMP4
rhBMP4+rhGDF-3 0.25 ug/mL
rhBMP4+rhGDF-3 1 ug/mL
rhBMP4+rhGDF-3 4 ug/mL
intact caps
dissociated caps
Sox2
Msx1
BU
ODC

However, this dorsalizing activity does not distinguish between BMP inhibition and Nodal-like activation. Therefore, I analyzed the activity of recombinant human GDF-3 protein (rhGDF-3) on cell fate in the frog embryo animal caps that had been disassociated into individual cells. It has previously been shown that this manipulation removes endogenous BMP signals and allows the animal cap cells to adopt a default neural fate, rather than the epidermal fate that BMPs induce (Wilson and Hemmati-Brivanlou, 1995). I then challenged these cells with exogenous BMP protein and tested the ability of rhGDF-3 to block the effects of this exogenous BMP signaling.

I found that, at the doses that I tested, rhGDF-3 protein did not induce mesoderm, although mesoderm was induced by the same dose of recombinant mouse Nodal protein (rmNodal), produced from a similar source (Figure 8C). While untreated disassociated cells became neural, rhBMP4 reverted these cells to epidermis. Increasing doses (0.5 - 4 ng/mL) of rhGDF-3 blocked this activity of rhBMP4 (Figure 8C). I also tested 15 ng/mL of rhGDF-3 and found that it had the same effect (data not shown). Therefore, at these protein doses, GDF-3 is a BMP inhibitor and does not act like a Nodal ligand.

2.5 - GDF-3 is required endogenously for full BMP inhibition

To study the physiological role of GDF-3, I analyzed the effects of reducing GDF-3 function in mouse embryonic stem cells. I used genetrap embryonic stem cells carrying an interruption of the GDF-3 locus (detailed in

Chapter 3.4). I injected these embryonic stem cells into host blastocysts to generate a line of mice with the genetrap insertion. Using these mice, I mated heterozygous pairs and obtained blastocysts that gave rise to wild-type, heterozygous, and homozygous genetrap mouse embryonic stem cells.

I characterized six embryonic stem cell lines – three wild-type lines, two heterozygous lines, and one homozygous genetrap line – and analyzed the state of TGF-β signaling in these cells. I first analyzed the ongoing signaling levels of the TGF-β/Activin/Nodal and BMP/GDF pathways in these cells by examining the phosphorylation status of Smads which mediate the intracellular signal transduction of these pathways.

I found that the heterozygous and homozygous genetrap lines, with reduced levels of GDF-3 protein, displayed mildly increased levels of BMP pathway activation. However, BMP signaling in embryonic stem cells is active at extremely low levels endogenously. To further examine the effect of reduced GDF-3 levels on BMP signaling, I stimulated the embryonic stem cells with recombinant BMP4 protein.

I found that all of the cell lines showed dramatically increased BMP signaling, but that this activation was most pronounced in heterozygous or homozygous ES lines that had reduced levels of GDF-3 signaling (Figure 9). After normalization to total Smad1 levels, quantification demonstrated that ES lines with reduced GDF-3 levels had 1.7 +/- 0.3 times Smad1 phosphorylation, compared with an average of three wild-type lines. There was no difference

between heterozygous and homozygous genetrap ES lines in activation of Smad1. There was an average increase in Smad2 phosphorylation in heterozygous and homozygous genetrap ES lines of 1.5 +/- 0.4 times, compared with the average of three wild-type lines. These results confirm that, in cells that normally express GDF-3, this factor is required for normal regulation of the BMP pathway, but does not play a role in activating the TGF-β/Activin/Nodal-like signaling.

Figure 9

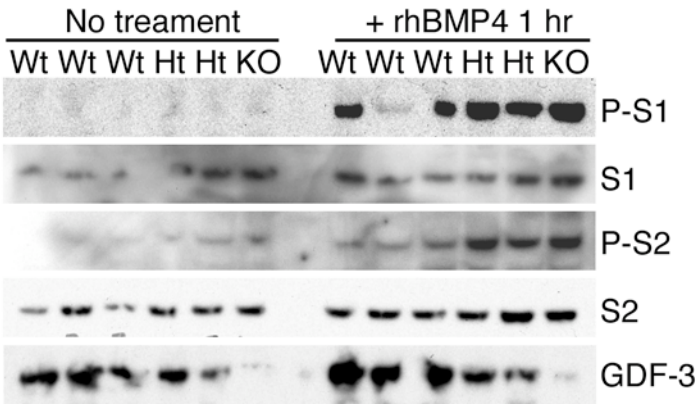

Figure 9: GDF-3 is an endogenous BMP inhibitor. Mouse embryonic stem cells that were wild-type (Wt), heterozygous (Ht), or homozygous (KO) for a genetrap insertional mutation in the GDF-3 locus were analyzed for activation status of Smad signaling. Cells were untreated (left) or treated with rhBMP4 for one hour (right). Phosphorylation at the MH2 site of Smads1/5/8 or Smad2/3 (P-S1 or P-S2) was used to assess activation of BMP signaling or Nodal signaling, respectively. Total Smad1 (S1) and Smad2 (S2) are shown as controls. Total levels of GDF-3 protein (full length prepro form) are shown.

2.6 - GDF-3 inhibitory properties reside in both the prepro form and the 'missing cysteine'

GDF-3 protein contains two elements that distinguish it from most TGF-β family members: it is missing the fourth canonical cysteine and it is poorly processed and, as such, is mainly in the prepro form in cells that express it endogenously (embryonic stem cells) or exogenously (frog embryos). I therefore sought to determine whether either of these characteristics endow GDF-3 with its unusual activity of inhibiting its own family members. I created two mutations in GDF-3 to pursue these experiments. The first mutation converts the cleavage recognition sequence of GDF-3, RKRR, into the sequence GNVG. This cleavage mutation (CM) prevents the cleavage maturation of GDF-3 so that the protein only exists in the prepro form. The second mutation replaces the 'missing' cysteine in GDF-3 by converting the valine at this residue to a cysteine (VtoC mutation).

As a preliminary test of the function of these constructs, I injected them into frog embryos and analyzed their ability to inhibit co-injected BMPs by luciferase assay. As shown in Figure 10, the cleavage mutant of GDF-3 retains the full ability to inhibit BMP signaling. To determine whether this activity requires the mature domain at all, I also tested the prepro domain of GDF-3 alone for its ability to inhibit BMP-induction of the luciferase reporter and found that the prepro domain is a weak BMP inhibitor.

Figure 10: Effect of GDF-3 mutations on BMP inhibitory activity. Luciferase activity (in arbitrary units) from a luciferase construct regulated by a BMP responsive element (BRE-Lux) was measured on whole embryos lysed at stage 10.5 after being injected at the two cell stage. Embryos were injected with reporter alone (first column), BMP4 RNA (green column, first lane of western blot), or BMP4 RNA together with RNA for GDF-3 constructs. The following constructs were tested: wild-type (Wt), cleavage mutant (CM), prepro domain alone (prepro), 'missing cysteine' reverted (VtoC), and a double mutant of VtoC and CM (VtoC/CM). Below the luciferase graph, a western blot of each lane is indicated showing prepro and mature forms of GDF-3.

Figure 10

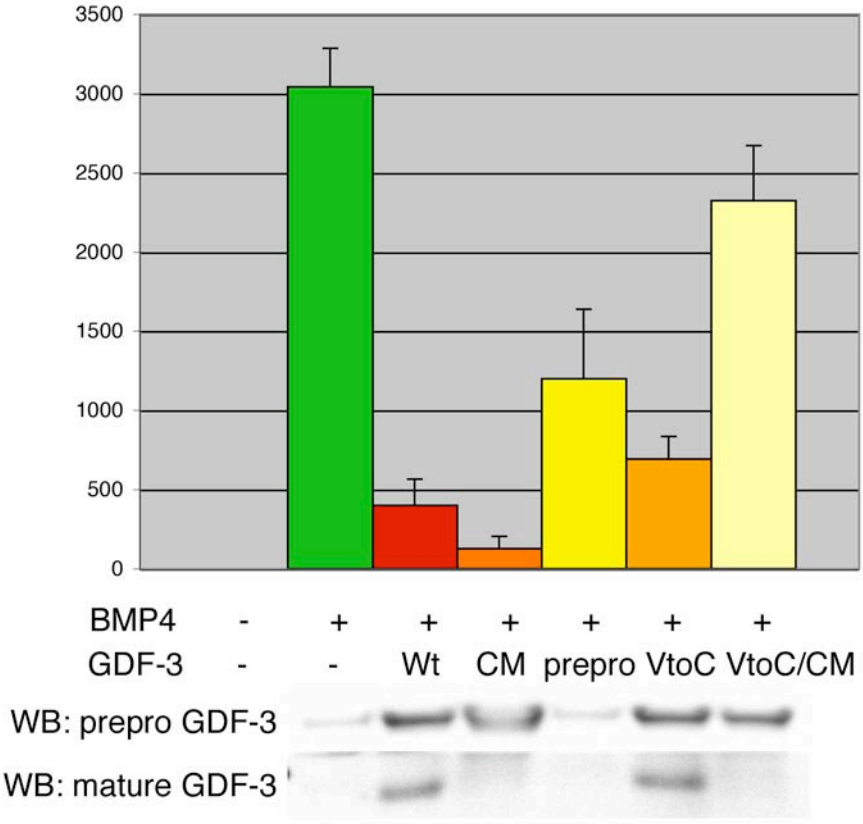
3500
3000
2500
2000
1500
1000
500
0
BMP4 - + + + + + +
GDF-3 - - Wt CM prepro VtoC VtoC/CM
WB: prepro GDF-3
WB: mature GDF-3

I also tested the activity of the VtoC mutant GDF-3 and observed that this mutant is also a weak BMP inhibitor. To test whether other aspects of the GDF-3 protein have inhibitory activity, I created a double mutant with both a mutated cleavage site and the VtoC substitution. This form of GDF-3 was only able to slightly reduce BMP-induced transcription, indicating that both of the unusual features of the GDF-3 protein (its predominant prepro form and missing cysteine) provide redundant mechanisms for blocking BMPs and account for most of the inhibitory behavior of GDF-3 (Figure 10).

2.7 - GDF-3 protein interacts physically with BMP proteins

To determine whether GDF-3 inhibition of BMPs may be direct, I performed reciprocal co-immunoprecipitation assays and found that GDF-3 and BMP4 protein interact. HA-tagged BMP4 (or untagged BMP4) and Flag-tagged GDF-3 were injected into the animal pole of frog embryos at the 2 to 4 cell stage, and embryos were cultured to gastrula stages. The animal caps were lysed and immunoprecipitated using anti-HA or anti-Flag. Flag-GDF-3 immunoprecipitates prepro and mature BMP4 (60 kDa and 25 kDa) and HA-BMP4 immunoprecipitates the prepro (45 kDa) and mature (20 kDa) forms of GDF-3 (Figure 11A).

I also tested whether GDF-3 interacts with other TGF-β members to determine whether the interaction between GDF-3 and BMP4 is specific or reflective of promiscuous binding by GDF-3. I found that GDF-3

immunoprecipitates xVg1 and xNR1 but not Activin upon over-expression in Xenopus animal caps (Figure 11B). Interestingly, although the prepro form is the major form produced in cells and immunoprecipitated in these assays, the interactions do not rely on the prepro domain. I tested this by using GDF-3 to immunoprecipitate BMP4 containing the BMP4 pro-domain or the Activin pro-domain and found that GDF-3 immunoprecipitates both forms (data not shown) whereas it does not interact with Activin.

I sought to determine whether GDF-3 can interact with BMPs extracellularly, providing a mechanism for its inhibition. I used COS cells that stably express either EYFP or GDF-3-Flag and transfected with EYFP or with mBMP4-HA. I performed immunoprecipitations on conditioned media or cell lysate from cells that co-expressed GDF-3-Flag and BMP4-HA as a positive control for interaction and compared these to immunoprecipitations performed on combined conditioned media or cell lysate from cells expressing either GDF-3 or BMP4. I found that GDF-3 and BMP4 interact whether they are co-secreted from the same cells, or expressed separately, confirming that this interaction could take place extracellularly (Figure 11C).

In this experiment, I also tested whether co-expression of GDF-3 and BMP4 altered the levels of production or secretion of either ligand but found no difference between BMP4 production or secretion when BMP4 was expressed alone or together with GDF-3, suggesting that GDF-3 does not inhibit BMPs in the producing cell (Figure 11C).

Figure 11: GDF-3 protein interacts physically with BMP4 protein. (A) Reciprocal co-immunoprecipitation of Flag-tagged GDF-3 and HA-tagged BMP4 protein produced by over-expression at the two cell stage of frog embryos, followed by lysis and precipitation at stage 11. The top two panels show western blot (WB) for 10% of the crude lysate for BMP4 and GDF-3. The third panel shows the result of the immunoprecipitation with GDF-3, probed for BMP4, and the fourth panel shows the immunoprecipitation of BMP4, probed for GDF-3. (B) GDF-3 was immunoprecipitated by BMP4-HA but not Activin-HA in an assay similar to that in 'A' followed by western blot for prepro and mature GDF-3. (C) Immunoprecipitation of GDF-3 and BMP4 in solution. GDF-3 and BMP4-HA were produced in COS cells and the conditioned media (CM) from these cells was immunoprecipitated with anti-HA antibodies and probes for GDF-3. In lanes 1 and 4, GDF-3 was produced alone in COS cells, in lane 2 BMP4 was produced alone, in 3 and 5, GDF-3 and BMP4 were co-expressed in the same cells, in lane 6 conditioned media from COS expressing either GDF-3 or BMP4 alone was mixed before immunoprecipitation. 10% of crude CM is shown in lanes 1-3, probed by western blot for prepro GDF-3 together with prepro and mature BMP4; immunoprecipitation is shown in lanes 4-6, probed by western blot for prepro and mature GDF-3.

Figure 11

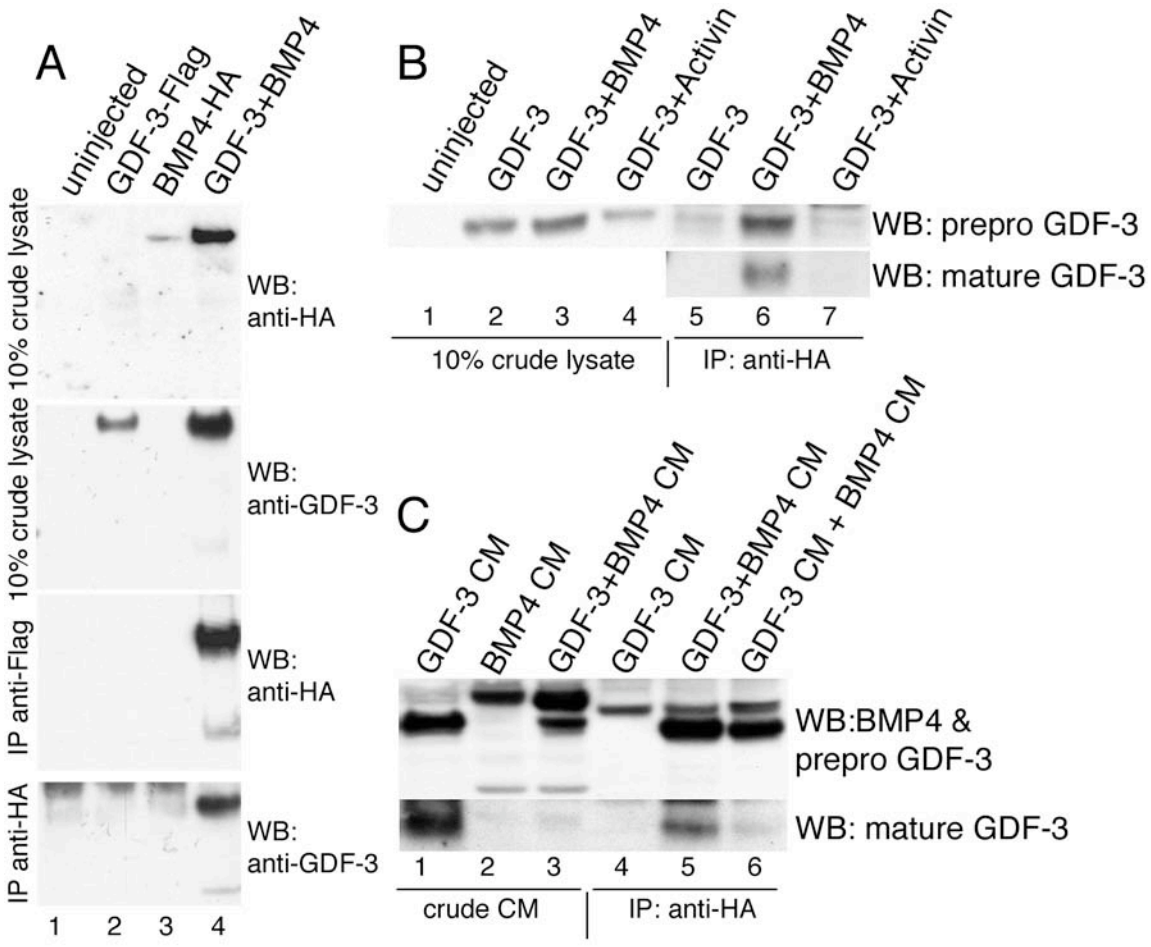
A
uninjected
GDF-3-Flag
BMP4-HA
GDF-3+BMP4
10% crude lysate
WB: anti-HA
10% crude lysate
WB: anti-GDF-3
IP anti-Flag
WB: anti-HA
IP anti-HA
WB: anti-GDF-3
1 2 3 4
B
uninjected
GDF-3
GDF-3+BMP4
GDF-3+Activin
GDF-3
GDF-3+BMP4
GDF-3+Activin
WB: prepro GDF-3
WB: mature GDF-3
1 2 3 4 5 6 7
10% crude lysate
IP: anti-HA
C
GDF-3 CM
BMP4 CM
GDF-3+BMP4 CM
GDF-3 CM
GDF-3+BMP4 CM
GDF-3 CM + BMP4 CM
WB:BMP4 & prepro GDF-3
WB: mature GDF-3
1 2 3 4 5 6
crude CM
IP: anti-HA

2.8 Chapter Summary

These experiments provide a foundation for understanding the mechanism of GDF-3 activity. I used gain-of-function analysis of GDF-3 mRNA in the frog embryo to reveal that GDF-3 is a BMP inhibitor and as such, can act as a direct neural inducer within the frog ectoderm. These results were confirmed using GDF-3 recombinant protein, which can neuralize individual dispersed cells of the animal cap. Reduction of GDF-3 protein levels in the endogenous context of embryonic stem cells further demonstrates that GDF-3 is a physiological BMP inhibitor, as enhanced activation of the BMP pathway is observed. To provide a possible biochemical explanation for GDF-3 activity, I performed immunoprecipitation binding assays and found that GDF-3 protein binds to BMP proteins, both in cells and in solution.

2.9 Chapter analysis

These findings identify GDF-3 as an inhibitory TGF-β superfamily ligand, together with BMP15, GDF9, BMP3, Xnr3 (a Nodal-related frog-specific ligand), and the divergent ligands LeftyA and LeftyB (Levine and Brivanlou, 2006a; Tabibzadeh and Hemmati-Brivanlou, 2006). Of these ligands, BMP15, GDF9, LeftyA, and LeftyB are also missing the fourth canonical cysteine. In addition, Xnr3 has a 'shifted' fourth cysteine that is a few amino acids earlier than in the canonical location. BMP3 has the normal complement of cysteines.

The mechanism of inhibition for most of these ligands has not been determined. However, it is very interesting to consider the role of the 'missing'

cysteine. As this cysteine is involved in intermolecular interactions (Groppe et al., 2002), and I have shown that GDF-3 protein interacts physically with BMP proteins, it is possible that GDF-3 forms a heterodimer with BMP proteins that has an atypical structure that inhibits the ability of BMP ligands to signal. However, several of my findings suggest that this model cannot explain fully the inhibitory activity of GDF-3. First, heterodimers are formed between the prepro forms of ligands before secretion from the cell of origin but I found that GDF-3 mature protein can inhibit BMP signaling when presented in solution with mature BMP proteins. Second, I found that introducing the 'missing' cysteine into the GDF-3 mature domain did not eliminate the ability of GDF-3 to inhibit BMP signaling. I did not determine whether endogenous GDF-3 mature protein is present as a monomer or dimer, but the recombinant GDF-3 protein that I used is described by the company (Peprotech) as being a dimer.

To determine which other features of the GDF-3 protein account for its inhibitory function, I also considered the prepro domain because cleavage mutants of other TGF-β ligands (particularly Nodal-related ligands) have been shown to act as BMP inhibitors (Eimon and Harland, 2002; Haramoto et al., 2004; Yeo and Whitman, 2001) and GDF-3 is present endogenously mainly in the prepro form. I found that both the cleavage mutant and the prepro domain of GDF-3 can inhibit BMP signaling. Interestingly, a double mutant of the 'missing' cysteine and the cleavage site lost most ability to block BMPs. Therefore, the ability of GDF-3 to inhibit BMP signaling resides redundantly in the prepro region

of the protein and in the mature domain that is ‘missing’ the fourth cysteine. This accounts for the inhibitory properties of GDF-3 and may inform the mechanisms of other inhibitory ligands.

CHAPTER 3: GDF-3 IN STEM CELLS

In the previous section, I established that GDF-3 is a BMP inhibitor. I next sought to characterize the outcome of this activity in the endogenous contexts of GDF-3 expression. My initial interest in GDF-3 began with the observation that its expression is tightly correlated with stemness in both human and mouse embryonic stem cells (Sato et al., 2003). I therefore returned to stem cells to study GDF-3 function through gain-of-function in human embryonic stem cells and reduction-of-function in mouse embryonic stem cells.

3.1 - GDF-3 expression is associated with pluripotency in mammlian cells

To confirm the micro-array findings that GDF-3 expression is associated with the undifferentiated state of embryonic stem cells (Sato et al., 2003), I performed RT-PCR to examine GDF-3 mRNA levels in both human and mouse embryonic stem cells. I cultured H1 human embryonic stem cells and 129Ola mouse embryonic stem cells either in conditioned media (CM) or LIF, respectively (that maintain their undifferentiated states) or in the absence of these factors to allow differentiation. I found that GDF-3 is present in the human embryonic stem cells grown in CM and the mouse embryonic stem cells grown in LIF, and it was significantly reduced when these embryonic stem cells were allowed to differentiate, together with the decreased expression of other stem cell markers (Figure 12).

Figure 12

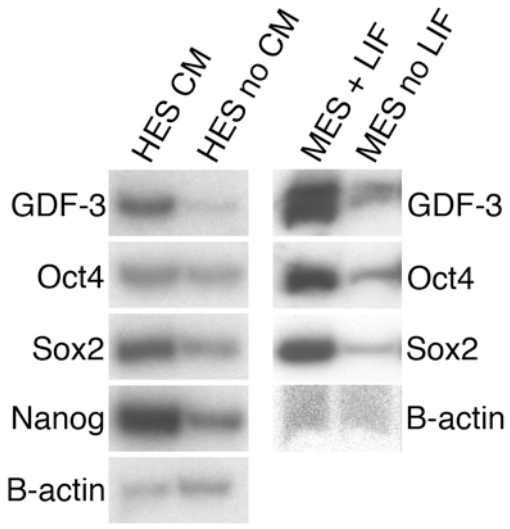

Figure 12: GDF-3 expression is associated with stemness in human and mouse embryonic stem cells. Human BGN1 embryonic stem cells (HES) and mouse CJ7 mouse embryonic stem cells (MES) were cultured in the presence of MEF-conditioned medium (CM) or leukemia inhibitory factor (LIF) to maintain stemness (lanes 1 and 3, respectively), or these treatments were removed to allow differentiation for four (HES) or three days (MES) (lanes 2 and 4). GDF-3, Oct4, Sox2, and Nanog are markers of stemness; β-actin is shown as a loading control.

3.2 – GDF-3 is a BMP inhibitor in pluripotent mammalian cells

In my analysis of GDF-3 activity in embryonic stem cells, I next sought to confirm its role as a BMP inhibitor in this context. My results in Chapter 2.4 of this thesis demonstrated that GDF-3 is an endogenous BMP inhibitor in mouse embryonic stem cells. To determine whether GDF-3 over-expression could suppress exogenous BMP signals in a pluripotent mammalian context, I performed experiments in P19 cells into which I transfected mGDF-3 with or without mBMP4. In order to generate a robust BMP signal this system was complemented by co-transfection of downstream signaling components: Smads 1, Smad 4, and OAZ (Hata et al., 2000). Figure 13 shows that in P19 cells, mGDF-3 reduced BMP4 signaling. This evidence confirms that GDF-3 is an inhibitory member of the BMP-GDF subfamily of TGF-βs.

Figure 13

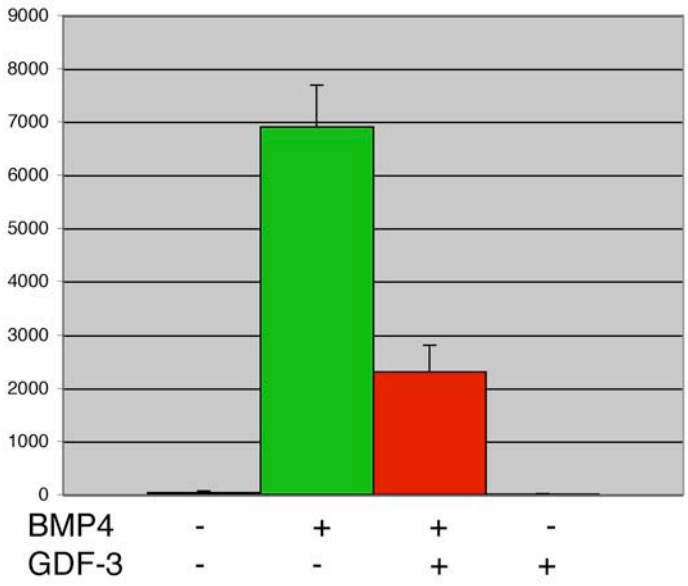

Figure 13: GDF-3 inhibits BMP4 signaling in P19 mouse teratoma cells. Luciferase activity (in arbitrary units) was analyzed using a BMP responsive element driving a luciferase reporter (BRE-Lux) in P19 cells expressing BMP4 alone (column 2), BMP4 together with GDF-3 (column 3), or GDF-3 alone (column 4). All P19 cells were transfected with BRE-Lux, together with BMP signaling components Smad1, Smad4, and OAZ.

3.3 - GDF-3 partially maintains pluripotent cell types in human embryonic stem cells

It has previously been shown that exogenous BMP signaling from classic BMPs promotes extra-embryonic cell fate differentiation in human embryonic stem cells (Xu et al., 2002). To determine whether, as a BMP inhibitor, GDF-3 can oppose these functions, I transiently transfected BGN1 or RUES1 human embryonic stem cells with GDF-3 plasmids and cultured these cells in CM that maintains the undifferentiated state or in the absence of CM, allowing heterogeneous differentiation, and I cultured them in the presence or absence of BMP4 protein. Figure 14A shows that GDF-3 transfected BGN1 human embryonic stem cells maintained significant levels of the pluripotency markers Oct3/4 and Nanog in conditions that normally promote differentiation. In RUES1 human embryonic stem cells, I found that GDF-3 over-expression resulted in limited maintenance of pluritpotency markers upon differentiation, but only upon the combined treatment of BMP4 protein and the absence of conditioned medium (Figure 14B). It is unclear what accounts for differences in the strength of GDF-3 activity between human embryonic stem cells lines, but it is possible that variable levels of endogenous GDF-3, or different transfection efficiencies account for these observations.

Figure 14: GDF-3 supports stemness markers in human embryonic stem cells and reduces extra-embryonic differentiation. (A,B) BGN1 (A) or RUES1 (B) human embryonic stem cells were transiently transfected with empty vector (V) or with a vector containing GDF-3 (G). Beginning 24 hours after transfection, cells were treated for four days with conditioned medium (CM), non-conditioned medium (no CM), conditioned medium containing 10 ng/mL recombinant human BMP4 protein (CM + BMP4), or non-conditioned medium with BMP4 (no CM + BMP4). Cells were then lysed and proteins were analysed by western blot for Oct4, Sox2, and Nanog (stem cell markers) and for cyclophilin B or tubulin (loading controls). (C) RUES1 HES were cultured for four days in the presence or absence of recombinant human GDF-3 protein (1 ug/mL) in CM, no CM, or CM containing rhBMP4 (10 ng/mL). Cells were harvested for RNA and real-time PCR was performed to analyze expression of the trophoblast marker cdx2, normalized to levels of a housekeeping gene, tbp1.

Figure 14

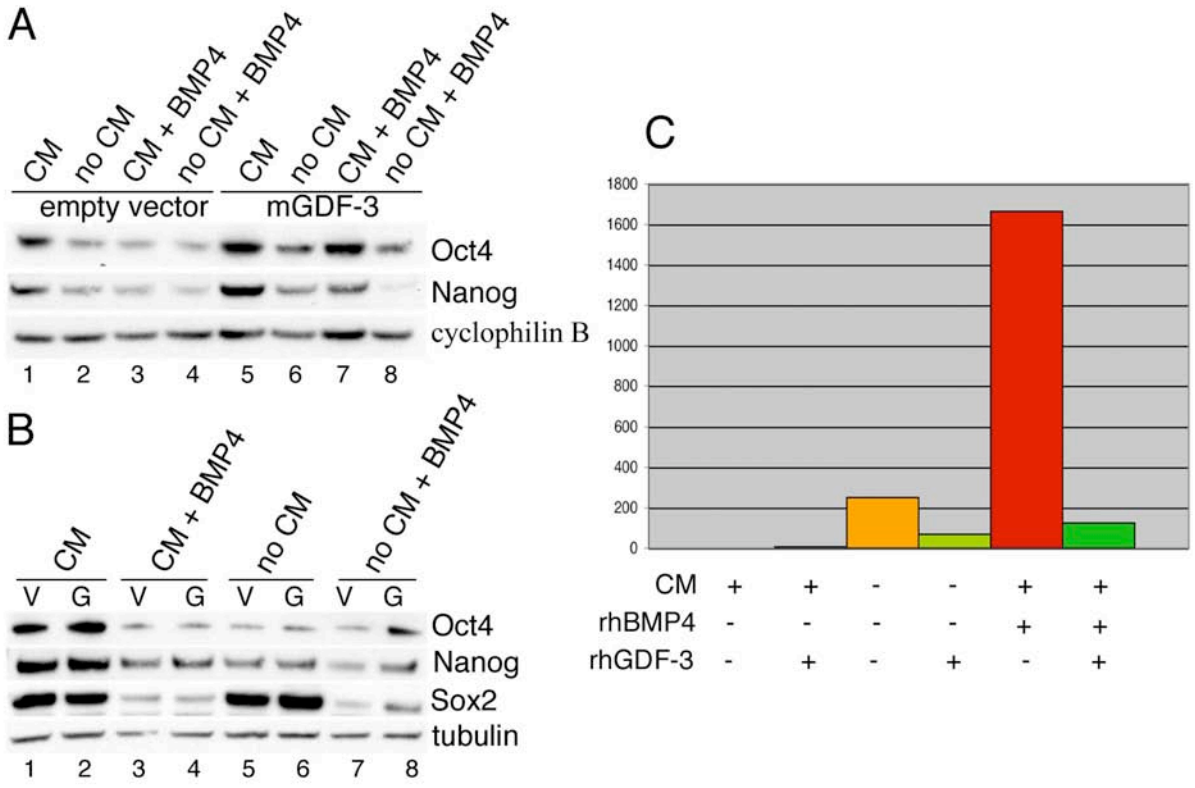
A
CM
no CM
CM + BMP4
no CM + BMP4
CM
no CM
CM + BMP4
no CM + BMP4
empty vector
mGDF-3
Oct4
Nanog
cyclophilin B
1 2 3 4 5 6 7 8
B
CM
CM + BMP4
no CM
no CM + BMP4
V G V G V G V G
Oct4
Nanog
Sox2
tubulin
1 2 3 4 5 6 7 8
C
1800
1600
1400
1200
1000
800
600
400
200
0
CM + + - - + +
rhBMP4 - - - - + +
rhGDF-3 - + - + - +

I next tested whether GDF-3 had the complementary ability to inhibit BMP-induced differentiation to extra-embryonic trophoblast. I cultured RUES1 cells in conditioned media, non-conditioned media, or conditioned media with BMP4 protein in the presence or absence of recombinant human GDF-3 protein (rhGDF-3). GDF-3 significantly reduced the expression of cdx2, a marker of trophoblast, either during heterogenous or directed trophoblast differentiation (Figure 14C). This demonstrates that GDF-3 contributed to the maintenance of pluripotent gene expression and the inhibition of differentiated extra-embryonic gene expression in human embryonic stem cells.

3.4 - GDF-3 activity is required for the full spectrum of in vitro differentiation of mouse embryonic stem cells grown without LIF

In contrast to the differentiative effect of BMP signaling in human embryonic stem cells, it has been shown that moderate levels of BMP signaling synergize with LIF to support the pluripotent state in mouse embryonic stem cells while high levels of BMP activation, as those obtained with a constituitively active BMP receptor, promote differentiation (Ying et al., 2003).

To study the required functions of GDF-3 in mouse ES, I obtained a genetrap embryonic stem cell line (Sanger Insitute line AD0857), in which the β-geo (a β-gal/neomycin resistance fusion) insertion is located in the single intron of the GDF-3 gene and creates a splice-fusion product with exon 1 (Figure 15A). Exon 1 of GDF-3 contains approximately one third of the prepro domain and has

no function upon over-expression in frog embryos (data not shown). Therefore, I predicted that this allele could produce a reduction-of-function for GDF-3. I characterized the phenotype of the heterozygous genetrap ES through expression and functional analysis. I first confirmed that these ES had significantly reduced levels of GDF-3 protein (Figure 15B).

Then, I examined the phenotypic effects of reduced GDF-3 levels. I cultured the heterozygous genetrap ES in the presence and absence of LIF. When cultured in the presence of LIF, wild-type mouse ES cells can be maintained in the undifferentiated state but in the absence of LIF, these cells differentiated to a flattened morphology after four days of culture. In contrast, genetrap cells maintained a normal, undifferentiated morphology even in the absence of LIF (Figure 15C). I analyzed these cells with molecular markers to determine what cell fates were formed and found that, in the absence of LIF, wild-type cells expressed high levels of brachyury, a mesoderm marker, and low levels of Oct3/4 and Sox2, markers of the undifferentiated state, and of FGF5, a marker of pluripotent epiblast; genetrap cells had reduced levels of brachyury and maintained significant levels of Oct3/4, Sox2, and FGF5 (Figure 15D). These findings suggest that the reduced level of GDF-3 protein precludes normal differentiation.

Figure 15: Reduction of GDF-3 in mouse embryonic stem cells (MES) blocks normal differentiation. (A) The genetrap allele AD0857. The β-geo insertion (β-gal/neomycin fusion protein; blue) is in the single intron of the GDF-3 gene. The prepro domain (red) of GDF-3 protein is on exon 1 and 2. The mature domain of GDF-3 protein (green) is entirely within exon2. Normal splicing of the endogenous locus produces GDF-3 mRNA. Splicing of the genetrap (GT) locus produces AD0857 mRNA containing a fragment of the prepro coding sequence and the β-geo insertion. (B) Western blot of WT MES and GT MES showing GDF-3 prepro and mature forms. Tubulin is a loading control. (C) Morphology of WT and GT ES after four days of culture in the with or without LIF (x10). (D) RT-PCR of WT and GT ES after four days of culture in the presence or absence of LIF. The following markers were used: FGF5 (pluripotent epiblast), BU (mesoderm), Sox2 (stem/epiblast/neural precursor) and Oct3/4 (stem/epiblast), β-actin (loading control). (E) The percent of hanging drops containing cells of each condition (WT and GT with and without LIF) that formed embryoid bodies. (F) Day 2 embryoid bodies for WT cells cultured in the presence of LIF, and GT cells cultured in the presence or absence of LIF (x10 magnification). Scale bar is 200 μm. (G) RT-PCR of markers for early embryonic cell fates on day 8 suspension culture embryoid bodies. The following markers were used: Oct4 ,FGF5, Sox2, Pax6 (neural), Rax (anterior neural), Nkx2.5 (cardiac mesoderm), Flk-1 (endothelial mesoderm), scl-1 (blood), AFP (endoderm), β-actin (loading control). No RT cotrol is shown for β-actin.

Figure 15

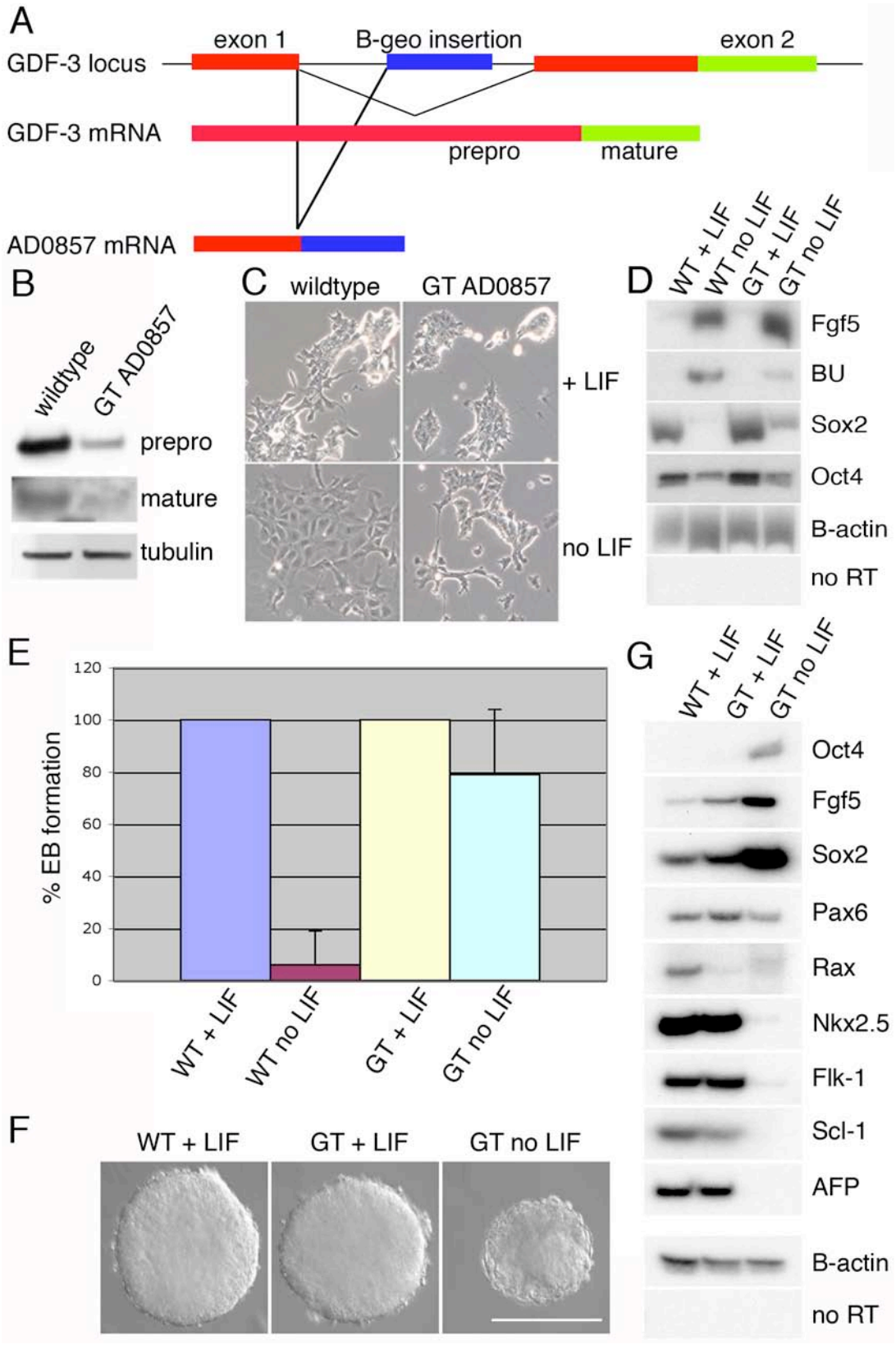
A
exon 1
B-geo insertion
exon 2
GDF-3 locus
GDF-3 mRNA
prepro
mature
AD0857 mRNA
B
wildtype
GT AD0857
prepro
mature
tubulin
C
wildtype
GT AD0857
+ LIF
no LIF
D
WT + LIF
WT no LIF
GT + LIF
GT no LIF
Fgf5
BU
Sox2
Oct4
B-actin
no RT
E
% EB formation
120
100
80
60
40
20
0
WT + LIF
WT no LIF
GT + LIF
GT no LIF
F
WT + LIF
GT + LIF
GT no LIF
G
WT + LIF
GT + LIF
GT no LIF
Oct4
Fgf5
Sox2
Pax6
Rax
Nkx2.5
Flk-1
Scl-1
AFP
B-actin
no RT

I tested the ability of the heterozygous genetrap cells to remain functionally pluripotent even in the absence of LIF by assaying for the formation of embryoid bodies (EBs). Upon culture in hanging drops, undifferentiated embryonic stem cells form aggregates, called EBs, that differentiate into many types of embryonic tissue. Wild-type and genetrap cells grown in the presence of LIF formed EBs in 100% of the hanging drops (+/- 0%). While wild-type cells grown in the absence of LIF rarely formed EBs (6% +/- 13%), genetrap cells without LIF formed EBs in 79% (+/-25%) of the hanging drops (Figure 15E). However, these 'EBs' were much smaller and less compact than EBs produced by cells grown in LIF (Figure 15F).

I examined the EBs on day 8 of suspension culture by RT-PCR to determine whether a reduction of GDF-3 levels alters cell fate outcomes in differentiated mouse embryonic stem cells. I studied mRNA levels of stem/primitive markers (Oct4, Fgf5, Sox2), neural markers (Sox2, Pax6, Rax), mesodermal markers (Nkx2.5, Flk-1, Scl-1), and endodermal markers (AFP, HNF-3β (data not shown); (Figure 15G). While wild-type or genetrap cells grown in the presence of LIF can give rise to a full profile of differentiated cells types, AD0857 cells grown in the absence of LIF retain a primitive phenotype with limited neural differentiation. However, these cells do not form mesoderm or endoderm, suggesting that the spheres formed are not true 'embryoid bodies.' This evidence establishes that wild-type levels of GDF-3 activity are required for

normal in vitro differentiation of the three embryonic germ layers: the signature of pluripotency.

I next sought to determine whether reduction of GDF-3 levels also precludes normal differentiation in vivo by injecting stable-GFP expressing wild-type or heterozygous genetrap ES cells cultured in the presence or absence of LIF into mouse blastocysts and assessing tissue contribution at mid-gestation (e9.5). In this assay of ES cell potential, I found that neither wild-type nor genetrap ES cells cultured without LIF gave rise to any differentiated cells within the host embryo. Further, I did not observe any difference in tissue contribution between wild-type and genetrap ES cultured in the presence of LIF, as both differentiated normally (data not shown). These data suggest that the effects of reduced GDF-3 levels on ES cell potential are confined to in vitro differentiation, possibly due to the greater robustness of in vivo development.

3.5 Chapter Summary

These experiments reveal that GDF-3 has dual roles in the context of embryonic stem cells, both of which are consistent with its role as a BMP inhibitor. I found that, as in the frog embryo, GDF-3 in pluripotent mammalian cells inhibits BMP signaling. The outcome of this activity in human embryonic stem cells is that GDF-3 supports the undifferentiated state, partially maintaining the expression of stem cells markers in multiple differentiation contexts. Specifically, it plays a role in reducing differentiation to the extra-embryonic

trophoblast, a fate that is induced by classic BMP ligands. In mouse embryonic stem cells, I found that reduced levels of GDF-3 protein, produced through a genetrap allele, preclude normal differentiation. Instead, cells that are heterozygous for the genetrap allele show maintenance of stem cell/epiblast markers and the ability to form embryoid bodies, even after they have been cultured in the absence of LIF. Together, these data establish that GDF-3 regulates both of the key features of embryonic stem cells – the ability to maintain stemness and the ability to differentiate.

3.6 Chapter analysis

GDF-3 achieves these functions in a species-specific manner that is consistent with, and extends, previous reports of BMP function in stem cells (Xu et al., 2002; Ying et al., 2003). I present four possibilities to explain the species-specificity of BMP/GDF activity in stem cells.

First, it is possible that distinct signaling profiles regulate the early cell fate decisions of human and mouse embryos. This is consistent with observations that LIF is sufficient to maintain stemness in mouse mES, but not in human ES (Daheron et al., 2004; Reubinoff et al., 2000; Sato et al., 2004) and that Nodal signaling is required for stemness in human ES, but not in mouse ES (James et al., 2005).

A second possibility is that human and mouse ES cells possess different sensitivities to BMP signaling and that different levels of effective BMP signaling

in these cells produces their disparate phenotypes. According to this concept, the absence of BMP signaling could promote neural differentiation, very low levels could promote stemness, and higher levels of BMP signaling could promote differentiation to extra-embryonic or mesendoderm cell fates. It is known that BMPs can act as morphogens, creating distinct cell fates based on different concentrations of the ligand at a given time window (Wilson et al., 1997). This concept is further supported by the observation that moderate BMP activation in mouse embryonic stem cells, if presented together with LIF, promote stemness; however, strong activation of the BMP pathway promotes differentiation, even in the presence of LIF. Thus, it is probable that GDF-3 expression helps to establish a BMP activity gradient.

Third, it is possible that human and mouse embryonic stem cells correspond to distinct stages of in vivo development. If mouse embryonic stem cells represent a slightly later cell type than the inner cell mass of the blastocyst, like the early epiblast, the role of BMP signaling in these cells is supported by the observation that decreased BMP signaling (through the BMPR1A knockout) result in precocious differentiation, suggesting that BMPs help to maintain the pluripotency of early epiblast cells (Di-Gregorio et al., 2007). Fourth, it is possible that the distinct signaling status and effect of GDF-3 in human and mouse ES could be an artifact of different derivation and culture conditions.

GDF-3 is first expressed zygotically in the blastocyst, and is somewhat enriched in the inner cell mass, the region that will form the entire mouse

embryo and from which embryonic stem cells can be derived. GDF-3 is therefore one of the earliest BMP inhibitors expressed in the mammalian embryo. Recent studies profiling genome-wide expression in early mouse embryos describe expression of only one other possible BMP inhibitor, Lefty, in pre-implantation mouse development (in addition to GDF-3) (Hamatani et al., 2004; Wang et al., 2004).

The localization of GDF-3 at blastocyst stages is particularly interesting because it is known that BMP4 is expressed at this stage (Coucouvanis and Martin, 1999) but that BMP signaling is not active (James et al., 2005). If GDF-3 is the unique BMP inhibitor at this stage, it would play a critical role in the earliest cell fate decisions of the mammalian embryo, that is, whether a cell should be inner cell mass or trophoblast and within the inner cell mass, whether a cell should become future embryonic tissue, or primitive endoderm.

In agreement with this suggestion, BMP promotes primitive endoderm in the mouse embryo (Coucouvanis and Martin, 1999) and trophoblast in human embryonic stem cells (Xu et al., 2002). I found that GDF-3 blocked BMP-induced trophoblast differentiation of human embryonic stem cells and it has been shown that BMP inhibition is sufficient to maintain human embryonic stem cells in the undifferentiated state, together with FGF activation (Xu et al., 2005). These findings demonstrate the importance of an inhibitory signal (rather than an activating, instructive signal) in establishing the inner cell mass/stemness fate and highlight the potential roles of ‘negative’ information.

CHAPTER 4: THE ROLE OF GDF-3 IN MOUSE EMBRYOGENESIS

The previous sections established the mechanism of GDF-3 function and its activity in embryonic stem cells. I next extended this analysis to determine other developmentally-relevant contexts for GDF-3 and to study its function in these settings through a reduction of GDF-3 protein levels in the mouse embryo.

4.1 - Expression of GDF-3 during early mouse embryogenesis

I first analyzed the expression of GDF-3 during early mouse embryogenesis to gain an understanding of what role it may play in development. Previously, GDF-3 was found to be expressed in e12.5-e15.5 embryos in bone (Jones et al., 1992b), so I focused my studies on early embryonic expression. Temporal analysis of GDF-3 expression by RT-PCR revealed that GDF-3 expression was present at blastocyst and gastrula stages and up-regulated at e8.5 (Figure 16A). Using in situ hybridization to study GDF-3 mRNA expression spatially, I found that GDF-3 is expressed within the inner cell mass of the blastocyst embryo; however, expression was weak and I cannot rule out lower levels of GDF-3 transcripts in the surrounding trophoblast cells (data not shown). Therefore, I performed immunofluorescence to localize GDF-3

protein. I found that GDF-3 protein is expressed throughout the blastocyst embryo and is either membrane-associated or extracellular (Figure 16B).

Figure 16: Expression of GDF-3 in early mouse development. (A) RT-PCR showing GDF-3 mRNA expression during pre-implantation (2-4 cell through blastocyst) through mid-gestation development (e6.5-e10.5). HPRT is shown as a loading control, no RT is a negative control for genomic DNA. (B) Immunofluorescence for GDF-3 protein (red) in a mouse blastocyst. Nuclei are visualized with Sytox green. The bottom panel shows a control with no primary anti-GDF-3 antibody. Scale bar is 50 μm.

Figure 16

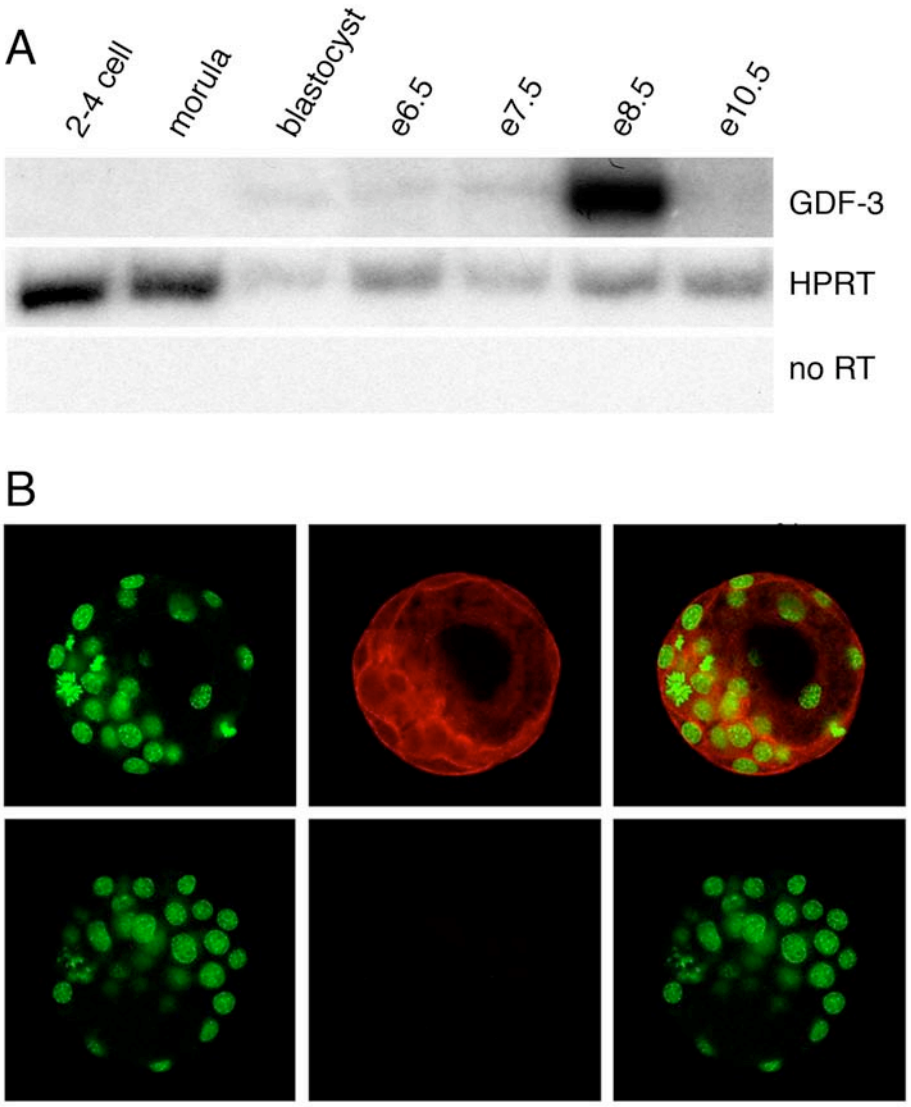

Subsequently, GDF-3 mRNA is confined to the node and the tissue immediately anterior to the node during gastrulation (Figure 17A,B). Shortly after gastrulation, GDF-3 mRNA is expressed in the forming cranial neural crest and in the ventral neural tube and notochord (Figure 17E,F).

Figure 17: Expression of GDF-3 mRNA in early post-gastrulation mouse embryos. In situ hybridization for GDF-3 mRNA is shown at e7.5 (A), e8.0 (B), and e8.5 (C,D). A 10 μm frozen section after whole mount in situ hybridization is shown in (D). (A) Lateral view, anterior is to the right, (B) posterior view, (C) dorsal view. Scale bar is 200 μm.

Figure 17

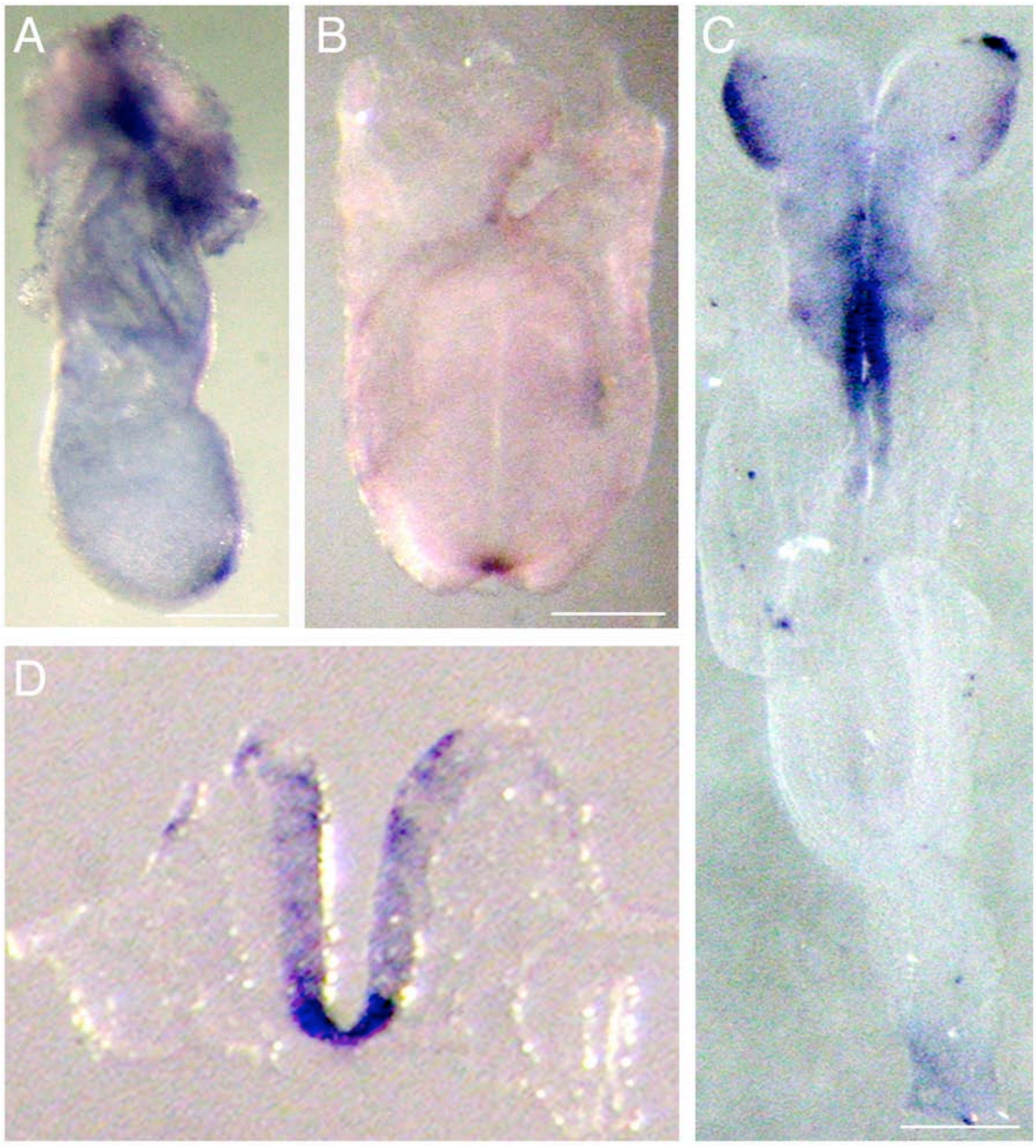

I next extended my characterization of GDF-3 expression from e7.75 through e8.5 embryos by analyzing the expression of the LacZ transgene inserted as a genetrap (see Chapter 3.4). I found LacZ protein only in the late node and notochord of embryos at these stages. This is distinct from the pattern of GDF-3 mRNA detected by in situ hybridization, which also includes staining in the prospective neural crest, and rostral ventral spinal cord. I considered that possibly this discrepancy reflects a lag in translation, such that GDF-3 locus mRNA produced at e8.0 in the node results in LacZ translation at e8.5 in node-derived structures, but not yet in structures that are newly expressing GDF-3 locus mRNA. However, I detected no LacZ protein in the e9.5 embryo, making this possibility unlikely. Alternatively, it is possible that the hybrid mRNA for intron 1 of GDF-3 and the LacZ coding sequence is either regulated post-transcriptionally in a tissue-specific manner, or that the hybrid protein is produced, secreted, and the LacZ staining that I observed represents the target tissue of GDF-3 secretion.

Figure 18

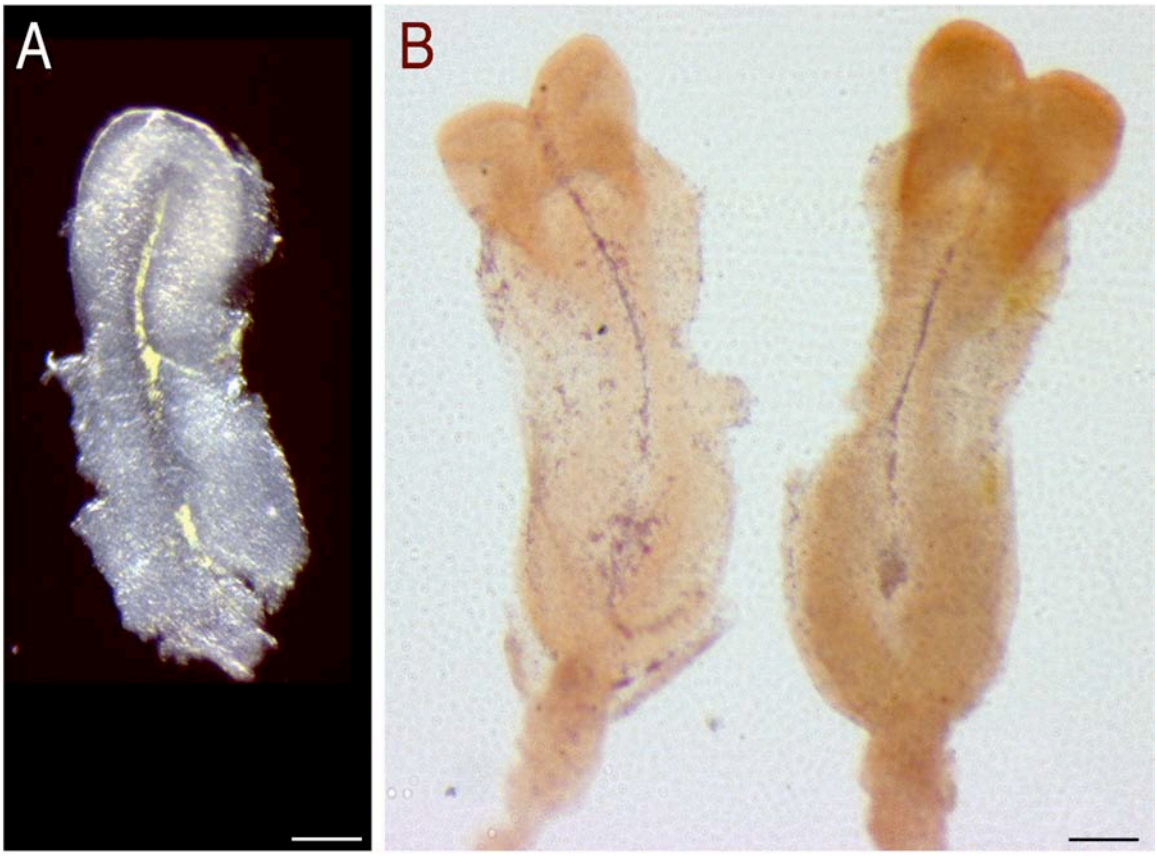

Figure 18: Expression of GDF-3 locus LacZ in early post-gastrulation mouse embryos. Red-GAL staining of embryos that are heterozygous for the LacZ genetrap insertion at e8.0 (A, yellow) and e8.5 (B, maroon). Embryos are shown in dorsal views. Scale bar is 200 μm.

To begin to study the role of GDF-3 in adult stem cells, I performed in situ hybrdization on adult testis and found that GDF-3 is surprisingly expressed specifically in the most differentiated cell types such as spermatids (Figure 19A). Using immunofluorescence, I found that GDF-3 protein is also present in the spermatids (Figure 19C-E), specifically localizing to the acrosome of the sperm (Figure 19F,G), as determined by co-localization with peanut agglutinin (G).

Figure 19: Expression of GDF-3 during male gametogenesis. (A) In situ hybridization shows GDF-3 expression in the mature spermatids in the testis. (B) A sense probe control for GDF-3 expression. (C,E) Immunofluorescence for GDF-3 showed protein expression in the mature spermatids. (D) Negative control for immunofluorescence performed by pre-absorbing anti-GDF-3 primary antibody with 10X recombinant GDF-3 protein. (F,G) Individual mouse sperm stained for GDF-3 protein (red) and the nucleus (F, green) or the acrosome (G, green). (A-E) were performed on 10 μm frozen sections of testis. (A-D) 10X magnification, (E) 40X magnification, scale bar is 200 μm. (F,G) 63X magnification, scale bar is 5 μm.

Figure 19

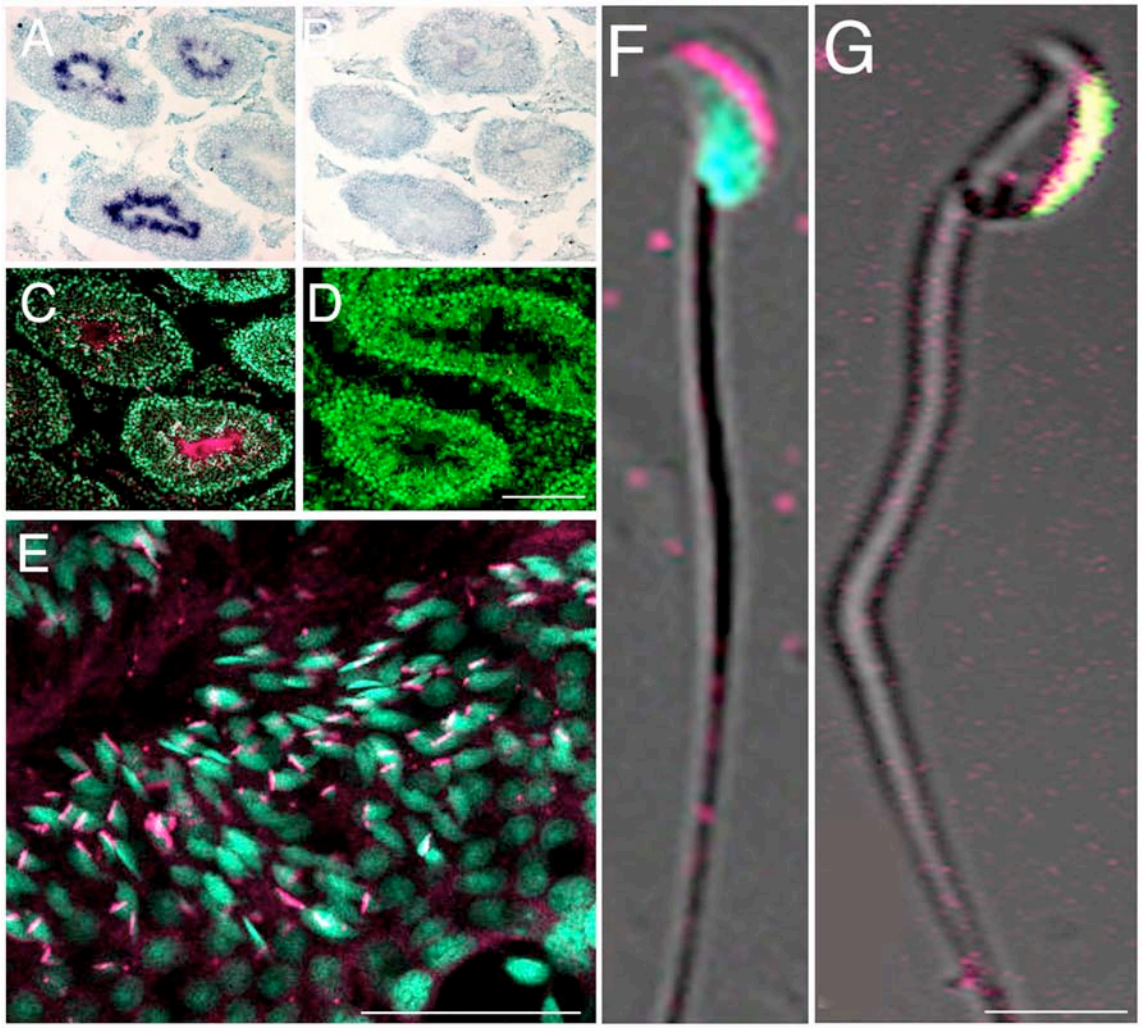

5.2 - Reduction-of-Function Analysis of GDF-3

To study the required roles for GDF-3 during mouse embryogenesis, I examined the effects of a genetrap allele that interrupts the GDF-3 genomic locus (described in Chapter 3.4). We also pursued creation of a conditional knockout for GDF-3, but this work could not be addressed within the time limitations of the thesis, and was not characterized.

Heterozygous genetrap embryonic stem cells (from Sanger Institute) were injected into host blastocysts to create chimeras, that were then used to propagate a genetrap (GT) line of mice. I tested the efficiency of loss of GDF-3 protein by deriving embryonic stem cells from blastocysts that were wild-type, heterozygous, or homozygous for the genetrap allele and found reduced GDF-3 protein in the heterozygous line and very low levels of GDF-3 protein in the homozygous genetrap line (Figure 20).

Figure 20

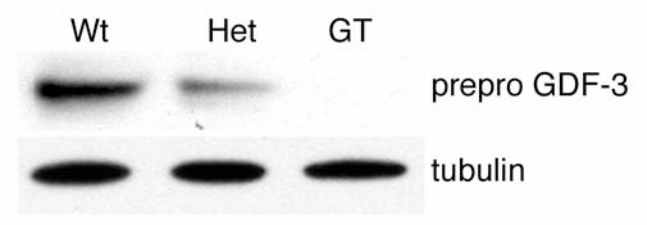

Figure 20: Genetrap AD0857 of the GDF-3 mouse genomic locus results in loss of GDF-3 protein. Western blot of full length (prepro) GDF-3 protein in wild-type (Wt), heterozygous (Het), and homozygous genetrap (GT) mouse embryonic stem cells. Tubulin is shown as a loading control. Upon very high exposure, a GDF-3 band can be seen in the homozygous GT cells.

I first observed that homozygous genetrap mice were present in the colony, but at lower levels than predicted (15/120 animals born of heterozygous matings; 12.5% observed versus 25% predicted). This suggested a partially penetrant embryonic lethality and I began dissecting embryos from timed matings to determine the embryonic stage of lethality. Beginning at e7.75 (early allantoic bud stage) through e8.5 (neurula stage), I found a dramatic phenotype in 42% of homozygous mutant embryos, (Figure 21, Table 1). The most severely affected embryos arrested at e8.5, but a fraction that had a similar, but slightly milder phenotype, survived to e9.5.

Figure 21: Gross morphological phenotype of affected homozygous GDF-3 genetrap embryos, compared with wild-type littermates. The following stages are shown: e7.75 (A,B), e8.0 (C,D), e8.5 (E,F), e9.5 (G,H). Homozgyous genetrap embryos are in the right column. *1 highlights the growth of the embryo, outside of the extra-embryonic membrances, *2 denotes the 'rod' shape of the embryo, and *3 shows the anterior neural truncation. In the first three rows, anterior is left and dorsal is up. In the fourth row, anterior is up and dorsal is right. Scale bar is 200 μm (A-F) or 400 μm (G,H).

Figure 21

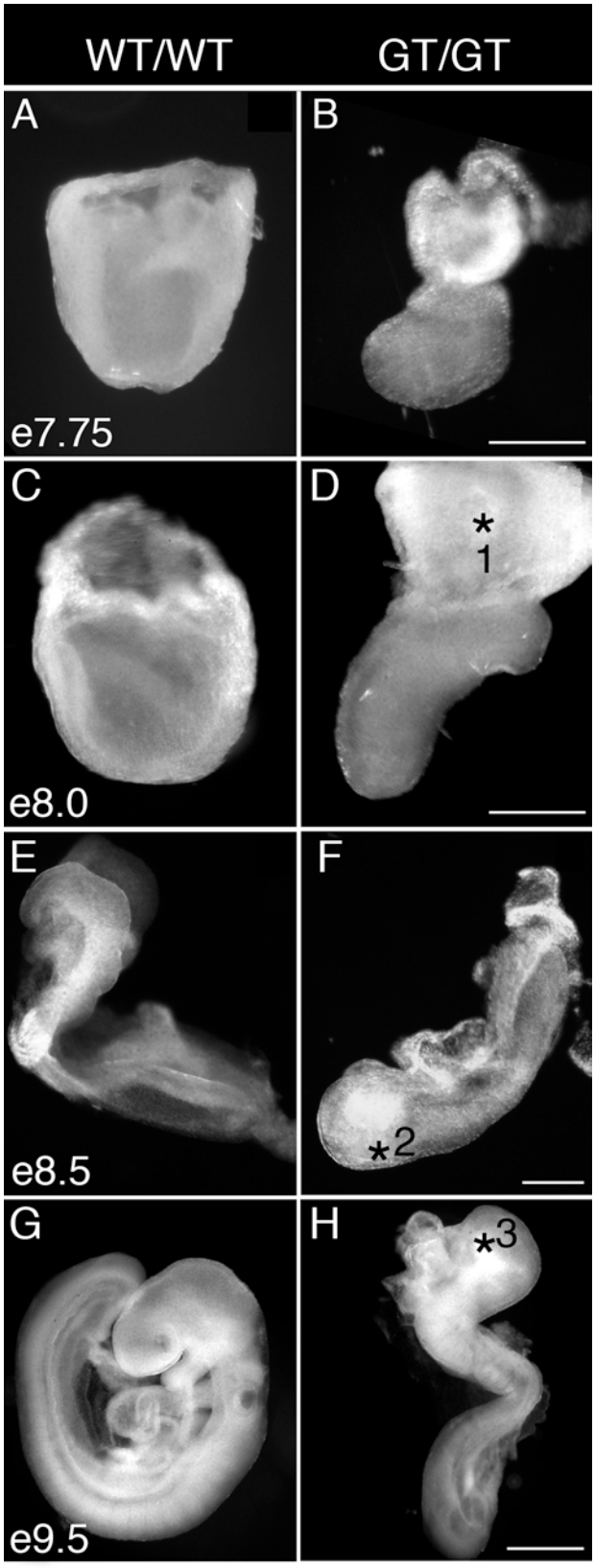

Table 1: Frequency of GDF-3 genetrap embryos and mice.

Embryonic Stage	Wild-type % (n)	Heterozygous % (n)	Homozygous % (n)	Phenotype % of homozygous (n)
e6.5-e7.5	16.5% (33)	57% (113)	25% (54)	0% (0)
e7.75-e8.5	25% (73)	54% (160)	21% (64)	42% (27)*
e9.5	19% (9)	40% (19)	34% (20)	10% (2)
Adult	27% (32)	61% (73)	12.5% (15)	0% (0)

* Four of these embryos were degenerated, with only the yolk sac remaining. Twenty three of these embryos displayed the common phenotype, shown in Figure 21A,C,E.

4.3 – Characterization of the phenotype of affected homozygous GDF-3 genetrap embryos

The gross phenotype at e8.5-e9.5 was most notable for the following elements: the embryo is not surrounded by extra-embryonic membranes, but is connected to them in its posterior region (Figure 21D *1); the embryo does not have an open neural plate but is instead a closed rod (Figure 21F *2); and the embryo seems to lack anterior neural structures (Figure 21H *3).

This gross phenotype is reminiscent to the phenotype of mutants that have perturbed formation of the anterior visceral endoderm (Kinder et al., 2001a). The phenotype also resembles embryos that are mutant for FoxA2 (Ang and Rossant, 1994; Weinstein et al., 1994), which lack anterior visceral endoderm and the node/notochord, and to sub-classes of Nodal hypomorph embryos that have strongly reduced or absent notochord (Lowe et al., 2001). To analyze these tissues directly, I characterized the expression of molecular markers. I found that, at e6.5, the anterior visceral endoderm markers Lim1 (5/5 homozygous mutant embryos, Figure 22B) and Hesx1 (3/3 homozygous mutant embryos) were normal, suggesting that this tissue is formed normally. I next examined the formation of the primitive streak, node, and anterior mesoderm by analyzing Brachyury (BU) and FoxA2 expression at e7.5, which were both normal (10/10 and 7/7 homozygous mutant embryos, respectively, Figure 22D, F), indicating that the anterior-posterior axis is normally established, that the primitive streak is formed normally, and that the node was induced normally.

Figure 22: Anterior visceral endoderm, primitive streak, and node induction are normal in affected homozygous genetrap GDF-3 embryos. Lim1 expression marks the anterior visceral endoderm in a wild-type embryo and mutant e6.5 embryo (A,B scale bar is 150 μm). FoxA2 expression marks the node in e7.5 embryos (C,D scale bar is 200 μm). Brachyury expression marks the primitive streak, node, and anterior axial mesoderm in e7.75 embryos (E-G, scale bar is 200 μm). Anterior is to the left (A), posterior is to the right (P).

Figure 22

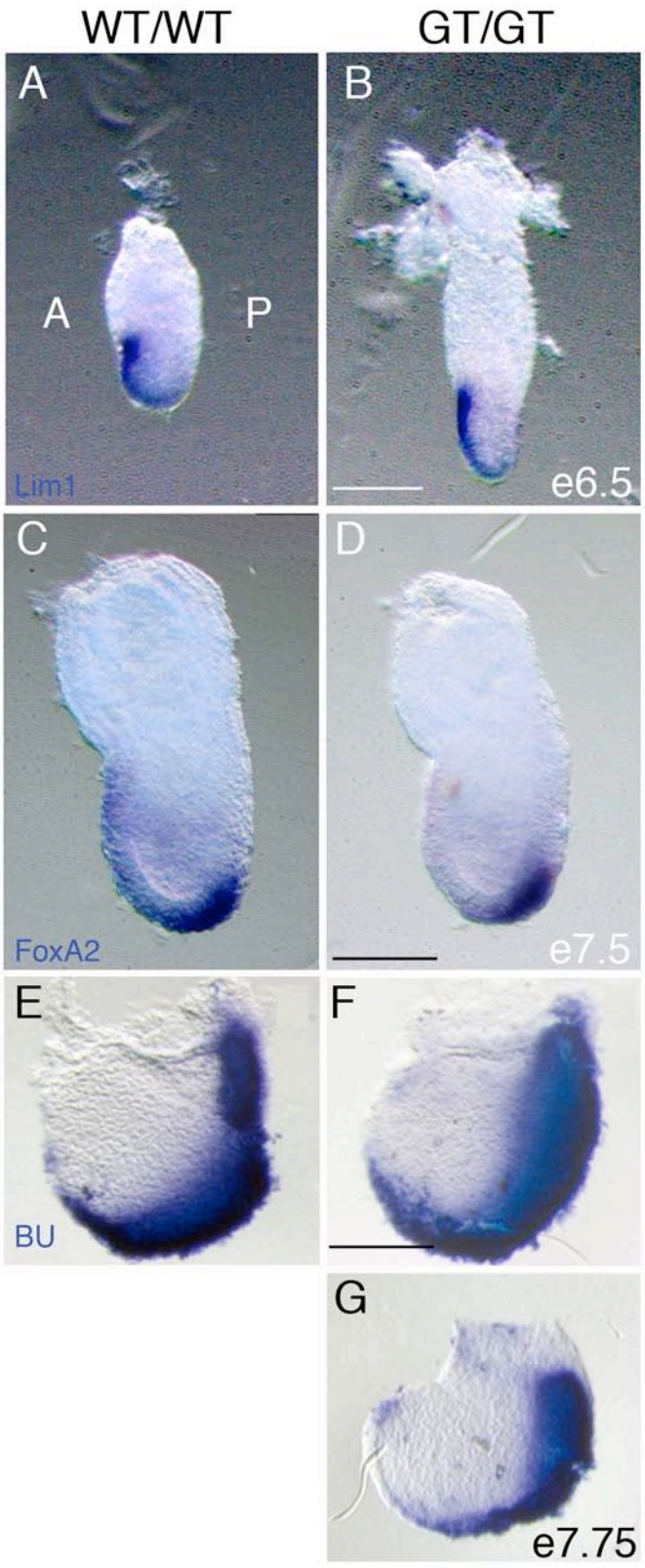

To analyze more carefully the phenotype of affected mutant embryos, I sectioned them at e8.5 and e9.5. I found that, strikingly, the embryos possessed a notochord, but it was located at the extreme ventral edge of the embryo (Figure 23). In a subset of late e8.5-e9.5 embryos, I even observed a notochord at the opposite end of the dorsal-ventral axis of the embryo from a morphologically normal heart (Figure 23). I next analyzed the neural tube and found that at early stages (e7.75-early e8.5), it opened into the body of the embryo, rather than out towards the dorsal edge of the embryo (Figure 24I,M). At later stages (late e8.5-e9.5), the neural tube was closed, as in wild-type littermate embryos (Figure 23).

Figure 23

Figure 23: Section of an affected homozygous GDF-3 genetrap e9.0 embryo, after in situ hybridization for Brachyury, to identify the notochord (red). The neural tube (blue) and heart (orange) are identified by their typical morphology. Ectopic tissue, of unknown character, is present in the interior of the embryo. This is a pseudo-colored image of a 10 μm frozen section after whole mount in situ hybridization. Scale bar is 150 μm.

Molecular markers revealed that affected homozygous mutant embryos had a dorsal-ventral arrangement of tissues as follows: heart/endoderm, dorsal neural tube, ventral neural tube, then notochord, rather than the typical dorsal-ventral arrangement of neural tube, notochord, then endoderm and heart (Figure 24). For instance, Fgf8 (cardiac progenitors), FoxA2 (foregut) and Hex (endoderm) showed 'dorsal' staining at e8.5 (2/2, 4/6, and 2/2, respectively). In the neural tube, Wnt1 and Pax3 stained the most internal, 'dorsal' structures (3/4 and 5/6, respectively), while FoxA2 stained a floorplate like structure in the 'ventral' neural tube (5/6). Shh was strongly downregulated, but present in the ventral notochord (2/2).

Figure 24: Marker analysis of dorso-ventral arrangement of tissues in affected homozygous GDF-3 genetrap e8.0-e8.5 embryos. Mutant embryo sections are shown on the left, wild-type littermates are shown on the right. The following markers were used: Hex (endoderm, A,B); Fgf8 (cardiac progenitors, C,D); FoxA2 (notochord, floorplate, foregut, E,F); BU (notochord, G,H); Pax3 (dorsal neural tube, I,J); Wnt1 (dorsal neural tube, K,L), Shh (notochord, floorplate, M,N). The same magnification was used for all sections but slight variations in embryonic stage and the position of the section along the anterior-posterior axis account for the differences in size. (O,P) Abstract version of the tissues in homozygous genetrap (O) versus wild-type (P) embryos. The notochord is shown in maroon, the heart and endoderm in orange, and the neural tube in blue, with the dorsal structures being a darker shade. Dorsal is up (D), ventral is down (V). Scale bar is 150 μm.

Figure 24

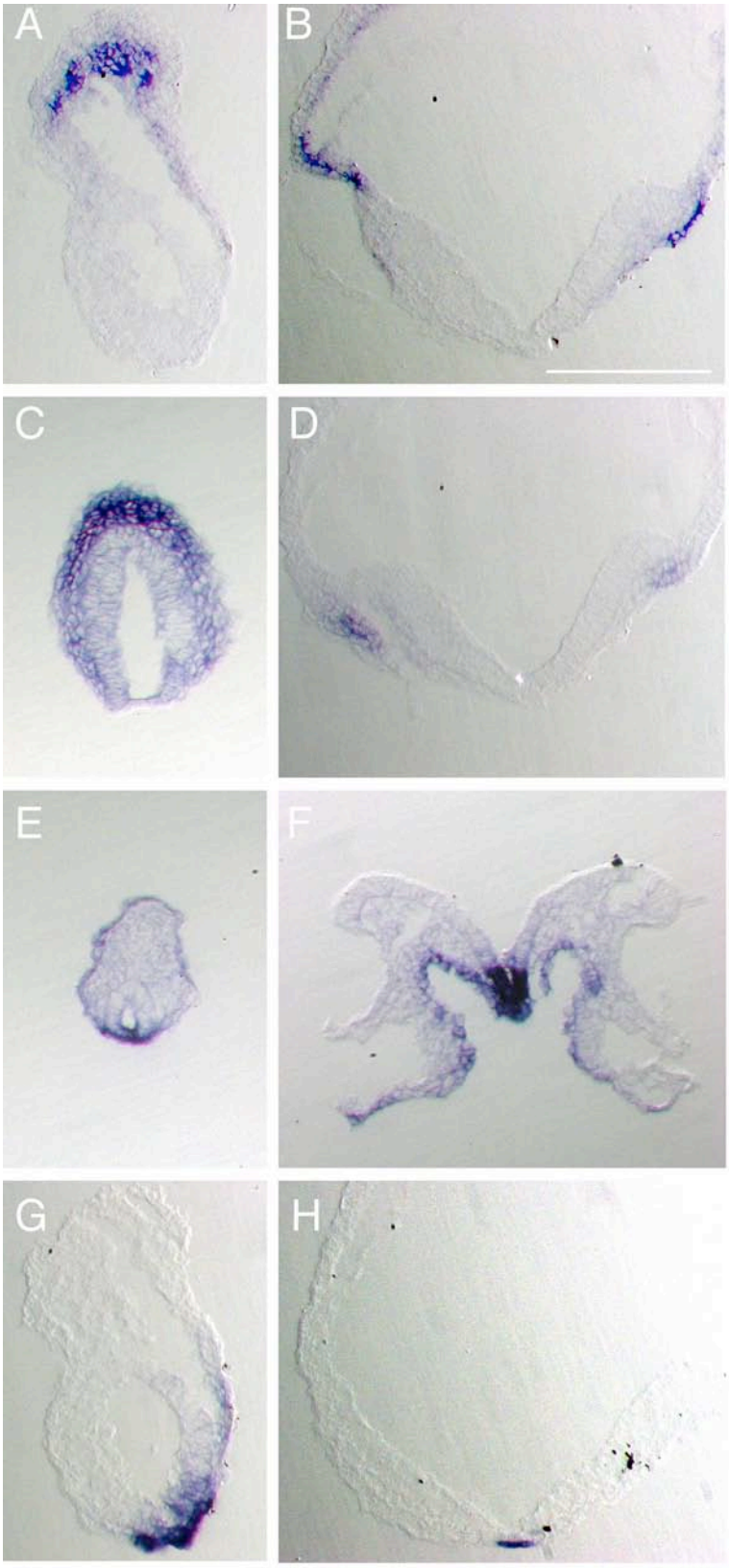

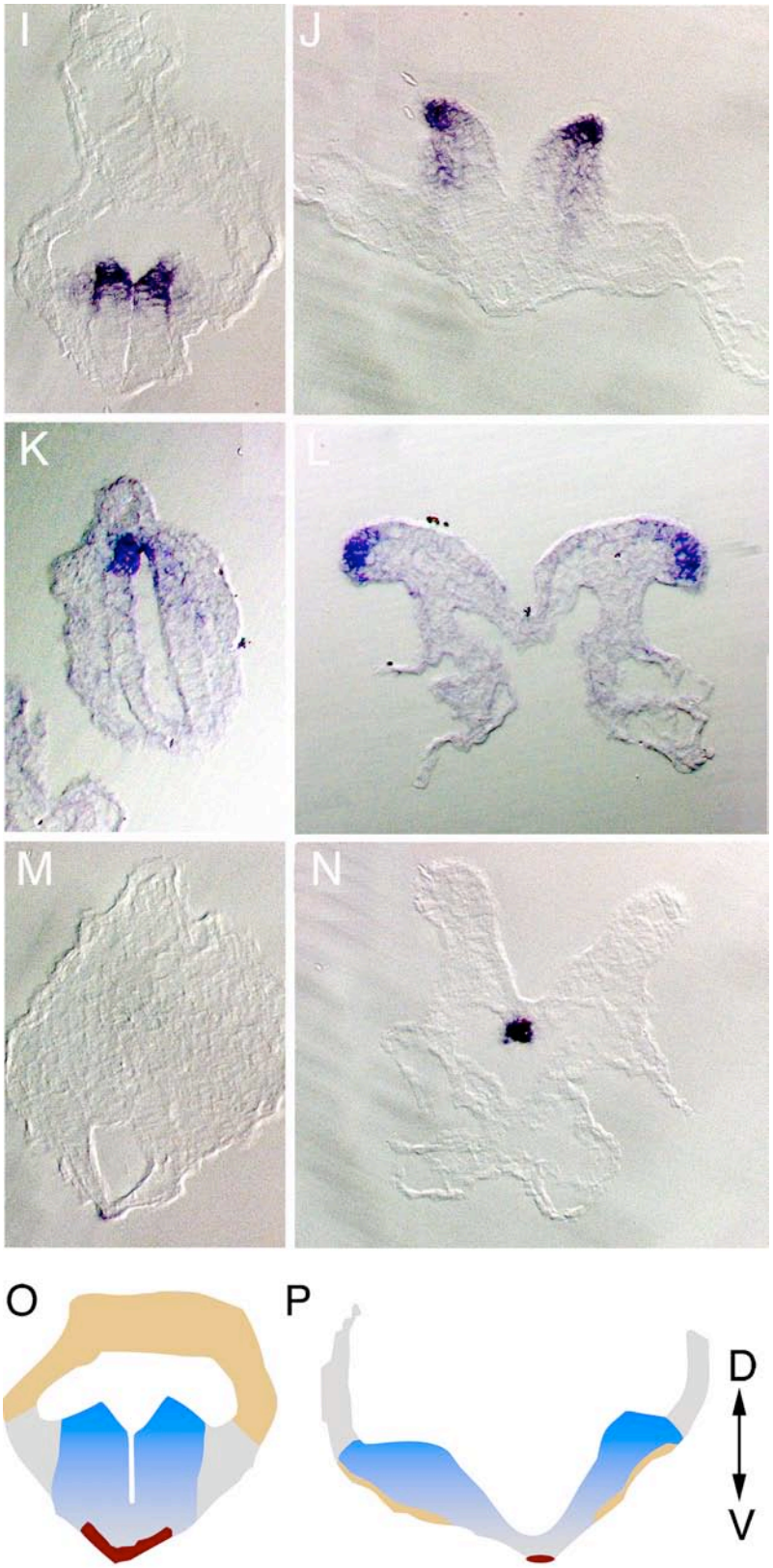
I
J
K
L
M
N
O
P
D
V

Ventral to the neural tube, a ‘cap’ of notochord was present (10/11 affected homozygous mutant embryos), that was positive for BU (10/11, Figure 24G) and FoxA2 (5/6, Figure 24E). Interestingly, Shh was severely reduced in this structure (2/2), indicating a possible second role for GDF-3 in the maintenance of Shh expression in the notochord (Figure 24M).

This cap was broader than the typical wild-type notochord and in e7.75/e8.0 affected homozygous embryos, I observed a wide stretch of BU-positive cells emanating from the node and extending anteriorly on the ventral surface of the embryo. This expression was present as a continuous cap or with small gaps. In contrast to the wild-type embryos, in which ventral observation revealed two thin BU-positive columns of cells that lead anteriorly from the node, joining to form the notochord, the affected mutant embryos displayed dispersed, disorganized BU-positive cells on the ventral surface (10/11 sectioned, Figure 24G; 5/5 whole mount, Figure 25). This is the earliest molecular abnormality in the GDF-3 genetrap embryos, and provides an important clue to the cause of the phenotypic defects, discussed in Chapter 4.5-4.6.

Figure 25: Notochord formation is perturbed in affected homozygous GDF-3 genetrap embryos. In situ hybridization for Brachury was performed on wild-type (A,C) and homozygous GDF-3 genetrap embryos (B,D. At e7.75-e8.0, lateral views (A,B) show that the primitive streak and node appear normal but ventral views (C,D) show that notochord/head process mesoderm migration anteriorly from the node is disorganized in the mutant embryos. Scale bar is 200 μm.

Figure 25

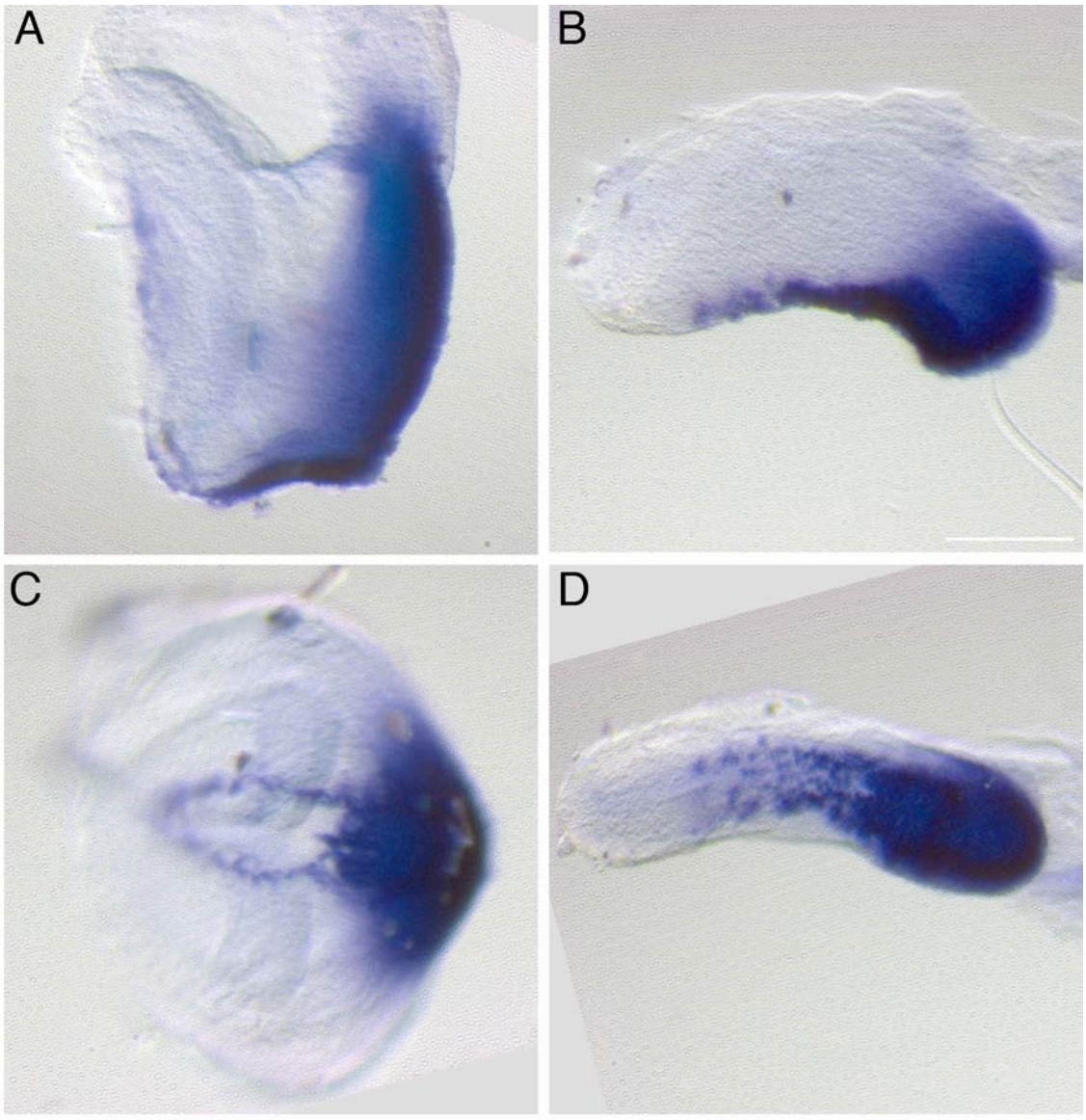

In addition to the abnormal overall dorsal-ventral patterning, another notable feature of the homozygous genetrap mutant embryos is their lack of anterior neural structures. I analyzed whether forebrain is induced in genetrap mutants and found that Six3 staining is normal at e7.75-e8.0 (8/8) and is subsequently lost by e8.5-e9.0 (2/5 have expression), as is Otx2, another anterior neural marker (2/2 e7.5 have expression, 6/11 e8.5-9.0 have expression) (Figure 26). This suggests that anterior neural structures are induced normally, but fail to be maintained.

Figure 26: Lack of forebrain maintenance in affected homozgygous GDF-3 genetrap embryos. In situ hybridization for Otx2 (A,B,C,D) and Six3 (E,F,G,H). Homozgyous genetrap embryos (B,C,F,H) do not show forebrain markers at e9.0-9.5 (B,F) but do show normal induction of forebrain markers at e7.0-e7.75 (C,H). Wild-type sibling embryos are shown in A,D,E,H. In A and B, embryos are also stained for the lateral mesoderm marker Lim1. In E and F, embryos are also stained for Brachyury, demonstrating the abnormal localization of the notochord at the ventral extreme of the mutant embryo (F). Scale bar is 500 μm in A,B; 150 μm in C,D,G,H; 300 μm in E,F.

Figure 26

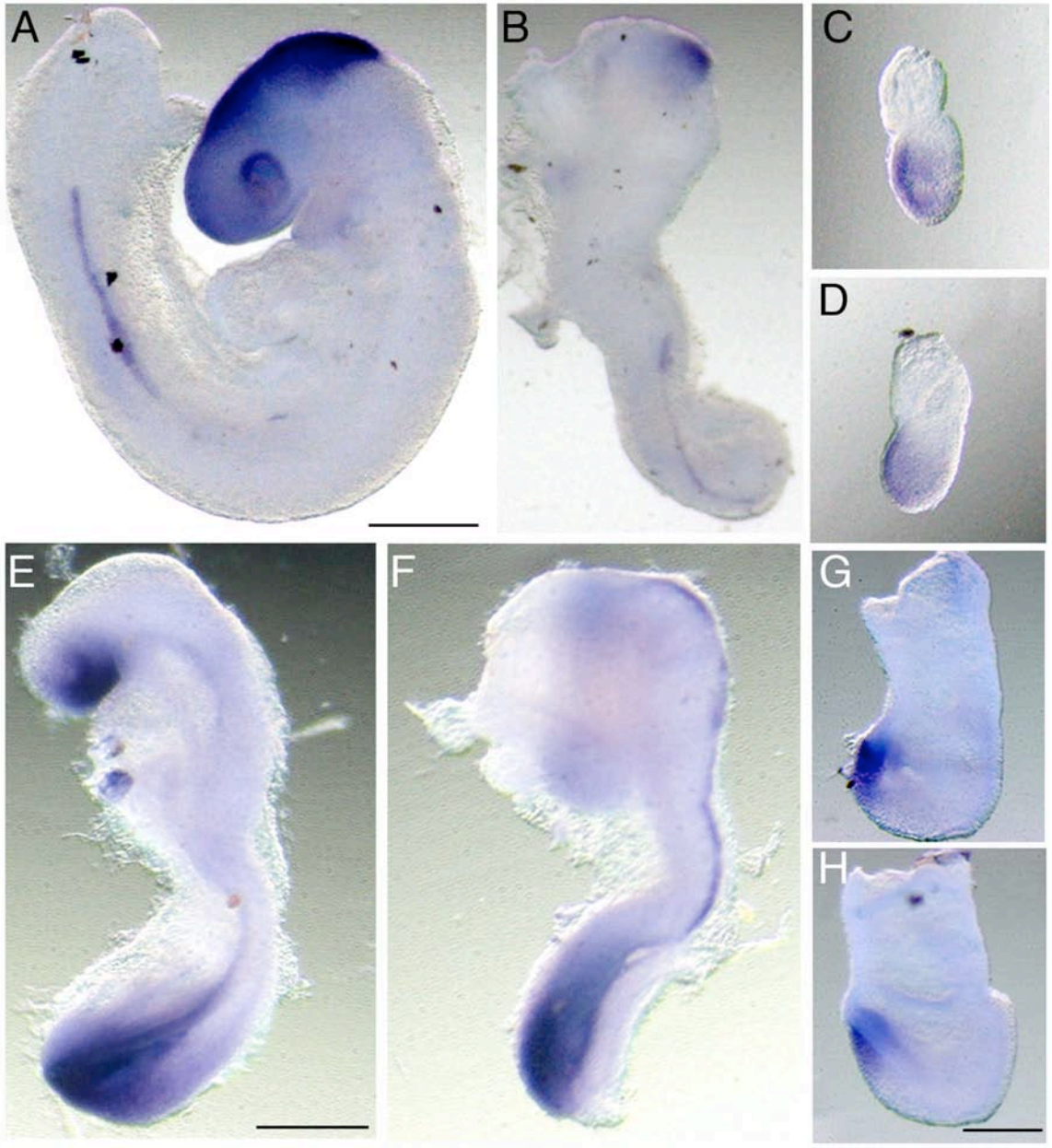

4.4 – BMP provides a repulsive cue to migrating node cells

I considered possible explanations for the abnormal axial mesoderm morphogenesis based on the central observations that GDF-3 is a BMP inhibitor whose expression in the post-implantation embryo begins at e7.5 in the node and then notochord. This correlates with the place and time of the earliest defects observed in the genetrap mutant.

As the notochord migration occurs along the distal-anterior edge of the embryo, and BMP signaling is active at the opposite end, I hypothesized that BMP signaling may negatively drive migration of this structure. I therefore explored the effect of BMP protein (supplied by rhBMP4 beads) on migration of the distal region of the e7.25 mouse embryo – the area of origin for the anterior axial mesoderm and the future anterior neural tissue.

To test this hypothesis, I analyzed the effect of exogenous BMP signaling on the migration of node explants. The distal fifth of e7.25 embryos was explanted and allowed to attach to a fibronectin substrate for several hours (Figure 27A). Subsequently, beads carrying rhBMP4 (or control human serum albumin (HSA)) protein were placed near the explant and then the explant was cultured for 48 hours. During this time, cells migrated away from the explant both as leading, dispersed cells and as a dense 'sheet'.

I measured the distance from the center of the node explant to the edge of the migrating cells, creating a ratio of the distance away from the beads, to the distance towards the beads. I found that beads carrying rhBMP4 provided a repulsive cue to cells migrating from the node, while control beads had no effect on cellular migration (Figure 27B). The ratio of the distance away from the bead over the distance toward the bead was 1.06 +/- 0.18 units in the control HSA treated explants (five sets, with a total 15 explants, and 1.44 +/- 0.55 in the BMP4 treated explants (five sets, with a total 20 explants). Figure 27B shows the percent of explants (blue, control and red, BMP4) in each range of distance ratios.

Figure 27: BMP protein provides a repulsive cue to migrating node explant cells. (A) On the left, an e7.25 mouse embryo that has been partially cut, showing the distal region that would be explanted. On the right, an explant that has attached to fibronectin for several hours, with beads (5X magnification, scale bar is 100 μm). (B) Percent of explants in each distance ratio category for BMP4 treated explants (red) or control HSA explants (blue). The ratios were calculated as the distance away from the bead over the distance towards the bead. (C,D) Nuclear stain showing the node explant (highlighted in white), next to the beads (dark circle with asterisk) containing BMP4 (C) or HSA (D), and the cells that have migrated away from the explant (yellow). Scale bar is 50 μm. The arrows indicate the distance measured for migration from the center of the explant to the edges, although the explant in (C) continues beyond the margin of the image (2.5X magnification).

Figure 27

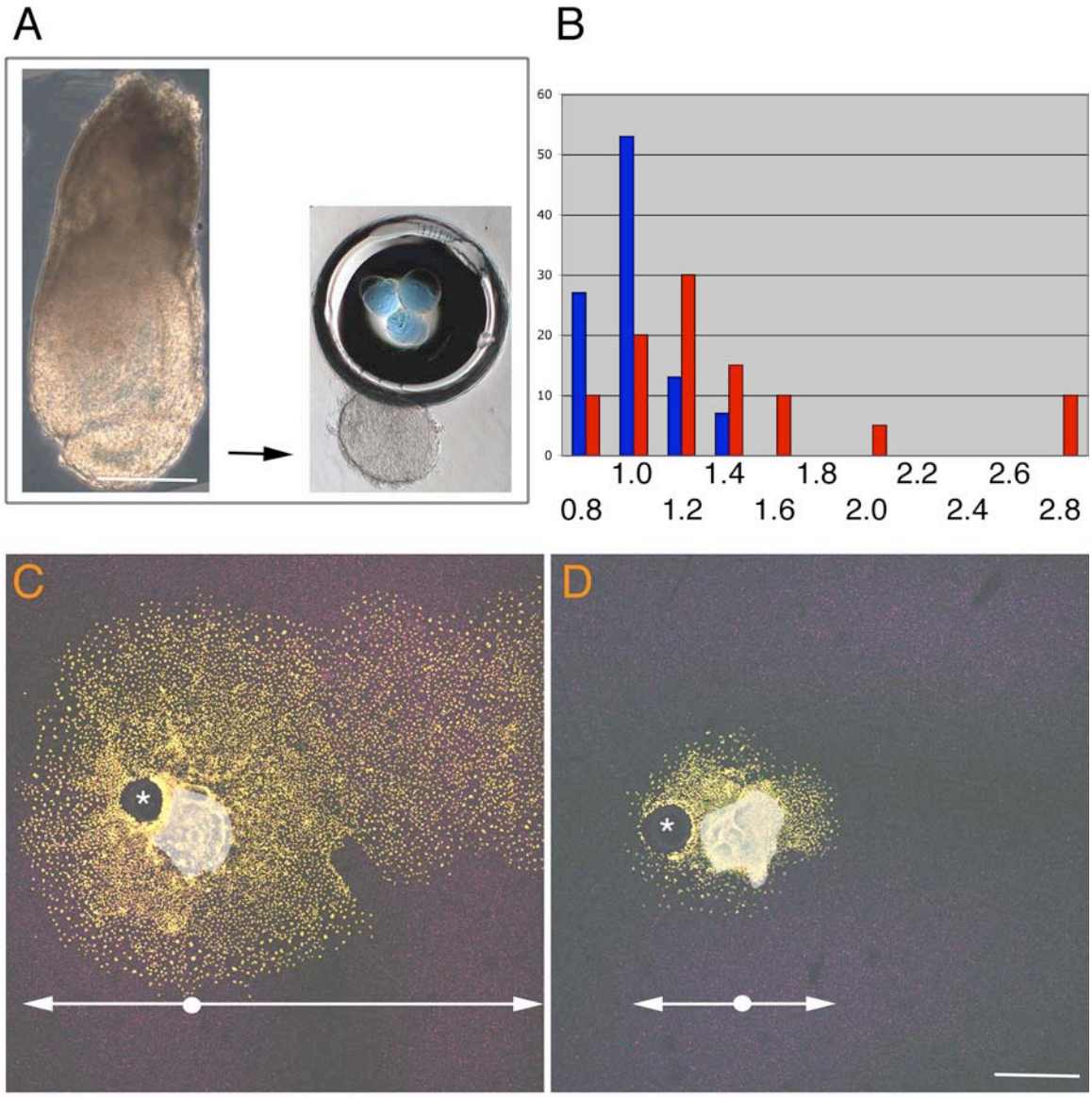

The variability in the ratio of the BMP4 treated explants is most likely is due to slight variations in the stage of the embryos and/or the size of the explants, and therefore the cellular makeup of the extirpated distal region. For instance, earlier embryos may have had a smaller population of perspective axial mesoderm cells in the distal tip, while slightly later embryos are closer to the definitive node stage, when distal explants include more axial mesoderm precursors. The two explants with a ratio of 2.8 and 2.9 (one of which is shown in Figure 27C) were from slightly older embryos, approximately e7.4.

4.5 Chapter Summary

These findings demonstrate that GDF-3 plays a critical role in the patterning of the early embryo. My descriptive analysis found GDF-3 mRNA in the sperm and within the embryo in the inner cell mass, node, notochord, floorplate and neural crest of the mouse embryo, while a LacZ analysis found the GDF-3 exon1-LacZ fusion exclusively in the node and notochord of head-fold and early somite stage embryos. My reduction-of-function studies using the genetrap line showed that GDF-3 is required for proper morphogenesis of the post-gastrulation embryo, and that in its absence, the embryo has abnormal dorsal-ventral patterning. Specifically, the ventral-most structure is the notochord, followed by the neural tube, then the heart and foregut, rather than the wild-type arrangment of heart and foregut, then notochord, and neural tube (Figure 28). The notochord itself is abnormal, being broad and 'dispersed.' This results in an embryonic lethality of affected embryos (42% of total homozygous genetrap embryos) around e9.0 through e9.5 of gestation.

I hypothesized that the reduced GDF-3 levels allow for enhanced BMP driven repulsory migration of the axial notochord and possibly the neural tube, while preserving the normal location of more lateral cell fates such as heart and foregut. I tested this by analyzing migration of an embryo explant in the presence of beads containing BMP protein, which I found indeed drove repelled migration. Together, these findings suggest that GDF-3 mediated inhibition of BMPs is important for early patterning of the mouse embryo.

Figure 28: Model of the phenotype of affected homozygous GDF-3 genetrap embryos. Abstracted embryos of stage e7.75 (A,B) and e8.0 (C,D and sections E,F) are shown, with a wild-type embryo on the left and a homozygous genetrap embryo on the right. Axial mesoderm/notochord is shown in maroon, neural tissue in blue, and heart/foregut is shown in light orange, and the primitive streak in dark orange.

Figure 28

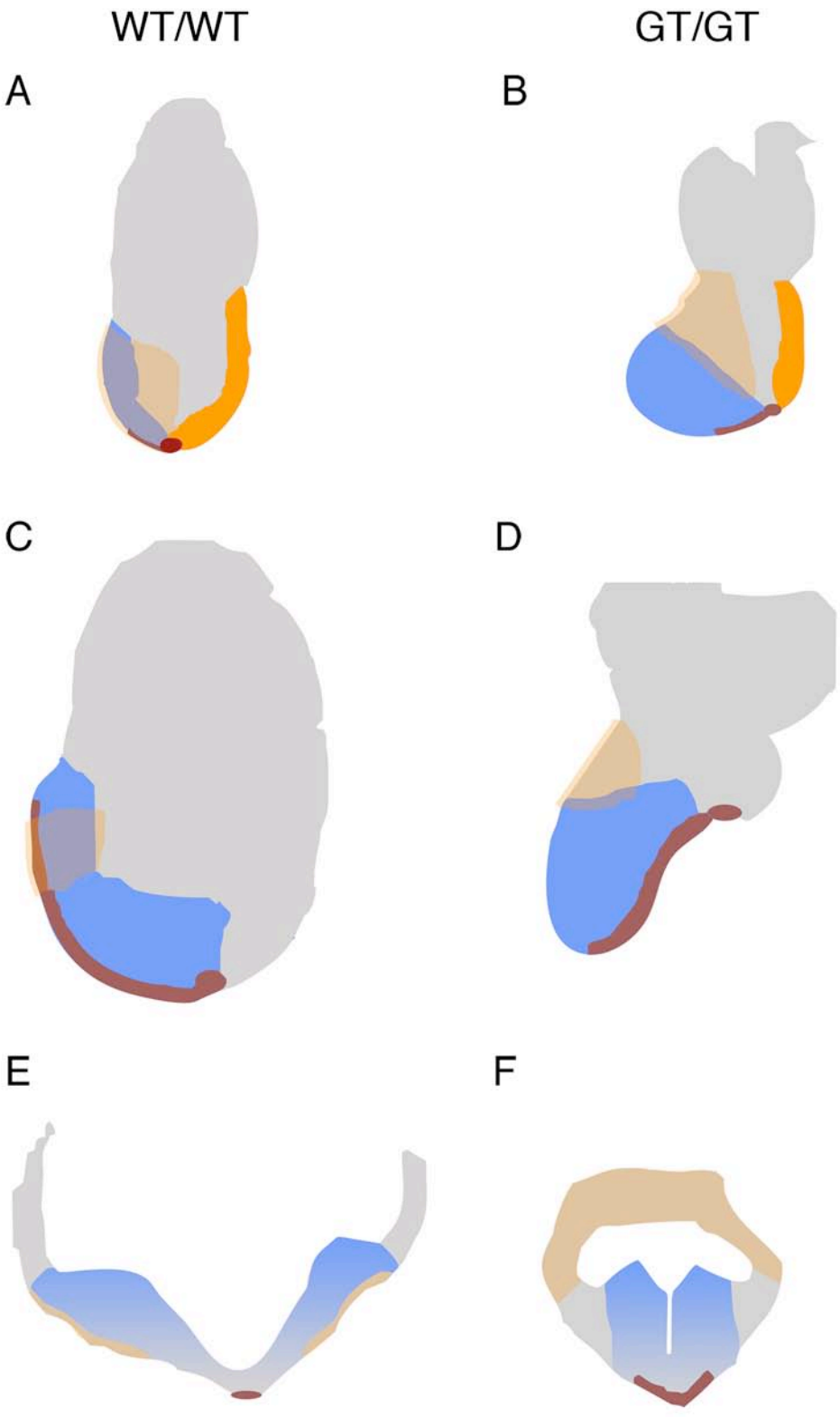

4.6 Chapter analysis

I compared the phenotype of the homozygous GDF-3 genetrap embryos with those of other mouse mutants, to gain a greater understanding of the processes regulating morphogenesis in the mouse embryo. Before this analysis, it is important to note that a knockout of GDF-3 has been published (Chen et al., 2006), with a distinct phenotype that it is discussed in Chapter 5.6.

The gross phenotype of the genetrap mutants most closely resembles the FoxA2 knockout (Ang and Rossant, 1994; Weinstein et al., 1994), the severe phenotype (class III) of the FoxH1 mutant (Yamamoto et al., 2001), and the severe phenotype (class III) of Nodal hypomorph embryos (Lowe et al., 2001). These three mutants perturb Nodal signaling. In addition, the genetrap phenotype is similar to embryos with defects in the anterior visceral endoderm, such as Otx2 and Lim1. Both of these classes of mutants result in embryos that develop outside of the extra-embryonic membranes, have anterior neural truncations, and a closed 'rod' structure.

However, there are several critical differences between the GDF-3 genetrap context and these other mutants. First, the aspects of the FoxA2 and FoxH1 phenotype that resemble the gross GDF-3 phenotype reflect the role of these genes in the anterior visceral endoderm. Perturbation of the anterior visceral endoderm results in failure to convert the proximal-distal axis of the early post-implantation embryo into the anterior-posterior axis of the gastrula, and causes the relevant phenotype, beginning at e7.0 with distal outgrowth of

the embryo (Kinder et al., 2001a). However, rescue of these genes only in the visceral endoderm rescues the anterior-posterior axis and the relevant phenotype (Dufort et al., 1998; Lowe et al., 2001; Rhinn et al., 1998; Yamamoto et al., 2001).

In GDF-3 genetrap embryos, the anterior visceral endoderm is normal, and the embryos display proper anterior-posterior polarity, as judged by appropriate placement of the primitive streak, and the embryos are morphologically normal until e7.75, when they begin to grow out anteriorly.

During gastrulation, the mammalian embryo undergoes explosive growth, with the embryo increasing in cell number from approximately 600 to over 14,000 (in the mouse) (Snow, 1977). Therefore, cell fate specification, morphogenesis, and growth must be tightly coupled. Perturbed outgrowth of the embryo, either due to improper patterning of the proximal-distal axis, or to abnormal migration and morphogenesis, may result in similar appearances. Therefore, the 'phenocopy' of the late gross phenotype may be superficial and does not reveal a mechanistic similarity in the genesis of the phenotype.

Several mutants of the Nodal pathway also display a lack of the node and notochord. This is seen in embryos that lack epiblast FoxA2 or FoxH1, or embryos mutant for GDF1-/-;Nodal+/-, the milder phenotypes of Nodal hypomorphs (class 1, class II), and Smad2 epiblast mutants (Andersson et al., 2006; Dufort et al., 1998; Lowe et al., 2001; Vincent et al., 2003; Yamamoto et al., 2001). The loss of anterior axial mesoderm results in a 'pin-head' phenotype

that is quite different from the GDF-3 genetrap phenotype. I clearly demonstrated that the GDF-3 genetrap embryos form a node and notochord, although the notochord is 'misplaced'. This distinction highlights the critical difference between an effect on cell fate in the Nodal pathway mutants, and the effect on morphogenesis, which I observed in the GDF-3 genetrap mutant.

The molecular mechanisms of notochord induction are known, but the signals that regulate mammalian notochord morphogenesis are poorly understood, in part because processes that govern mammalian notochord formation and migration are slightly different than in other vertebrates.

In the mouse, cells ingress as individuals or small clusters through the primitive streak, by changing their adhesive properties and undergoing an epithelial-to-mesenchymal transition as they leave the epiblast layer (Burdsal et al., 1993; Nakatsuji et al., 1986). The early and mid-gastrula organizer that are at the anterior edge of the primitive streak are the main source of the prechordal plate, while the node contributes to the notochord (Kinder et al., 2001b). Labeling of the mid-gastrula organizer reveals that the descendants migrate in a column that is several cell diameters wide and deposit a trail of cells that reaches caudally to the node (Kinder et al., 2001b; Sulik et al., 1994). During this time and continuing through e8.5, the node regresses caudally, laying down the notochord principally by cell accretion, though some cell division and convergent extension also contribute to the elongation of the notochord (Sausedo and Schoenwolf, 1994; Sulik et al., 1994). Initially, the notochord is incorporated into

the endodermal layer and then converges more medially and folds off dorsally, forming a rod in between the endoderm and neural tissue (Jurand, 1974).

In the frog, Activin has been implicated in endowing the notochord with anterior-posterior polarity, to coordinate extension along this axis (Ninomiya et al., 2004). However, this type of regulation does not explain the active anterior cell migration that forms the prechordal plate and anterior notochord in the mouse. In the Hex mouse mutant, the axial mesendoderm is induced, but does not migrate anteriorly from the node (Martinez Barbera et al., 2000). As a result of Hex loss, markers such as FoxA2 and Lim1 have expanded expression in the node and reduced expression anteriorly. However, the phenotype of the Hex mutant is usually explained as the result of a defect in induction of the most anterior endoderm and prechordal plate (Brickman et al., 2000; Martinez Barbera et al., 2000; Martinez-Barbera and Beddington, 2001; Zamparini et al., 2006). It is important to determine whether BMP/GDF regulation of axial mesoderm morphogenesis is related to a possible role of Hex in this process, or whether GDF-3 provides the only genetic means to uncouple mammalian notochord induction and migration.

One of the most notable features of the gross phenotype of homozygous GDF-3 genetrap embryos is the anterior truncation that results from forebrain loss. It is possible that the lack of GDF-3 in the notochord allows enhanced BMP signaling that could abrogate forebrain maintenance. Similarly, in Chordin-/- ;Noggin+/- embryos, lack of these factors in the anterior mesendoderm results in

failure to maintain forebrain tissue (Anderson et al., 2002). Further, in explants of 'late-bud' stage embryos, the forebrain has already been specified but markers of forebrain disappear after prolonged culture or upon treatment with exogenous BMPs, unless these explants are co-cultured with anterior mesendoderm (Yang and Klingensmith, 2006). Alternatively, the dramatic reduction of Shh in the notochord of affected mutants may indirectly prevent secretion of a necessary forebrain maintenance signal. Of note, rostral Shh is lost in the Noggin/Chordin double mutant (Bachiller et al., 2000).

Another possibility is that misplacement of the notochord relative to the forebrain, or improper migration of the most anterior prechordal plate results in the failure to maintain the forebrain. Several mouse mutants reveal the necessity of this notochord-derived ongoing maintenance, as defects in mesendoderm generally result in anterior neural truncations and post-gastrulation loss of forebrain markers that were normally induced during gastrulation. Lack of forebrain maintenance is seen in several Nodal pathway mutants that do not induce anterior axial mesoderm, such as the Gdf1-/-;Nodal+/- mutant, the FoxH1 mutant, and a mutant that reduces Smad2/3 levels in the epiblast (Andersson et al., 2006; Vincent et al., 2003; Yamamoto et al., 2001).

It is important to consider my observations of the GDF-3 genetrap phenotype as a 'reduction-of-function' analysis. I studied the required functions of GDF-3 in the mouse embryo using a genetrap allele that strongly reduces production of GDF-3 protein. While the phenotype that I observed is dramatic,

the allele itself is a ‘knock-down’ and the results must be interpreted in this context. We also intended to create a conditional knockout of GDF-3, but this work, done in collaboration with Regeneron was not successful.

Genetrap-based removal of GDF-3 probably results in partial enhancement of BMP signaling, whereas a full null allele would cause greater BMP pathway activation. As BMPs are morphogens, producing distinct cell fates at distinct doses, this could show a different result from that of a true knockout, and one that yields different information about the balance of BMP/GDF signals. However, as I observed a probable effect of BMP signaling on chemotaxis, not just cell fate, the residual GDF-3 protein might be of limited importance because different doses of BMP could simply provide more or less notochord repulsion, but produce the same type of phenotype.

It is possible that Noggin and/or Chordin mediate the rescue that allows 50-60% of homozygous genetrap embryos to escape the phenotype and survive to adulthood. The shared expression of GDF-3, Noggin, and Chordin suggests that only combined removal of all three factors would provide maximal BMP activation. As a result, full removal of GDF-3 through a null allele would still only produce an intermediate level of BMP inhibition.

In contrast to the phenotype of the GDF-3 genetrap mutation that I observed, embryos that are missing either of the ‘classic’ BMP inhibitors Noggin or Chordin have distinct, generally less severe phenotypes. Loss of Noggin alone results in perinatal lethality, with defects in patterning of the neural tube

and somites (McMahon et al., 1998). Loss of Chordin alone causes the majority of mutant embryos to die perinatally, with head and neck abnormalities (Bachiller et al., 2003; McMahon et al., 1998). However, a small percentage of Chordin knockout embryos arrest shortly after gastrulation, with 'ventralization' that includes reduced neural tissue and absence of dorsal mesodermal derivatives such as the notochord and somites. Combined loss of Noggin and Chordin results in embryonic lethality (Bachiller et al., 2000). These embryos do not induce forebrain, but morphogenesis proceeds normally for the majority of the embryo and the embryos arrest later in development. In addition, these embryos have defects in left-right axis determination and in specifying and/or maintaining certain cell fates, such as anterior notochord and trachea.

It is possible that the different phenotypes of the GDF-3 genetrap mutant and the Noggin/Chordin double mutant reveal distinct requirements for BMP inhibition mediated by atypical TGF-β ligands, such as GDF-3 in morphogenesis, and by non-ligand factors such as Noggin and Chordin in establishing cell fate (such as neural tissue and dorsal mesoderm). If this is the case, my work also provides the first basis for genetically distinguishing the effects of BMPs on cell fate determination and cell movement in the mouse embryo. Further, it highlights the functional importance of the variety of regulatory mechanisms for the TGF-β superfamily.

CHAPTER 5: Does GDF-3 also act as a Nodal-like agonist?

During this work, another group reported that GDF-3 is a Nodal-like agonist required for early mouse development. My finding that GDF-3 acts as a BMP inhibitor does not exclude the possibility that GDF-3 could have other functions, and it is even possible that GDF-3 is a bi-functional ligand. Throughout development, the reciprocal regulation of these two branches of TGF-β family signaling is a very common phenomenon. These pathways are oppositely regulated in human ES and possibly in the endogenous state of mouse ES as well, reviewed in (Brivanlou and Levine, 2007). In the frog embryo, blocking ongoing BMP signaling with concomitant activation of TGF-β/Activin/Nodal signaling is required for dorsal mesoderm induction and one mechanism for this is intracellular competition for factors required in both signal transduction pathways (Candia et al., 1997; Graff et al., 1996; Graff et al., 1994). Given the importance of coordinately regulating these two pathways, a very interesting and general mechanism could be bi-functional ligands. Nodal itself has been shown to act as a BMP inhibitor, directly suppressing the activation of Smad1/5/8 at the same dose at which it acts as a Smad2/3 activator (Yeo and Whitman, 2001). However, my findings demonstrate that the major activity of GDF-3 is mediated through its ability to inhibit BMP signaling, and Nodal-like functions may be minor, or represent an artifactual activity.

5.1 - Summary of the findings by Chen and colleagues

I present here a comparison of our data, together with data that directly addresses the basis for our different conclusions. Chen et al made the following central observations: 1) That GDF-3 is a 'relative' of xVg1. 2) GDF-3 over-expression in frog embryos causes a secondary dorsal axis and results in mesoderm induction in animal caps. 3) GDF-3 can stimulate Activin/Nodal-responsive transcription in cell culture, and is inhibited by the Nodal inhibitor Lefty. 4) GDF-3 interacts with Nodal receptors, in a complex with the co-receptor Cripto. 5) GDF-3 is expressed in the inner cell mass and epiblast, but not in any other tissues before mid-gestation (e9.5). 6) Loss of GDF-3 exon 2 results in 35% of homozygous mutant embryos arresting by e8.5, with a constriction at the embryonic/extra-embryonic border, reduced anterior structures, ectopic, abnormal mesodermal derivatives, and defects in extra-embryonic tissue. Molecular defects include the failure of anterior visceral endoderm to be induced and/or migrate, and defects in mesoderm and definitive endoderm induction.

5.2 - The relationship between GDF-3 and Vg1

GDF-3 was first cloned from a mouse e6.5 cDNA embryonic library by homology to Xenopus Vg-1 (Jones et al., 1992b). However, it is not the mammalian ortholog of Vg1. Mature mouse GDF-3 shares only 53% identity with mature xVg1, while it has 84% identity with mature human GDF-3. Frog and mammalian homologues of TGF-β superfamily ligands typically share greater than 80% homology. More importantly, Vg1 retains the fourth cysteine, a

defining feature of classic TGF-β superfamily ligands, and mutation of this cysteine abrogates the ability of Vg1 to induce mesoderm (Joseph and Melton, 1998). Chen and colleagues do not identify GDF-3 as the true ortholog of Vg1, but rather suggest that functions of Vg1 in the frog have been split between its two close relatives, GDF-1(which has the same cysteine arrangement as Vg1), and GDF-3, which represent functional homologs. As described in Chapter 2.1, xVg1 is not syntenic with GDF-3, but is syntenic with GDF1. In summary, I find no basis for considering GDF-3 to be a homolog of Vg1, but find that Vg1 is the homolog of GDF-1, as judged by function, sequence, and synteny.

5.3 - GDF-3 over-expression in frog embryos and animal caps, and effects on luciferase transcription

Secondary dorsal axis formation can result from either BMP inhibition or Nodal-like activation. However, these two possibilities can be resolved by assays such as over-expression in the animal cap in which BMP inhibition results in direct neural induction, whereas Nodal activation induces mesoderm, with secondary neural induction. As both groups performed the same assay, with different results, I first analyzed the constructs that each group used to produce GDF-3 mRNA. I studied GDF-3 over-expression with a construct containing only the coding region of GDF-3. Other groups had used either a construct containing both the coding region and untranslated regions (UTRs) (Richard Harland and Julie Baker, personal communication), a construct

containing the coding region followed by an SV40 polyA region (Chen et al., 2006), or a chimeric GDF-3 mRNA encoding the prepro domain of BMP2 with the mature domain of GDF-3 (Chen et al., 2006), a strategy that has been used frequently in enhancing processing of TGF-β ligands. I therefore hypothesized that the presence of the UTRs, the viral polyA, or the enhanced processing of GDF-3 could promote higher levels of GDF-3 mature protein and thus account for the different activities as a dose threshold effect.

To test whether the GDF-3 mRNA 5' and 3' UTRs enhanced production of GDF-3 protein, I injected 1 pg, 10 pg, 100 pg, and 1000 pg of mRNA of each construct and analyzed the amount of GDF-3 protein produced. As I hypothesized, I found that the presence of the UTRs allowed production of significantly more GDF-3 protein for each dose of mRNA injected (Figure 29A).

Therefore, injection of the coding region or the coding region plus UTRs of GDF-3 give rise to very different 'doses' of GDF-3 protein. I predicted that at high levels, the coding region alone could acquire mesoderm-inducing activity and at low levels, the coding region plus UTRs would acquire BMP inhibitory activity. I analyzed whether these different constructs possess different cell fate inductive activities using the animal cap assay in the frog embryo. I found that, throughout the dose range of the coding region alone construct, GDF-3 acted as a BMP inhibitor, inducing neural tissue directly. I tested up to 3 ng/frog embryo and still observed this phenotype but did not test higher doses because of non-specific lethality of the embryos (data not shown). However, I found that at low

doses (1, 10 pg), the coding region plus UTRs construct acted as a direct neural inducer, the hallmark of BMP inhibition, while at higher doses (100 pg, 1 ng), it acted as a mesoderm inducer, a classic response to Nodal signaling (Figure 29A).

In addition to my analysis of cell fate in animal caps, I tested the ability of GDF-3 constructs to induce the typical elongated morphology of dorsal mesoderm in animal caps. I injected RNA for increasing doses of GDF-3 CDS alone and GDF-3 CDS plus UTRs. I found that the CDS alone did not induce elongated dorsal mesoderm and caps maintained a spherical shape, similar to uninjected caps or caps injected with Noggin, another BMP inhibitor. In contrast, the CDS plus UTRs induced dorsal mesoderm elongation at 100 pg and 1 ng of RNA injection (Figure 29B).

Figure 29: Dose effect of GDF-3 over-expression in frog embryos. (A) Over-expression of GDF-3 coding region only (CDS) and coding region plus untranslated regions (CDS+UTRs) by injection of RNA (1, 10, 100, or 1000 pg). The top panel shows a western blot of GDF-3 protein and panels 2-5 show RT-PCR on the animal caps. The following markers were used: Sox2 (neural), Msx1 (epidermal marker), BU (mesodermal marker), and ODC (loading control). Lanes 1,2 show whole embryo (st 11) with and without reverse transcription as positive and negative controls for each RT-PCR marker, respectively. Lane 3 shows an uninjected control. (B) Morphology of animal caps that were uninjected (left middle, indicated '(-)'), injected with Noggin (a control BMP inhibitor, indicated 'nog') or a dose range of GDF-3 CDS (middle column) or CDS+UTRs (right column). An intact stage 17 embryo is shown in the upper left corner as a stage-matched control. Scale bar is 1 mm. (C) Luciferase assay (arbitrary units) using an Activin/Nodal responsive element (ARE) or a BMP responsive element (BRE) driving luciferase reporters (Lux). A dose range of each GDF-3 construct (CDS or CDS+UTRs) was tested against the ARE-Lux alone or against the BRE-Lux together with BMP4 RNA (100 pg). Lanes 1 and 10 show reporter alone controls. Lane 11 shows BMP4 RNA alone as a positive control for BRE-Lux activation. (D) Over-expression of GDF-3 CDS+UTRs with or without α-amanitin. Lane 1 shows stage 6 as a negative control for Smad phosphorylation (Phospho-Smad1 and Phospho-Smad2) because the Smad pathways are not active at this stage. Tubulin is shown as a loading control.

Figure 29

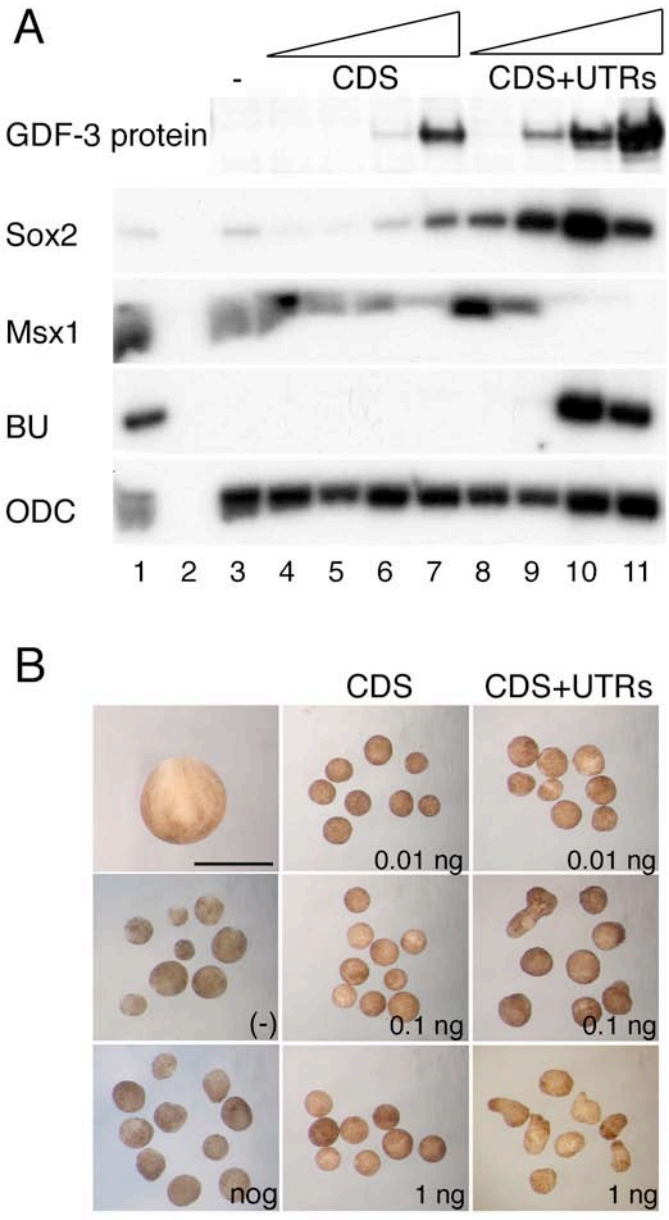
A
-
CDS
CDS+UTRs
GDF-3 protein
Sox2
Msx1
BU
ODC
1 2 3 4 5 6 7 8 9 10 11
B
CDS
CDS+UTRs
0.01 ng
0.01 ng
(-)
0.1 ng
0.1 ng
nog
1 ng
1 ng

C

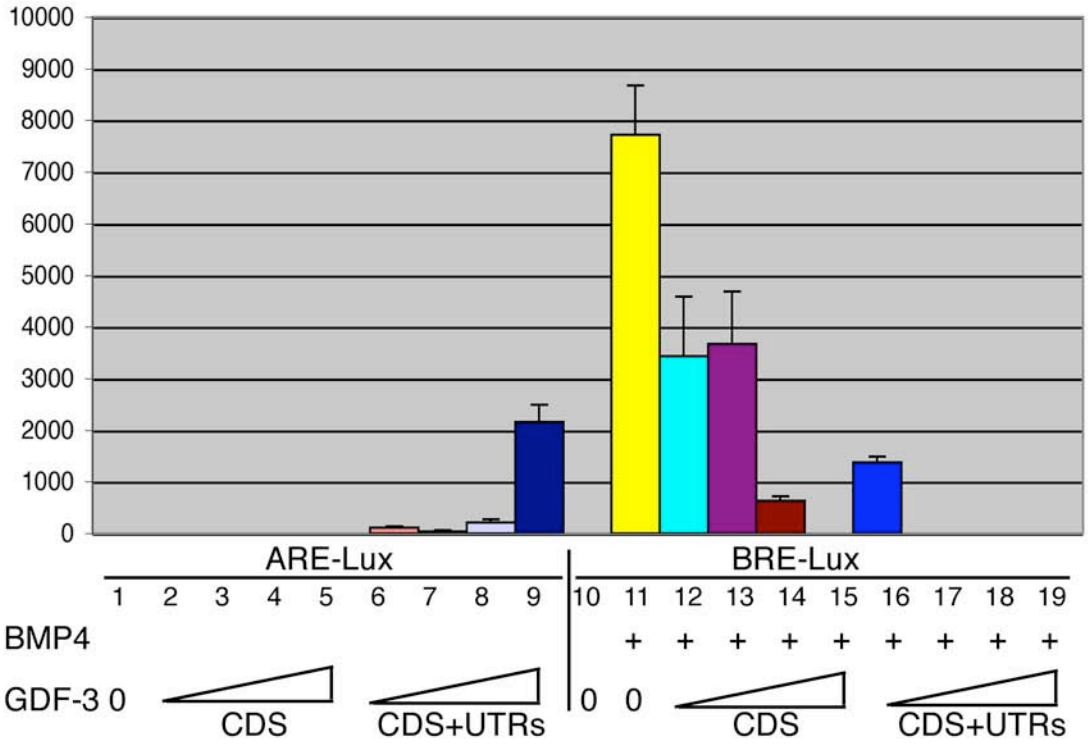
10000
9000
8000
7000
6000
5000
4000
3000
2000
1000
0
ARE-Lux
BRE-Lux
1 2 3 4 5 6 7 8 9 10 11 12 13 14 15 16 17 18 19
BMP4
+ + + + + + + + +
GDF-3 0
0 0
CDS
CDS+UTRs
CDS
CDS+UTRs

D

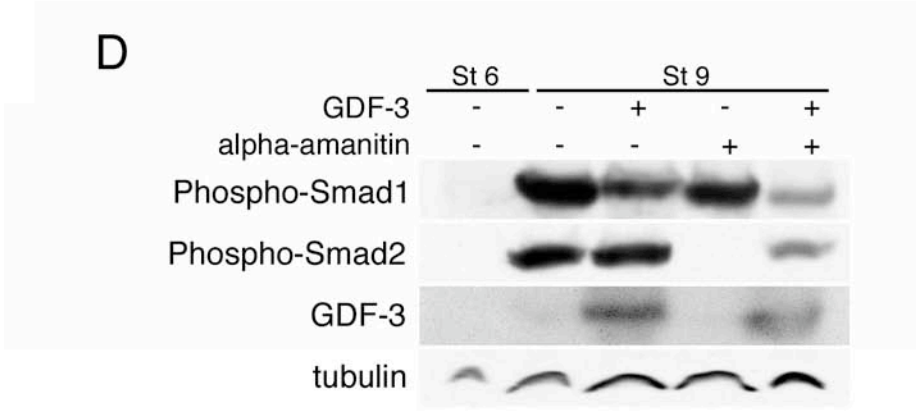
St 6
St 9
GDF-3 - - + - +
alpha-amanitin - - - + +
Phospho-Smad1
Phospho-Smad2
GDF-3
tubulin

I confirmed the effects of a dose range of the coding region plus UTRs using a luciferase assay. I tested the effects of this construct on activation of a luciferase gene regulated by a BMP-responsive element (BRE) and an Activin/Nodal responsive element (ARE). These experiments showed that even 1 pg of the GDF-3 coding region plus UTRs is sufficient for BMP inhibition, while 100 pg -1 ng is required to activate Nodal-like signaling (Figure 29C). To determine whether this type of activity switching dose response is a common feature of Nodal-like ligands, I tested the luciferase response to a similar dose curve using a known Nodal-like ligand, Xnr1. Xnr1 was not able to inhibit BMP signaling at low doses. 1 ng of Xnr1 mRNA activated the ARE luciferase and inhibited the BRE luciferase, most likely indirectly through induction of BMP inhibitors in dorsal mesoderm (data not shown).

I next sought to determine whether GDF-3 switches activity at a certain dose threshold or acquires Nodal-like activity while retaining the ability to inhibit BMP signaling. To do this, I analyzed the effects of over-expressing 1 ng (high dose) of GDF-3 coding region plus UTRs with or without α-amanitin, an inhibitor of translation that prohibits indirect effects of manipulating signal transduction pathways. This approach allowed me to observe the primary effects of GDF-3, but not secondary effects mediated by new transcription. This is important because activation of Nodal signaling induces dorsal mesoderm, which then expresses new transcripts of BMP inhibitors such as Noggin and Chordin, and thus includes primary mesoderm induction and secondary BMP inhibition. I

found that a high dose of GDF-3 caused inhibition of Smad1/5/8 and direct activation of Smad2/3 in either the absence or presence of α-amanitin (Figure 29D). Therefore, I showed that GDF-3 is a Smad1/5/8 inhibitor throughout its dose range and that, at high doses, this activity is coincident with Smad2/3 activation.

5.4 - GDF-3 protein interacts physically with various factors in the TGF-β pathway

While I detected GDF-3 interaction with BMP4, I also observed that GDF-3 can interact with a Nodal like ligand and with xVg1, but not with Activin. However, neither my data, nor those of Chen and colleagues describe endogenous protein interactions. Therefore, both sets of data could reflect promiscuous or artificial binding.

5.5 - The expression of GDF-3 in the early mouse embryo

The different findings on mRNA spatial localization in the mouse embryo, between my findings and those of Chen and colleagues, can probably be explained by the use of different in situ probes. We both detected GDF-3 in the inner cell mass, but observed different patterns in post-implantation stages. Chen and colleagues used the full-length anti-sense RNA as a probe, whereas I used the 3' 500 bp of the coding region to produce the anti-sense probe. However, I used RT-PCR to confirm the temporal expression pattern of GDF-3,

and detected the highest signal at e8.5, when Chen and colleagues report no expression of GDF-3. Further, I performed LacZ staining on genetrap heterozygous embryos, providing an independent strategy for confirming GDF-3 expression in the notochord.

5.6 - The required roles of GDF-3 in early development

The phenotype of the GDF-3 genetrap allele resembles the gross morphology of the exon 2 knockout, described by Chen and colleagues. However, it is important to note striking molecular differences. While the knockout displays failure to induce (or proper migration of) anterior visceral endoderm, I found that this tissue is normal. In addition, the knockout has defects in mesoderm and definitive endoderm induction, while I observed proper induction of the primitive, node, notochord, heart, and foregut.

One explanation for the different findings could be that the genetrap allele reduces, but does not remove the wild-type GDF-3 allele, whereas the knockout is a true loss-of-function. As such, the genetrap may allow minimal, but sufficient levels of wild-type GDF-3 to be expressed during the establishment of anterior visceral endoderm and induction of mesendoderm, allowing the genetrap mutants to perform these steps properly, while the knockout fails to do so. However, higher levels of GDF-3 may be required for morphogenesis, causing this process to be perturbed in the genetrap.

It is also possible that the knockout phenotype reflects earlier failure to regulate the BMP pathway. Enhanced BMP signaling has been shown to perturb anterior visceral endoderm induction (Soares et al., 2005), but it is difficult to understand how elevated Smad1/5/8 activity could block mesoderm formation.

I compared the GDF-3 genetrap phenotype to Nodal pathway mutants in Chapter 4, and note that a critical difference is that the node and notochord are induced normally in the genetrap mutant embryos, but do not form in embryos with reduced Nodal signaling. This latter defect results in a distinct phenotype from either the GDF-3 genetrap or the GDF-3 exon 2 knockout.

5.7 - GDF-3 is an endogenous BMP inhibitor

Despite some evidence for the ability of GDF-3 to act like Nodal, I feel that this is probably an artifact of high levels of over-expression of GDF-3. The real question in studying this potential model is whether the BMP inhibitory and Nodal-like activating roles for GDF-3 are physiological. I first characterized the activity of GDF-3 protein because over-expression of RNA or DNA of other TGF-β ligands could yield artificial results. These experiments demonstrated that GDF-3 mature protein is a BMP inhibitor (Figure 8).

I also studied the endogenous role of GDF-3 in regulating TGF-β signaling. To do this, I characterized the activation state of the BMP pathway (through Smad1/5/8 phosphorylation) and TGF-β/Activin/Nodal pathway (through Smad2/3 phosphorylation) in mouse embryonic stem cells that contain

a genetrap insertion, interrupting the GDF-3 gene. I found that in steady-state, cells with reduced GDF-3 levels had slightly increased Smad1/5/8 activation with no difference in Smad2/3 signaling. Exogenous BMP signaling accentuated this effect, such that cells with reduced GDF-3 levels had notably higher Smad1/5/8 signaling (Figure 9). As Nodal signaling is only activated by the highest doses of GDF-3 mRNA, reduction of GDF-3 levels should impinge on this activity first. However, these data show that GDF-3 is a physiological BMP inhibitor and do not reveal any endogenous role in activating the Nodal pathway.

CHAPTER 6: DISCUSSION AND CONCLUSIONS

This thesis work used comparative embryology to study the regulation of early developmental processes by the TGF-β superfamily, with a focus on the unusual GDF-3 ligand. Through biochemistry, gain-of-function, and reduction-of-function approaches in multiple developmental contexts, I have created the first comprehensive analysis of GDF-3 embryonic function.

My data show that GDF-3 is an inhibitory ligand, interacting with and blocking classic BMP/GDF ligands. Through this mechanism, GDF-3 induces a secondary dorsal axis in the frog embryo, and acts as a direct neural inducer in the frog ectoderm. In embryonic stem cells, GDF-3 opposes BMP activity to regulate the balance between stemness and differentiation. Within the context of the mouse embryo, GDF-3 is required for normal morphogenesis of the notochord and dorso-ventral patterning of the body plan. In addition to my specific findings on the GDF-3 ligand, my work provides the basis for several general concepts and conclusions.

First, my findings represent a special example of the high degree of evolutionary conservation of developmental modules. The ability of GDF-3 to elicit a secondary dorsal axis in the frog embryo relies on the formation of a molecular equivalent to Spemann's organizer at the ventral site of injection. Local BMP inhibition in the ventral body dorsalizes the local mesoderm to include notochord and paraxial mesoderm, and concomitantly induces neural

tissue. Together, these tissues constitute the secondary axis (Figure 30A). The phenotype that I observed in the GDF-3 genetrap mutant mouse embryos echoes this phenomenon. Through mis-placement of the notochord, the final derivative of the organizer, the entire dorsal axis is mislocalized, including the notochord, neural tube, and paraxial mesoderm (Figure 30B). However, ventral and lateral cell fates such as endoderm and heart, are not perturbed and maintain their typical location. This reflects the continuing role of the organizer derivatives in establishing and patterning the dorsal axis.

Figure 30

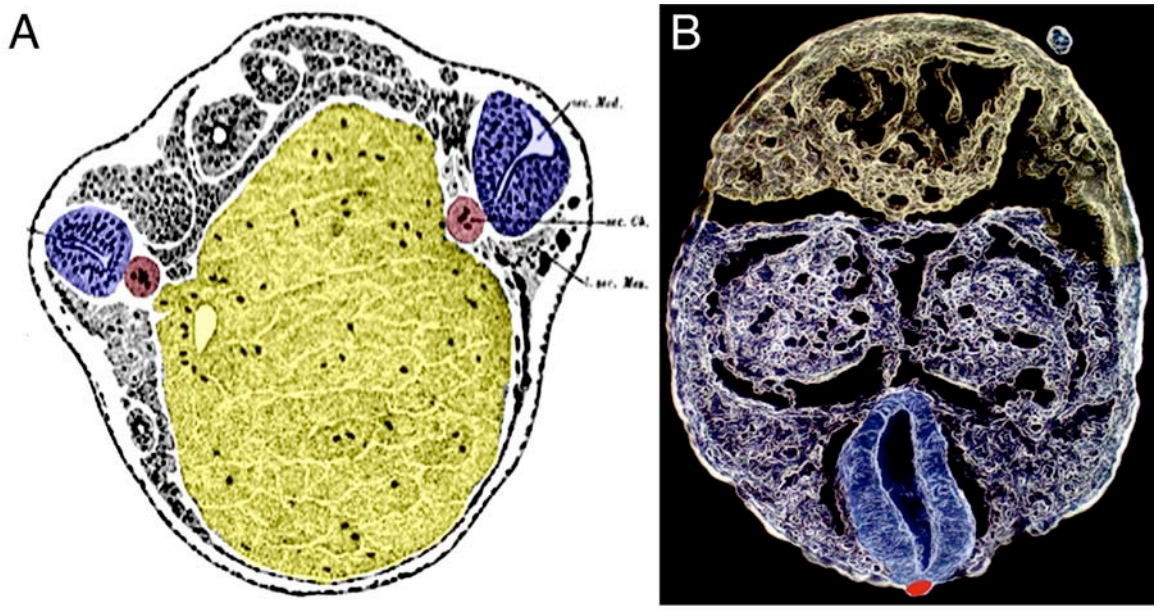

Figure 30: The organizer directs formation of the dorsal axis in multiple contexts. (A) depicts the formation of a double axis by transplantation of an organizer graft to the ventral side of a host frog embryo, from Figure 23 (Spemann and Mangold, 1924). The graft formed a secondary notochord (maroon) and induced a secondary neural tube (blue) on the right. (B) shows the arrangement of the dorsal axis (notochord (maroon), neural tube (blue) in the GDF-3 genetrap mouse mutants with the lateral/ventral tissues in yellow.

Interestingly, in embryonic stem cells, GDF-3 contributes to a molecular pattern that is similar to that of the organizer and its derivatives: including BMP inhibition, Nodal activation, and possibly IGF activation, although Wnt signaling is inhibited by the organizer, and active in embryonic stem cells ((Bendall et al., 2007; James et al., 2005; Pera et al., 2001; Sato et al., 2004; Vincent et al., 2003), reviewed in (Brivanlou and Levine, 2007; Harland and Gerhart, 1997; Levine and Brivanlou, 2007). It is not clear whether this is a coincidence, or whether it could reflect a co-option by embryonic stem cells of a molecular program that allows the organizer to give rise to derivatives of all three germ layers, albeit in a more limited manner (Beddington, 1994; Mangold, 1933). Together, these data demonstrate a recurring theme of molecular embryology – that after the original establishment of signaling centers and transcriptional networks for a given role, this module may be 're-used' in both conserved and independent contexts.

Many of my observations demonstrate that GDF-3 activity in a given cell type or tissue is opposite to that of published reports for BMP. As such, it is possible to limit a view of this unusual TGF-β ligand to that of a decoration on the elaborately regulated BMP pathway and to limit my conclusions to supporting, in negative and inhibitory form, models about a positive, activating pathway. However, as the critical example of 'neural default' demonstrates, negative information can be just as important in cell-cell communication as positive signaling. In contrast to this limited view, I consider that GDF-3 and

BMPs are opposite poles of an axis – what is typically described as the 'BMP' pathway. As such, inhibition of BMPs by GDF-3 and other factors in embryonic stem cells helps to endow them with 'stemness.' Further, my findings regarding the required role of GDF-3 for normal morphogenesis of the mouse embryo extends beyond known functions for BMP signaling and furthers our understanding of the overall function of this GDF-3-BMP axis in regulating early embryonic development.

Third, my work highlights the remarkable specialization of large families of factors, here of the TGF-β superfamily into multiple activating branches and inhibitory branches. Further, my findings on GDF-3 may be informative about general mechanisms of inhibitory ligands, including LeftyA, LeftyB, BMP3, Xnr3, BMP15, and GDF9. An important outstanding question is whether there are distinct qualities of TGF-β inhibition, provided by ligand-inhibitors versus non-ligand inhibitorys, such as Noggin and Chordin. This concept is suggested by my finding that GDF-3 is co-expressed with other BMP inhibitors such as Noggin and Chordin; however, removal of GDF-3 perturbs cell movement, while removal of both Noggin and Chordin affect cell fate. If GDF-3 is representative of inhibitory-ligands, my work provides a basis for understanding the mechanisms of nearly one sixth of the ligands in the TGF-β superfamily. Therefore, my findings contribute to an integrated understanding of this pathway during early vertebrate embryogenesis.

MATERIALS AND METHODS:

Xenopus Embryos and Explants:

Embryos were obtained and manipulated as previously described (Hemmati-Brivanlou et al., 1989) and staged as described in Niewkoop and Faber (1967). Embryo explants (animal caps, ventral and dorsal marginal zones) were isolated in 0.1X MMR, washed once and transferred immediately to 0.5X MMR with gentamycin for culture. For animal cap disassociation, caps were isolated in CMFM media (88mM NaCl, 1 mM KCl, 2.4 mM $NaHCO_3$, 5 mM HEPES). Cut caps were transferred to fresh CMFM with 0.5% BSA in an agarose coated dish for several minutes with the sensorial layer down, to allow the epithelial layer to peel away; this step was aided with a hair knife. Disassociated cap cells were then transferred to 100 ul/well of CMFM/BSA in pre-coated 96-well plates for protein co-culture for four hours. During culture, cells were mixed every thirty minutes by pipetting. Cells were then transferred to a pre-BSA-coated eppendorf tube containing 0.75X MMR and 10 mM Ca^{2+}/Mg^{2+} and spun at 800 rpm for two minutes to reaggregate the cells. The cell pellet was then cultured until sibling embryos reached stage 11.5 and harvested for mRNA. Staging was determined using sibling embryos.

Cell Culture:

Human embryonic stem cells were maintained in conditioned medium produced by mouse embryonic fibroblasts. The media is DMEM/F12 with 20% KSR, pencillin/streptomycin, 2 mM L-glutamine, 1X non-essential amino acids, 55 μM β-mercaptoethanol, and FGF (4 ng/mL). 10 ng/mL of recombinant human BMP4 (rhBMP4) (R&D) or 1 ug/mL of recombinant human GDF-3 (Peprotech) was used for treatments. P19 cells were maintained in MEM-α-modified media (Sigma) with 7.5% CBS, 2.5% FBS. C2C12 cells were maintained in DMEM (Sigma) with 15% FBS. For differentiation of C2C12 cells, cells were grown to confluence, changed to DMEM with 2% serum and BMP4 (100 ng/mL) or TGF-β1 (R&D) (1 ng/mL) was added. Genetrap ES cells (The Wellcome Trust Sanger Institute) parent strain 12901a and genetrap AD0857 cells were cultured on gelatin with 1400 U LIF/mL in 1X GMEM containing 10% FBS, 2 mM l-glutamine, 1 mM sodium pyruvate, 1X non-essential amino acids, and 55 μM β-mercaptoethanol. New genetrap mouse embryonic stem cells were derived by allowing blastocysts to attach to mouse embryonic fibroblasts (MEFs) grown in 1000 U/mL of LIF and outgrow for three days. Outgrowths were then isolated with a micropipette, briefly trypsinized, and transferred to new MEFs to propagate the new line.

Embryoid Body Formation:

Cells were trypsinized to a single cell suspension, counted, and diluted to 10,000 cells/mL in ES growth media with no LIF. Twenty-five μL droplets of cell suspension were placed on the lid of a 10 cm bacterial culture dish and cultured inverted over media for two days. Embryoid bodies were then flushed into EB media (DMEM with 10% FBS) and cultured for seven days. % EB formation was assessed by counting the number of embryoid bodies formed/number of droplets per condition x 100%.

Node explants:

The distal fifth of the embryonic regions of e7.25-e7.5 mouse embryos was explanted with siliconized glass needles (dipped in sigmacote, as described in (Nagy et al., 2003)) and transferred to fibronectin-coated (Sigma human plasma fibronectin at 0.1 mg/mL in PBS for several hours) plastic dishes, with one node per well. Explants were cultured in human ES media (above) without FGF. Dissection was performed in the same media, containing 25 mM HEPES pH 7.4. After 4-5 hours allowed for attachment, divets were created in the plastic immediately next to each explant and one to four beads were placed in the divet. Beads (Affigel Blue from BioRad) were washed twice in PBS, then soaked in rhBMP4 or human serum albumin (final concentration 5 ug/mL) for two hours at 37 °C, then washed twice and placed into the divet. A pre-wetted plastic or glass

coverslip was placed on top to prevent the beads from moving out of the divet. After 48 hours, the explants were fixed, and nuclei were stained with Sytox orange (1:25,000) for visualization.

RT-PCR:

For *Xenopus*, ten animal caps or one embryo were isolated. For mouse, five pre-implantation embryos, three gastrulation stage embryos, or one post-gastrulation stage embryo were used. For real-time PCR The following primers were used.

Table 2: RT-PCR primers

PRIMER	MARKER	SENSE	ANTISENSE
hB-actin	housekeeping gene	TGGCACCACACCTTCTACAATGAGC	GCACAGCTTCTCCTTAATGTC
hCdx2-RT	Trophoblast	TGGAGCTGGAGAAGGAGTTTCACT	CTCCTTTGCTCTGCGGTTCTC
hNanog	stem cell	ACCAGAACTGTAGGGGGAAA	GGTTGCTCCAGGTTGAATTGT
hOct4	stem cell	GAAGGATGTGGTCCGAGTGT	GTGACAGAGACAGGGGGAAA
hSox2	stem cell/neural	ACCAGCTCGCAGACCTACAT	GGTAGTGCTGGGACATGTGA
hTbp1-RT	housekeeping gene	GCTGGCCCATAGTGATCTTT	CTTCACACGCCAAGAAACAGT
mAFP	Endoderm	ATTCCTTCTTCATGCCAG	ACACGTCCCCATCTGAAG
mB-actin	housekeeping gene	GGCCCAGAGCAAGAGAGGTATCC	ACGCACGATTTCCCTCTCAGC
mBU	Mesendoderm	GCTGTGACTGCCTACCAGCAGAATG	GAGAGAGAGCGAGCCTCCAA
mFGF5	Epiblast	AAAGTCAATGGCTCCCACGAA	CTTCAGTCTGTACTTCACTGG
mFlk1	Endothelium	CACCTGGCACTCTCCACCTTC	GATTTCATCCCACTACCGAAA
mGDF-3	gene of interest	CACTTGATTAGCTCCCAGGC	TCTGGAGACAGGAGCCATCT
mHPRT	housekeeping gene	GCTGGTGAAAAGGACCTCT	CACAGGACTAGAACAACCTG
mNkx2.5	Heart	TGCAGAAGGCAGTGGAGCTGGACAAGCC	TGCACTTGTAGCGACGGTTC
mOct4	stem cell	GGCGTTCTCTTTGGAAAGGTGTTC	CTCGAACCACATCCTTCTCT
mPax6	anterior neural/eye	GCTTCATCCGAGTCTTCTCCGTTAG	CCATCTTGCTTGGGAAATCCC
mRax	anterior neural	GAGTTGCTGCGAGCCCTGTGT	CCGATGATAGGCGCTGATGC
mScl-1	Blood	ATTGCACACACGGGATTCTG	GAATTCAGGGTCTTCCTTAG
mSox2	stem cell/neural	GGCAGCTACAGCATGATGCAGG	CTGGTCATGGAGTTGTACTGC
xGlobin	Blood	CAGGCTGGTGAGCTGCCC	GCCTACAACCTGAGAGTGG
xBU	Mesoderm	GGATCGTTATCACCTCTG	GTGTAGTCTGTAGCAGCA
xCollagen II	Notochord	GGATTCAAGGACTCTAGTGC	GATCTCAGCATTGGGGCAAT
xM-actin	Muscle	GCTGACAGAATGCAGAAG	TTGCTTGGAGTGTGT
xMsx1	epidermis	ACTGGTGTGAAGCCGTCCCT	TTCTCTCGGGACTCTCAGGC
xNCAM	neural	AGATGCAGTCATTATTTGTGATGTC	CTGGATGTCCTTATAGTTGAT
xODC	housekeeping gene	AATGGATTTCAGAGACCA	CCAAGGCTAAAGTTGCAG
xOtx2	neural	GGAGGCCAAAACAAAGTG	TCATGGGGTAGGTCCTCT
xSox2	neural	CAGGAGGAAAACCAACC	TGGGGGTATCCAAGCTGCTC
xWnt8	ventral mesoderm	GTTCAAGCATTACCCCGGAT	CTCCTCAATTCCATTCTGCG

Luciferase Assays:

All luciferase assays were done in three separate experiments, each in triplicate; representative individual triplicate experiments are shown in the results section. In *Xenopus* embryos, 20 pg of luciferase DNA construct (BRE-Lux or ARE-Lux) was injected into the animal region of two cell embryos together with the indicated RNAs transcribed from constructs in pCS2++. Pools of four embryos were harvested at stage 11 in 50 μL of lysis buffer. In P19 cells, cells were transfected with 150 ng of reporter, 3.3 ng of renilla reporter, 0.25 μg of Smad1 and Smad4 (each), 0.1 μg of OAZ and test constructs in pCS2++ or empty vector for a total of 1.6 μg/well. After six hours of transfection, media was changed to MEM-α-modified media with 0.2% serum. After 32 hours, cells were lysed in 150 μL of lysis buffer and analyzed for luciferase activity. The error bars indicate standard deviation.

Immunoprecipitations and Western Blots:

Immunoprecipitations on over-expressed proteins were performed as previously described (Yeo and Whitman, 2001) with mαFlag (Sigma; 1 ul/sample) or mαHA (Babco; 5 ul/sample). Antibodies used in western blots were mαα-tubulin (Sigma; 1:1000); rαcyclophillinB (Affinity BioReagents; 1:2000); mαSmad1 (Santa Cruz; 1:750); mαSmad2 (BD Biosciences; 1:750); rαP-Smads (Cell Signaling; 1:1000); mαOct3 (BD Transduction Laboratories; 1:1000); mαTROMA-1 (Dev Studies Hybridoma Bank; 1:75); gαGDF-3 (R&D; 1:10,000);

mαFlag (Sigma; 1:10,000); mαHA (Covance; 1:1000). Mα indicates mouse monoclonal antibody; rα and gα indicate rabbit and goat polyclonal antibody, respectively.

In situ Hybridization:

Whole mount in situ hybridization was performed as described (Merrill et al., 2004). Probes were prepared from GDF-3 in pCS2++ (anti-sense Pst1/T3; full-lenth sense Not1/Sp6). Sectioning of whole mount embryos was performed with 10 μm cryosections after embedding in OCT. Section in situ hybridizations were performed on adult Swiss Webster male testis and was performed as in Rouzankina et al., 2004 except that hybridization was performed by dipping slides into solution.

Immunofluorescence:

Immunofluoresence (IF) on testis was carried out on 10 μm frozen sections post-fixed in 4% paraformaldehyde (PFA). IF on sperm was carried out on sperm dissected from the cauda epididymis that was teased apart and incubated at 37°C for one hour, after which the supernatant was passed over a cell sorter screen to remove any debris. The sperm were then added in solution to a well containing a poly-L-lysine coated coverslip, spun at 450 xg, fixed in 4% PFA (added 1:1 as 8% PFA), and respun at 450xg for ten minutes. IF on blastocyst embryos was done after fixation for 15 minutes in 4% PFA. All IF samples were

washed in PBS containing 0.25% BSA, blocked and permeabilized in 10% donkey serum with 3% Triton, and incubated in primary antibody gαGDF-3 (R&D) (1:500 for sections, 1:100 for sperm) in 10% donkey serum for three hours at room temperature. Testis control samples were incubated with 1:500 primary antibody pre-incubated with recombinant mouse GDF-3 peptide (R&D) at a five times molar excess. Samples were then washed and incubated in secondary antibody then counterstained with either SytoxGreen (Molecular Probes) for nuclear stain or with peanut agglutinin (PNA) (Vector Laboratories) for acrosomal stain.

LacZ staining:

Embryos were dissected in cold PBS and fixed for 15 minutes on ice in fixation buffer (0.1M phosphate buffer pH 7.3, 0.2% gluteraldehyde, 5 mM EGTA, 2 mM $MgCl_2$). Embryos were then washed three times 15-30 minutes each (0.1M phosphate buffer pH 7.3, 2 mM $MgCl_2$, 0.01% sodium deoxycholate, 0.02% NP-40), and stained at 37°C (wash buffer, including 5 mM K_3Fe, 5 mM K_4Fe, 20 mM Tris pH 7.3, 1 mg/mL Red-GAL). Staining of Chd-rtTA/TEToLacZ embryos took 0.5-2 hrs, staining of GDF-3 genetrap embryos took 2 days.

Constructs:

The coding region of GDF-3 and the coding region of GDF-3 plus UTRs were generously provided by S.J. Lee and R.M. Harland, respectively. They were both

subcloned into the EcoR1/Not1 sites of pCS2++. For sense RNA, GDF-3 was linearized with Not1 and transcribed with SP6. The cleavage mutant of GDF-3 (coding region alone) in pCS2++ was produced by site-directed mutagenesis with the Stratagene QuickChange kit using the following primers: CATCCTTCTTCCGGAAACGTGGGGGCGGCCATCTCTGTCCCC (sense) and GGGGACAGAGATGGCCGCCCCCACGTTTCCGGAAGAAGGATG (anti-sense). The amino acid coding was converted from RKRR to GNVG. BMP4 untagged is in pSP64T and RNA was produced with EcoR1/SP6. BMP4-HA was produced with AvrII/T7. ActivinB-HA is in pCS2++ and was produced with Not1/SP6. Vg1-HA (provided by S. Cheng) is in pcDNA3.1 and was produced with AvrII/T7. xNR1 is in pCS2++ and was produced with Not1/SP6. Recombinant human GDF-3 protein was purchased from Peprotech. Recombinant mouse Nodal protein was purchased from R&D Systems.

Genetrap Mouse Genotyping

Tail tips or embryos were lysed in 750 or 200 ul of SNET buffer (20 mM Tris-HCl pH 8.0, 5 mM EDTA pH 8.0, 400 mM NaCl, 1% SDS) containing 400 ug/mL Proteinase K overnight at 55°. An equal volume of phenol/chloroform/isoamyl alcohol was then added, samples were shaken for 30 seconds, and samples were rotated for 30 minutes. The aqueous phase was then isolated and a final concentration of 0.2M NaCl and 70% ethanol was added to precipitate genomic DNA without SDS. Precipitated genomic DNA (gDNA) was washed once with

70% ethanol and gDNA from tail tips was resuspended in 300 ul of TE and embryo DNA was resuspended in 50 ul of TE and samples were allowed to resuspend at room temperature for at least three hours. 1 ul of tail tip gDNA or 5 ul of embryo gDNA was used in each PCR reaction. All PCR reactions were performed in duplicate and were only considered if the cycle number that passed an arbitrary threshold (ΔCT) for each sample was within 1 cycle (but duplicates were usually less than 0.3 cycles apart). Genotyping was performed using three pairs of primers: LacZ, intron boundary (5770-5892), and a normal two-copy gene (Wnt2b). The LacZ and Wnt2b primer sequences were taken from a genotyping strategy at Regeneron.

Table 3

PRIMER	SENSE	ANTISENSE
LacZ	GGAGTGCGATCTTCCTGAGG	CGCATCGTAACCGTGCATC
5770-5892 “D”	AGCCAAGGCTAGACAGAGAA	GGTCAGCATCAGCTTCCTCTTCAA
Wnt2b	GCAGCTGTGACCCATATACCC	CACTACAGCCACCCCAGTCAA
Chd-rtTA	TCCGCGTCCAATTCACCATGTCTA	AGTTTCCTTGTCGTCAGGCCTTC
TRE-BMP4	TTAGTGAACCGTCAGATCGCCT	TCCCGGTCTCAGGTATCAAACT
TRE-DTA	TTAGTGAACCGTCAGATCGCCT	TAACCAGGTTTAGTCCCGTGGT

REFERENCES

Adewumi, O., Aflatoonian, B., Ahrlund-Richter, L., Amit, M., Andrews, P. W., Beighton, G., Bello, P. A., Benvenisty, N., Berry, L. S., Bevan, S. et al. (2007). Characterization of human embryonic stem cell lines by the International Stem Cell Initiative. *Nat Biotechnol* **25**, 803-16.

Agius, E., Oelgeschlager, M., Wessely, O., Kemp, C. and De Robertis, E. M. (2000). Endodermal Nodal-related signals and mesoderm induction in Xenopus. *Development* **127**, 1173-83.

Anderson, R. M., Lawrence, A. R., Stottmann, R. W., Bachiller, D. and Klingensmith, J. (2002). Chordin and noggin promote organizing centers of forebrain development in the mouse. *Development* **129**, 4975-87.

Andersson, O., Reissmann, E., Jornvall, H. and Ibanez, C. F. (2006). Synergistic interaction between Gdf1 and Nodal during anterior axis development. *Dev Biol* **293**, 370-81.

Ang, S. L. and Rossant, J. (1994). HNF-3 beta is essential for node and notochord formation in mouse development. *Cell* **78**, 561-74.

Aono, A., Hazama, M., Notoya, K., Taketomi, S., Yamasaki, H., Tsukuda, R., Sasaki, S. and Fujisawa, Y. (1995). Potent ectopic bone-inducing activity of bone morphogenetic protein-4/7 heterodimer. *Biochem Biophys Res Commun* **210**, 670-7.

Ariizumi, T., Sawamura, K., Uchiyama, H. and Asashima, M. (1991). Dose and time-dependent mesoderm induction and outgrowth formation by activin A in Xenopus laevis. *Int J Dev Biol* **35**, 407-14.

Bachiller, D., Klingensmith, J., Kemp, C., Belo, J. A., Anderson, R. M., May, S. R., McMahon, J. A., McMahon, A. P., Harland, R. M., Rossant, J. et al. (2000). The organizer factors Chordin and Noggin are required for mouse forebrain development. *Nature* **403**, 658-61.

Bachiller, D., Klingensmith, J., Shneyder, N., Tran, U., Anderson, R., Rossant, J. and De Robertis, E. M. (2003). The role of chordin/Bmp signals in mammalian pharyngeal development and DiGeorge syndrome. *Development* **130**, 3567-78.

Beattie, G. M., Lopez, A. D., Bucay, N., Hinton, A., Firpo, M. T., King, C. C. and Hayek, A. (2005). Activin A maintains pluripotency of human embryonic stem cells in the absence of feeder layers. *Stem Cells* **23**, 489-95.

Beddington, R. S. (1994). Induction of a second neural axis by the mouse node. *Development* **120**, 613-20.

Bendall, S. C., Stewart, M. H., Menendez, P., George, D., Vijayaragavan, K., Werbowetski-Ogilvie, T., Ramos-Mejia, V., Rouleau, A., Yang, J., Bosse, M. et al. (2007). IGF and FGF cooperatively establish the regulatory stem cell niche of pluripotent human cells in vitro. *Nature* **448**, 1015-21.

Brickman, J. M., Jones, C. M., Clements, M., Smith, J. C. and Beddington, R. S. (2000). Hex is a transcriptional repressor that contributes to anterior identity and suppresses Spemann organiser function. *Development* **127**, 2303-15.

Brivanlou, A. H. and Darnell, J. E., Jr. (2002). Signal transduction and the control of gene expression. *Science* **295**, 813-8.

Brivanlou, A. H., Gage, F. H., Jaenisch, R., Jessell, T., Melton, D. and Rossant, J. (2003). Stem cells. Setting standards for human embryonic stem cells. *Science* **300**, 913-6.

Brivanlou, A. H. and Levine, A. J. (2007). Molecular Basis of Pluripotency. In *Principles of Regenerative Medicine*, (ed. A. Atala R. Lanza R. Nerem and J. Thomson): Elsevier Academic Press.

Burdsal, C. A., Damsky, C. H. and Pedersen, R. A. (1993). The role of E-cadherin and integrins in mesoderm differentiation and migration at the mammalian primitive streak. *Development* **118**, 829-44.

Camus, A., Perea-Gomez, A., Moreau, A. and Collignon, J. (2006). Absence of Nodal signaling promotes precocious neural differentiation in the mouse embryo. *Dev Biol* **295**, 743-55.

Candia, A. F., Watabe, T., Hawley, S. H., Onichtchouk, D., Zhang, Y., Derynck, R., Niehrs, C. and Cho, K. W. (1997). Cellular interpretation of multiple TGF-beta signals: intracellular antagonism between activin/BVg1 and BMP-2/4 signaling mediated by Smads. *Development* **124**, 4467-80.

Chen, C., Ware, S. M., Sato, A., Houston-Hawkins, D. E., Habas, R., Matzuk, M. M., Shen, M. M. and Brown, C. W. (2006). The Vg1-related protein Gdf3 acts in a Nodal signaling pathway in the pre-gastrulation mouse embryo. *Development* **133**, 319-29.

Conlon, F. L., Lyons, K. M., Takaesu, N., Barth, K. S., Kispert, A., Herrmann, B. and Robertson, E. J. (1994). A primary requirement for nodal in the formation and maintenance of the primitive streak in the mouse. *Development* **120**, 1919-28.

Coucouvanis, E. and Martin, G. R. (1999). BMP signaling plays a role in visceral endoderm differentiation and cavitation in the early mouse embryo. *Development* **126**, 535-46.

Daheron, L., Opitz, S. L., Zaehres, H., Lensch, W. M., Andrews, P. W., Itskovitz-Eldor, J. and Daley, G. Q. (2004). LIF/STAT3 signaling fails to maintain self-renewal of human embryonic stem cells. *Stem Cells* **22**, 770-8.

Dale, L., Howes, G., Price, B. M. and Smith, J. C. (1992). Bone morphogenetic protein 4: a ventralizing factor in early Xenopus development. *Development* **115**, 573-85.

Di-Gregorio, A., Sancho, M., Stuckey, D. W., Crompton, L. A., Godwin, J., Mishina, Y. and Rodriguez, T. A. (2007). BMP signalling inhibits premature neural differentiation in the mouse embryo. *Development*.

Dosch, R., Gawantka, V., Delius, H., Blumenstock, C. and Niehrs, C. (1997). Bmp-4 acts as a morphogen in dorsoventral mesoderm patterning in Xenopus. *Development* **124**, 2325-34.

Dufort, D., Schwartz, L., Harpal, K. and Rossant, J. (1998). The transcription factor HNF3beta is required in visceral endoderm for normal primitive streak morphogenesis. *Development* **125**, 3015-25.

Dunn, N. R., Vincent, S. D., Oxburgh, L., Robertson, E. J. and Bikoff, E. K. (2004). Combinatorial activities of Smad2 and Smad3 regulate mesoderm formation and patterning in the mouse embryo. *Development* **131**, 1717-28.

Durbec, P., Marcos-Gutierrez, C. V., Kilkenny, C., Grigoriou, M., Wartiowaara, K., Suvanto, P., Smith, D., Ponder, B., Costantini, F., Saarma, M. et al. (1996). GDNF signalling through the Ret receptor tyrosine kinase. *Nature* **381**, 789-93.

Eimon, P. M. and Harland, R. M. (2002). Effects of heterodimerization and proteolytic processing on Derriere and Nodal activity: implications for mesoderm induction in Xenopus. *Development* **129**, 3089-103.

Graff, J. M., Bansal, A. and Melton, D. A. (1996). Xenopus Mad proteins transduce distinct subsets of signals for the TGF beta superfamily. *Cell* **85**, 479-87.

Graff, J. M., Thies, R. S., Song, J. J., Celeste, A. J. and Melton, D. A. (1994). Studies with a Xenopus BMP receptor suggest that ventral mesoderm-inducing signals override dorsal signals in vivo. *Cell* **79**, 169-79.

Green, J. B., New, H. V. and Smith, J. C. (1992). Responses of embryonic Xenopus cells to activin and FGF are separated by multiple dose thresholds and correspond to distinct axes of the mesoderm. *Cell* **71**, 731-9.

Green, J. B. and Smith, J. C. (1990). Graded changes in dose of a Xenopus activin A homologue elicit stepwise transitions in embryonic cell fate. *Nature* **347**, 391-4.

Gritsman, K., Zhang, J., Cheng, S., Heckscher, E., Talbot, W. S. and Schier, A. F. (1999). The EGF-CFC protein one-eyed pinhead is essential for nodal signaling. *Cell* **97**, 121-32.

Groppe, J., Greenwald, J., Wiater, E., Rodriguez-Leon, J., Economides, A. N., Kwiatkowski, W., Affolter, M., Vale, W. W., Belmonte, J. C. and Choe, S. (2002). Structural basis of BMP signalling inhibition by the cystine knot protein Noggin. *Nature* **420**, 636-42.

Grunz, H. and Tacke, L. (1989). Neural differentiation of Xenopus laevis ectoderm takes place after disaggregation and delayed reaggregation without inducer. *Cell Differ Dev* **28**, 211-7.

Hamatani, T., Daikoku, T., Wang, H., Matsumoto, H., Carter, M. G., Ko, M. S. and Dey, S. K. (2004). Global gene expression analysis identifies molecular pathways distinguishing blastocyst dormancy and activation. *Proc Natl Acad Sci U S A* **101**, 10326-31.

Haramoto, Y., Tanegashima, K., Onuma, Y., Takahashi, S., Sekizaki, H. and Asashima, M. (2004). Xenopus tropicalis nodal-related gene 3 regulates BMP signaling: an essential role for the pro-region. *Dev Biol* **265**, 155-68.

Harland, R. and Gerhart, J. (1997). Formation and function of Spemann's organizer. *Annu Rev Cell Dev Biol* **13**, 611-67.

Harland, R. M. (2004). Dorsoventral Patterning of the Mesoderm. In *Gastrulation: From Cells to Embryos*, (ed. C. D. Stern), pp. 373-388. Cold Spring Harbor, NY: Cold Spring Harbor Laboratory Press.

Hata, A., Lagna, G., Massague, J. and Hemmati-Brivanlou, A. (1998). Smad6 inhibits BMP/Smad1 signaling by specifically competing with the Smad4 tumor suppressor. *Genes Dev* **12**, 186-97.

Hata, A., Seoane, J., Lagna, G., Montalvo, E., Hemmati-Brivanlou, A. and Massague, J. (2000). OAZ uses distinct DNA- and protein-binding zinc fingers in separate BMP-Smad and Olf signaling pathways. *Cell* **100**, 229-40.

Hemmati-Brivanlou, A., Kelly, O. G. and Melton, D. A. (1994). Follistatin, an antagonist of activin, is expressed in the Spemann organizer and displays direct neuralizing activity. *Cell* **77**, 283-95.

Hemmati-Brivanlou, A. and Melton, D. A. (1992). A truncated activin receptor inhibits mesoderm induction and formation of axial structures in Xenopus embryos. *Nature* **359**, 609-14.

Hemmati-Brivanlou, A. and Melton, D. A. (1994). Inhibition of activin receptor signaling promotes neuralization in Xenopus. *Cell* **77**, 273-81.

Hemmati-Brivanlou, A. and Thomsen, G. H. (1995). Ventral mesodermal patterning in Xenopus embryos: expression patterns and activities of BMP-2 and BMP-4. *Dev Genet* **17**, 78-89.

Hemmati-Brivanlou, A., Wright, D. A. and Melton, D. A. (1992). Embryonic expression and functional analysis of a Xenopus activin receptor. *Dev Dyn* **194**, 1-11.

James, D., Levine, A. J., Besser, D. and Hemmati-Brivanlou, A. (2005). TGFbeta/activin/nodal signaling is necessary for the maintenance of pluripotency in human embryonic stem cells. *Development* **132**, 1273-82.

Jing, S., Wen, D., Yu, Y., Holst, P. L., Luo, Y., Fang, M., Tamir, R., Antonio, L., Hu, Z., Cupples, R. et al. (1996). GDNF-induced activation of the ret protein tyrosine kinase is mediated by GDNFR-alpha, a novel receptor for GDNF. *Cell* **85**, 1113-24.

Jones, C. M., Lyons, K. M., Lapan, P. M., Wright, C. V. and Hogan, B. L. (1992a). DVR-4 (bone morphogenetic protein-4) as a posterior-ventralizing factor in Xenopus mesoderm induction. *Development* **115**, 639-47.

Jones, C. M., Simon-Chazottes, D., Guenet, J. L. and Hogan, B. L. (1992b). Isolation of Vgr-2, a novel member of the transforming growth factor-beta-related gene family. *Mol Endocrinol* **6**, 1961-8.

Joseph, E. M. and Melton, D. A. (1998). Mutant Vg1 ligands disrupt endoderm and mesoderm formation in Xenopus embryos. *Development* **125**, 2677-85.

Jurand, A. (1974). Some aspects of the development of the notochord in mouse embryos. *J Embryol Exp Morphol* **32**, 1-33.

Kinder, S. J., Tsang, T. E., Ang, S. L., Behringer, R. R. and Tam, P. P. (2001a). Defects of the body plan of mutant embryos lacking Lim1, Otx2 or Hnf3beta activity. *Int J Dev Biol* **45**, 347-55.

Kinder, S. J., Tsang, T. E., Wakamiya, M., Sasaki, H., Behringer, R. R., Nagy, A. and Tam, P. P. (2001b). The organizer of the mouse gastrula is composed of a dynamic population of progenitor cells for the axial mesoderm. *Development* **128**, 3623-34.

Korkola, J. E., Houldsworth, J., Chadalavada, R. S., Olshen, A. B., Dobrzynski, D., Reuter, V. E., Bosl, G. J. and Chaganti, R. S. (2006). Down-regulation of stem cell genes, including those in a 200-kb gene cluster at 12p13.31, is associated with in vivo differentiation of human male germ cell tumors. *Cancer Res* **66**, 820-7.

Lander, E. S. Linton, L. M. Birren, B. Nusbaum, C. Zody, M. C. Baldwin, J. Devon, K. Dewar, K. Doyle, M. FitzHugh, W. et al. (2001). Initial sequencing and analysis of the human genome. *Nature* **409**, 860-921.

Lawson, K. A., Dunn, N. R., Roelen, B. A., Zeinstra, L. M., Davis, A. M., Wright, C. V., Korving, J. P. and Hogan, B. L. (1999). Bmp4 is required for the generation of primordial germ cells in the mouse embryo. *Genes Dev* **13**, 424-36.

Levin, M., Johnson, R. L., Stern, C. D., Kuehn, M. and Tabin, C. (1995). A molecular pathway determining left-right asymmetry in chick embryogenesis. *Cell* **82**, 803-14.

Levine, A. J. and Brivanlou, A. H. (2006a). GDF3 at the crossroads of TGF-beta signaling. *Cell Cycle* **5**, 1069-73.

Levine, A. J. and Brivanlou, A. H. (2006b). GDF3, a BMP inhibitor, regulates cell fate in stem cells and early embryos. *Development* **133**, 209-16.

Levine, A. J. and Brivanlou, A. H. (2007). Proposal of a model of mammalian neural induction. *Dev Biol* **308**, 247-56.

Lowe, L. A., Yamada, S. and Kuehn, M. R. (2001). Genetic dissection of nodal function in patterning the mouse embryo. *Development* **128**, 1831-43.

Mangold, O. (1933). Uber die Induktionsfahighkeit der verschiedenen Bezirke der Neurula von Urodelen. *Naturewissenshaften* **21**, 761-766.

Martinez Barbera, J. P., Clements, M., Thomas, P., Rodriguez, T., Meloy, D., Kioussis, D. and Beddington, R. S. (2000). The homeobox gene Hex is required in definitive endodermal tissues for normal forebrain, liver and thyroid formation. *Development* **127**, 2433-45.

Martinez-Barbera, J. P. and Beddington, R. S. (2001). Getting your head around Hex and Hesx1: forebrain formation in mouse. *Int J Dev Biol* **45**, 327-36.

McMahon, J. A., Takada, S., Zimmerman, L. B., Fan, C. M., Harland, R. M. and McMahon, A. P. (1998). Noggin-mediated antagonism of BMP signaling is required for growth and patterning of the neural tube and somite. *Genes Dev* **12**, 1438-52.

Munoz-Sanjuan, I., Bell, E., Altmann, C. R., Vonica, A. and Brivanlou, A. H. (2002). Gene profiling during neural induction in Xenopus laevis: regulation of BMP signaling by post-transcriptional mechanisms and TAB3, a novel TAK1-binding protein. *Development* **129**, 5529-40.

Munoz-Sanjuan, I. and Brivanlou, A. H. (2002). Neural induction, the default model and embryonic stem cells. *Nat Rev Neurosci* **3**, 271-80.

Nagy, A., Gertsenstein, M., Vintersten, K. and Behringer, R. R. (2003). Manipulating the Mouse Embryo. Cold Spring Harbor, NY: Cold Spring Harbor Laboratory Press.

Nakatsuji, N., Snow, M. H. and Wylie, C. C. (1986). Cinemicrographic study of the cell movement in the primitive-streak-stage mouse embryo. *J Embryol Exp Morphol* **96**, 99-109.

Ninomiya, H., Elinson, R. P. and Winklbauer, R. (2004). Antero-posterior tissue polarity links mesoderm convergent extension to axial patterning. *Nature* **430**, 364-7.

Pedersen, R. A., Wu, K. and Balakier, H. (1986). Origin of the inner cell mass in mouse embryos: cell lineage analysis by microinjection. *Dev Biol* **117**, 581-95.

Pera, E. M., Wessely, O., Li, S. Y. and De Robertis, E. M. (2001). Neural and head induction by insulin-like growth factor signals. *Dev Cell* **1**, 655-65.

Perea-Gomez, A., Vella, F. D., Shawlot, W., Oulad-Abdelghani, M., Chazaud, C., Meno, C., Pfister, V., Chen, L., Robertson, E., Hamada, H. et al. (2002). Nodal antagonists in the anterior visceral endoderm prevent the formation of multiple primitive streaks. *Dev Cell* **3**, 745-56.

Reubinoff, B. E., Pera, M. F., Fong, C. Y., Trounson, A. and Bongso, A. (2000). Embryonic stem cell lines from human blastocysts: somatic differentiation in vitro. *Nat Biotechnol* **18**, 399-404.

Rhinn, M., Dierich, A., Shawlot, W., Behringer, R. R., Le Meur, M. and Ang, S. L. (1998). Sequential roles for Otx2 in visceral endoderm and neuroectoderm for forebrain and midbrain induction and specification. *Development* **125**, 845-56.

Robertson, E. J., Norris, D. P., Brennan, J. and Bikoff, E. K. (2003). Control of early anterior-posterior patterning in the mouse embryo by TGF-beta signalling. *Philos Trans R Soc Lond B Biol Sci* **358**, 1351-7; discussion 1357.

Rodriguez, S., Jafer, O., Goker, H., Summersgill, B. M., Zafarana, G., Gillis, A. J., van Gurp, R. J., Oosterhuis, J. W., Lu, Y. J., Huddart, R. et al. (2003). Expression profile of genes from 12p in testicular germ cell tumors of adolescents and adults associated with i(12p) and amplification at 12p11.2-p12.1. *Oncogene* **22**, 1880-91.

Sato, N., Meijer, L., Skaltsounis, L., Greengard, P. and Brivanlou, A. H. (2004). Maintenance of pluripotency in human and mouse embryonic stem cells through activation of Wnt signaling by a pharmacological GSK-3-specific inhibitor. *Nat Med* **10**, 55-63.

Sato, N., Sanjuan, I. M., Heke, M., Uchida, M., Naef, F. and Brivanlou, A. H. (2003). Molecular signature of human embryonic stem cells and its comparison with the mouse. *Dev Biol* **260**, 404-13.

Sausedo, R. A. and Schoenwolf, G. C. (1994). Quantitative analyses of cell behaviors underlying notochord formation and extension in mouse embryos. *Anat Rec* **239**, 103-12.

Shi, Y. and Massague, J. (2003). Mechanisms of TGF-beta signaling from cell membrane to the nucleus. *Cell* **113**, 685-700.

Shibuya, H., Yamaguchi, K., Shirakabe, K., Tonegawa, A., Gotoh, Y., Ueno, N., Irie, K., Nishida, E. and Matsumoto, K. (1996). TAB1: an activator of the TAK1 MAPKKK in TGF-beta signal transduction. *Science* **272**, 1179-82.

Skotheim, R. I., Autio, R., Lind, G. E., Kraggerud, S. M., Andrews, P. W., Monni, O., Kallioniemi, O. and Lothe, R. A. (2006). Novel genomic aberrations in testicular germ cell tumors by array-CGH, and associated gene expression changes. *Cell Oncol* **28**, 315-26.

Smith, J. C. (1987). A mesoderm-inducing factor is produced by Xenopus cell line. *Development* **99**, 3-14.

Smith, W. C. and Harland, R. M. (1992). Expression cloning of noggin, a new dorsalizing factor localized to the Spemann organizer in Xenopus embryos. *Cell* **70**, 829-40.

Snow, M. H. L. (1977). Gastrulation in the mouse: growth and regionalization of the epiblast. *J Embryol Exp Morphol* **42**, 293-303.

Soares, M. L., Haraguchi, S., Torres-Padilla, M. E., Kalmar, T., Carpenter, L., Bell, G., Morrison, A., Ring, C. J., Clarke, N. J., Glover, D. M. et al. (2005). Functional studies of signaling pathways in peri-implantation development of the mouse embryo by RNAi. *BMC Dev Biol* **5**, 28.

Sokol, S., Wong, G. G. and Melton, D. A. (1990). A mouse macrophage factor induces head structures and organizes a body axis in Xenopus. *Science* **249**, 561-4.

Spemann, H. and Mangold, H. (1924). Uber Induktion von Embryonalanlangen durch Implantation artfremder Organisatoren. *Archiv fur Mikroskopische Anatomie und Entwikslungsmechanik* **100**.

Sulik, K., Dehart, D. B., Iangaki, T., Carson, J. L., Vrablic, T., Gesteland, K. and Schoenwolf, G. C. (1994). Morphogenesis of the murine node and notochordal plate. *Dev Dyn* **201**, 260-78.

Suzuki, A., Thies, R. S., Yamaji, N., Song, J. J., Wozney, J. M., Murakami, K. and Ueno, N. (1994). A truncated bone morphogenetic protein receptor affects dorsal-ventral patterning in the early Xenopus embryo. *Proc Natl Acad Sci U S A* **91**, 10255-9.

Tabibzadeh, S. and Hemmati-Brivanlou, A. (2006). Lefty at the crossroads of "stemness" and differentiative events. *Stem Cells* **24**, 1998-2006.

Takahashi, S., Yokota, C., Takano, K., Tanegashima, K., Onuma, Y., Goto, J. and Asashima, M. (2000). Two novel nodal-related genes initiate early inductive events in Xenopus Nieuwkoop center. *Development* **127**, 5319-29.

Thomsen, G., Woolf, T., Whitman, M., Sokol, S., Vaughan, J., Vale, W. and Melton, D. A. (1990). Activins are expressed early in Xenopus embryogenesis and can induce axial mesoderm and anterior structures. *Cell* **63**, 485-93.

Trupp, M., Arenas, E., Fainzilber, M., Nilsson, A. S., Sieber, B. A., Grigoriou, M., Kilkenny, C., Salazar-Grueso, E., Pachnis, V. and Arumae, U. (1996). Functional receptor for GDNF encoded by the c-ret proto-oncogene. *Nature* **381**, 785-9.

Vallier, L., Alexander, M. and Pedersen, R. A. (2005). Activin/Nodal and FGF pathways cooperate to maintain pluripotency of human embryonic stem cells. *J Cell Sci* **118**, 4495-509.

Vallier, L., Reynolds, D. and Pedersen, R. A. (2004). Nodal inhibits differentiation of human embryonic stem cells along the neuroectodermal default pathway. *Dev Biol* **275**, 403-21.

Varlet, I., Collignon, J. and Robertson, E. J. (1997). nodal expression in the primitive endoderm is required for specification of the anterior axis during mouse gastrulation. *Development* **124**, 1033-44.

Vincent, S. D., Dunn, N. R., Hayashi, S., Norris, D. P. and Robertson, E. J. (2003). Cell fate decisions within the mouse organizer are governed by graded Nodal signals. *Genes Dev* **17**, 1646-62.

Vonica, A. and Brivanlou, A. H. (2007). The left-right axis is regulated by the interplay of Coco, Xnr1 and derriere in Xenopus embryos. *Dev Biol* **303**, 281-94.

Wall, N. A., Craig, E. J., Labosky, P. A. and Kessler, D. S. (2000). Mesendoderm induction and reversal of left-right pattern by mouse Gdf1, a Vg1-related gene. *Dev Biol* **227**, 495-509.

Wang, Q. T., Piotrowska, K., Ciemerych, M. A., Milenkovic, L., Scott, M. P., Davis, R. W. and Zernicka-Goetz, M. (2004). A genome-wide study of gene activity reveals developmental signaling pathways in the preimplantation mouse embryo. *Dev Cell* **6**, 133-44.

Weinstein, D. C., Ruiz i Altaba, A., Chen, W. S., Hoodless, P., Prezioso, V. R., Jessell, T. M. and Darnell, J. E., Jr. (1994). The winged-helix transcription factor HNF-3 beta is required for notochord development in the mouse embryo. *Cell* **78**, 575-88.

Wilson, P. A. and Hemmati-Brivanlou, A. (1995). Induction of epidermis and inhibition of neural fate by Bmp-4. *Nature* **376**, 331-3.

Wilson, P. A., Lagna, G., Suzuki, A. and Hemmati-Brivanlou, A. (1997). Concentration-dependent patterning of the Xenopus ectoderm by BMP4 and its signal transducer Smad1. *Development* **124**, 3177-84.

Xu, R. H., Chen, X., Li, D. S., Li, R., Addicks, G. C., Glennon, C., Zwaka, T. P. and Thomson, J. A. (2002). BMP4 initiates human embryonic stem cell differentiation to trophoblast. *Nat Biotechnol* **20**, 1261-4.

Xu, R. H., Peck, R. M., Li, D. S., Feng, X., Ludwig, T. and Thomson, J. A. (2005). Basic FGF and suppression of BMP signaling sustain undifferentiated proliferation of human ES cells. *Nat Methods* **2**, 185-90.

Yamaguchi, K., Shirakabe, K., Shibuya, H., Irie, K., Oishi, I., Ueno, N., Taniguchi, T., Nishida, E. and Matsumoto, K. (1995). Identification of a member of the MAPKKK family as a potential mediator of TGF-beta signal transduction. *Science* **270**, 2008-11.

Yamamoto, M., Meno, C., Sakai, Y., Shiratori, H., Mochida, K., Ikawa, Y., Saijoh, Y. and Hamada, H. (2001). The transcription factor FoxH1 (FAST) mediates Nodal signaling during anterior-posterior patterning and node formation in the mouse. *Genes Dev* **15**, 1242-56.

Yang, Y. P. and Klingensmith, J. (2006). Roles of organizer factors and BMP antagonism in mammalian forebrain establishment. *Dev Biol* **296**, 458-75.

Yeo, C. and Whitman, M. (2001). Nodal signals to Smads through Cripto-dependent and Cripto-independent mechanisms. *Mol Cell* **7**, 949-57.

Ying, Q. L., Nichols, J., Chambers, I. and Smith, A. (2003). BMP induction of Id proteins suppresses differentiation and sustains embryonic stem cell self-renewal in collaboration with STAT3. *Cell* **115**, 281-92.

Yost, H. J. (2001). Establishment of left-right asymmetry. *Int Rev Cytol* **203**, 357-81.

Zamparini, A. L., Watts, T., Gardner, C. E., Tomlinson, S. R., Johnston, G. I. and Brickman, J. M. (2006). Hex acts with beta-catenin to regulate anteroposterior patterning via a Groucho-related co-repressor and Nodal. *Development* **133**, 3709-22.

Zeng, X., Miura, T., Luo, Y., Bhattacharya, B., Condie, B., Chen, J., Ginis, I., Lyons, I., Mejido, J., Puri, R. K. et al. (2004). Properties of pluripotent human embryonic stem cells BG01 and BG02. *Stem Cells* **22**, 292-312.

Ziomek, C. A. and Johnson, M. H. (1982). The roles of phenotype and position in guiding the fate of 16-cell mouse blastomeres. *Dev Biol* **91**, 440-7.